



May 2019



Phase 3 Algal Flow-Way Pilot Testing Program at Dundalk Marine Terminal

Prepared for: U.S. Department of Transportation Maritime Administration
Maryland Department of Transportation Maryland Port Administration
Maryland Environmental Service

May 2019

Phase 3 Algal Flow-Way Pilot Testing Program at Dundalk Marine Terminal

Prepared for

U.S. Department of Transportation
Maritime Administration
1200 New Jersey Avenue, SE
Washington, DC 20590

Maryland Department of Transportation
Maryland Port Administration
401 East Pratt Street
Baltimore, Maryland 21202

Maryland Environmental Service
259 Najoles Road
Millersville, Maryland 21108

Prepared by

Anchor QEA, LLC
10320 Little Patuxent Parkway, Suite 1140
Columbia, Maryland 21044

TABLE OF CONTENTS

1	Introduction	5
1.1	Project Objectives	6
1.2	Adaptive Management	7
1.3	Algal Flow-Way Operations	8
1.3.1	Project History	8
1.3.2	MARAD Phase 3 Operations	8
1.4	Algal Flow-Way Harvests.....	11
1.5	Nutrient Calculations	13
1.5.1	Laboratory Analysis.....	13
1.5.2	First Flush Samples.....	14
2	Algal Flow-Way Operations	15
2.1	Environmental Conditions	15
2.2	Algal Flow-way Operational Changes in 2018.....	18
2.2.1	Pump Relocation, Water Flow Rate and Biofouling	18
2.2.2	Self-Siphoning Surge System	20
2.2.3	Surface Material of the Flow-Way.....	20
2.2.4	Sand Filter.....	21
3	Biomass Recovery and Algae Dewatering Methods	24
3.1	Biomass Dewatering Methods	25
3.1.1	Evaporation Bed.....	25
3.1.2	Dewatering Pad.....	25
3.1.3	Hanging Bag.....	27
3.1.4	Merit Tile.....	29
3.1.5	Wedge Wire Screen.....	30
3.1.6	Perpendicular Harvest + Side Channel	31
3.1.7	Sand Filter.....	32
3.1.8	Small-Scale Dewatering Tests.....	33
3.2	Recommended Algal Solids Recovery and Dewatering Method.....	35
4	Algal Digester Testing	36
4.1	Algal Digester Operation.....	36
4.2	Biogas Production.....	38
4.3	Summary of Algal Digester Testing	41

4.4	Feasibility of Fuel Cell Use at Dundalk Marine Terminal.....	41
4.4.1	Description of Fuel Cell Technology	42
4.4.2	Operational Considerations.....	43
4.4.3	Emissions and Economic Analysis.....	44
5	Project Recommendations	46
5.1	Biomass Productivity.....	46
5.1.1	Flow-Way Surface Material.....	46
5.1.2	Biofouling and the Linear Hydraulic Loading Rate.....	46
5.1.3	Surge/Pulsed Flow	46
5.1.4	Water Quality Monitoring.....	47
5.2	Algal Flow-Way Design.....	47
5.2.1	Perpendicular Harvest and Side Channel Dewatering	47
5.2.2	Wedge Wire.....	48
5.2.3	Sand Filter.....	48
5.3	Algal Digesters	48
6	References	49

TABLES

Table 1-1	2018 Dates of Algal Biomass Harvests.....	12
Table 3-1	Dates for Testing of Dewatering Methods.....	24
Table 4-1	Quantity of Algae Fed to the Digesters.....	37
Table 4-2	Biogas Production and Composition, Weeks 1-13	38
Table 4-3	Greenhouse Gas Emission Reductions for Deployment Options	44

FIGURES

Figure 1-1	Location of Algal Flow-Way at DMT	7
Figure 1-2	Surge System.....	9
Figure 2-1	Daily Total Rainfall in 2018 at Dundalk Marine Terminal Weather Station.....	16
Figure 2-2	Salinity in Baltimore Harbor in 2018	16
Figure 2-3	Algal Productivity from Algal Flow-Way at Dundalk Marine Terminal in 2017 and 2018.....	17
Figure 2-4	Water Inflow Linear Hydraulic Loading Rate (LHLR).....	19
Figure 2-5	Linear Hydraulic Loading Rate (LHLR) for Algal Flow-way Operations.....	19

Figure 2-6	Algal Flow-Way Design for Phase 3 Project	22
Figure 2-7	Two Algal Flow-way Sections with Roughened Concrete Surface.....	23
Figure 3-1	Evaporation Bed.....	26
Figure 3-2	Dewatering Pad.....	26
Figure 3-3	Hanging Bag Testing	28
Figure 3-3	Solids Retained During Parallel Hanging Bags Tests.....	28
Figure 3-4	Merit Tile Testing.....	29
Figure 3-5	Wedge Wire Screen Testing	31
Figure 3-6	Perpendicular Harvest and Side Channel	31
Figure 3-7	Sand Filter Testing.....	33
Figure 3-8	Wedge Wire Screen Effluent After 24 Hours of Settling.....	35
Figure 4-1	Total Biogas Production from Algal Digestion.....	39
Figure 4-2	Total Methane Production from Algal Digestion.....	40
Figure 4-3	Methane Production Normalized by Algae Fed.....	40
Figure 4-4	Performance Regression Model for a Variety of Fuel Cell System Sizes	45

APPENDICES

Appendix A	Project Photographs
Appendix B	Field Data Tables
Appendix C	Analytical Data for Algal Flow-Way Testing

ATTACHMENTS

Attachment A	Algal Digester Report, University of Maryland
Attachment B	Feasibility of Fuel Cell Use at Ports, Environmental Defense Fund Report

ABBREVIATIONS

µm	micron
AD	anaerobic digestion
AFT	algal flow-way technology
ASTM	American Society for Testing and Materials
BGE	Baltimore Gas and Electric
BMP	best management practice
CH ₄	methane
CO ₂	carbon dioxide
DMT	Dundalk Marine Terminal
EPDM	ethylene propylene diene terpolymer
ft	feet
gpm	gallons per minute
HydroMentia	HydroMentia Technologies, LLC
kW	kilowatt
L	liter
lf	linear foot
LHLR	linear hydraulic loading rate
MARAD	U.S. Department of Transportation Maritime Administration
MDE	Maryland Department of the Environment
MDOT MPA	Maryland Department of Transportation Maryland Port Administration
MES	Maryland Environmental Service
mg/L	milligram per liter
MS4	Municipal Separate Storm Sewer System
N ₂	balance gas
NMP	NMP Engineering Consultants, Inc.
NPDES	National Pollutant Discharge Elimination System
NTU	nephelometric turbidity unit
O ₂	oxygen
PNG	pipeline natural gas
ppt	parts per thousand
SOFC	solid oxide fuel cells
TN	total nitrogen
TP	total phosphorus
TSS	total suspended solids
UMD	University of Maryland

1 Introduction

The U.S. Department of Transportation Maritime Administration (MARAD) and Maryland Department of Transportation Maryland Port Administration (MDOT MPA), through a cooperative agreement, provided funding for an Integrated Algal Flow-Way and Biogas Production project at Dundalk Marine Terminal (DMT) in Baltimore, Maryland. The 2018 Phase 3 project was a continuation of work that was initiated with laboratory studies in 2016 (Phase 1) and continued with field studies completed in 2017 (Phase 2) (Anchor QEA 2018). The initial field studies in 2017 used algae grown on an algal flow-way to produce biogas and power a fuel cell.

The MARAD Phase 3 project represents a collaboration between MARAD and MDOT MPA, which was supported by Maryland Environmental Service (MES); Anchor QEA, LLC (Anchor QEA), HydroMentia Technologies, LLC (HydroMentia); NMP Engineering Consultants, Inc. (NMP); and the University of Maryland (UMD). Operation of the algal flow-way and experiments to enhance the biomass handling procedures were implemented by MES, Anchor QEA, HydroMentia, and NMP. The algal digester and biogas production component of the project was implemented by UMD with support from MES staff on-site at DMT (Section 4 and Attachment A).

The MARAD Phase 3 project used the algae grown on the flow-way as feedstock for an algal digester system that produced biogas. The MARAD Phase 3 testing program built on work conducted previously with a focus on enhancing the efficiency of dewatering and handling of the biomass. By decreasing the water content in the feedstock, the digester system should be able to more efficiently convert the algal biomass to biogas. Although the Phase 2 project included operation of a fuel cell, Phase 3 did not include any further fuel cell testing. A feasibility report on the potential future use of a fuel cell at DMT was completed by an Environmental Defense Fund Climate Corps fellow and the results of the study are summarized in Section 4. The full report is included as Attachment B.

MDOT MPA also implemented several testing procedures to quantify water quality improvements from the removal of total nitrogen (TN) and total phosphorus (TP) from Patapsco River water from algal growth and removal. Data from the pilot study were used to determine the TN and TP credit that could be applied to MDOT MPA's National Pollutant Discharge Elimination System (NPDES) municipal separate storm sewer system (MS4) permit or traded through the nutrient trading program. Maryland Department of the Environment (MDE) allows for use of alternative best management practices (BMPs) such as algal flow-way technologies to receive nutrient credit, specifically TN and TP, toward NPDES MS4 permit impervious acre restoration requirements. The algal flow-way is an alternative BMP that is accepted by MDE for inclusion in the nutrient credit trading program.

The overall approach to operations, testing, and nutrient sampling for the MARAD Phase 3 project was developed based on MDOT MPA's discharge permit for the algal flow-way and two guidance documents:

- Nutrient and Sediment Reductions from Algal Flow-way Technologies (AFT), Recommendations to the Chesapeake Bay Program's Water Quality Goal Implementation Team from the Algal Flow-way Technologies BMP Expert Panel (Bott et al. 2015)
- Accounting for Stormwater Wasteload Allocations and Impervious Acres Treated, Guidance for National Pollutant Discharge Elimination System Stormwater Permits (MDE 2014), specifically Appendix D

This report documents the testing conducted during the MARAD Phase 3 project. Results from UMD's data analyses and operations of the digesters in the field and laboratory studies of biogas production from algal digestion are briefly summarized within this report in Section 4. Project photographs, field data tables, and analytical data tables for algal flow-way testing are presented in Appendices A, B, and C, respectively. A description and analysis of UMD's project setup, testing procedures, results, and data analysis are included as Attachment A.

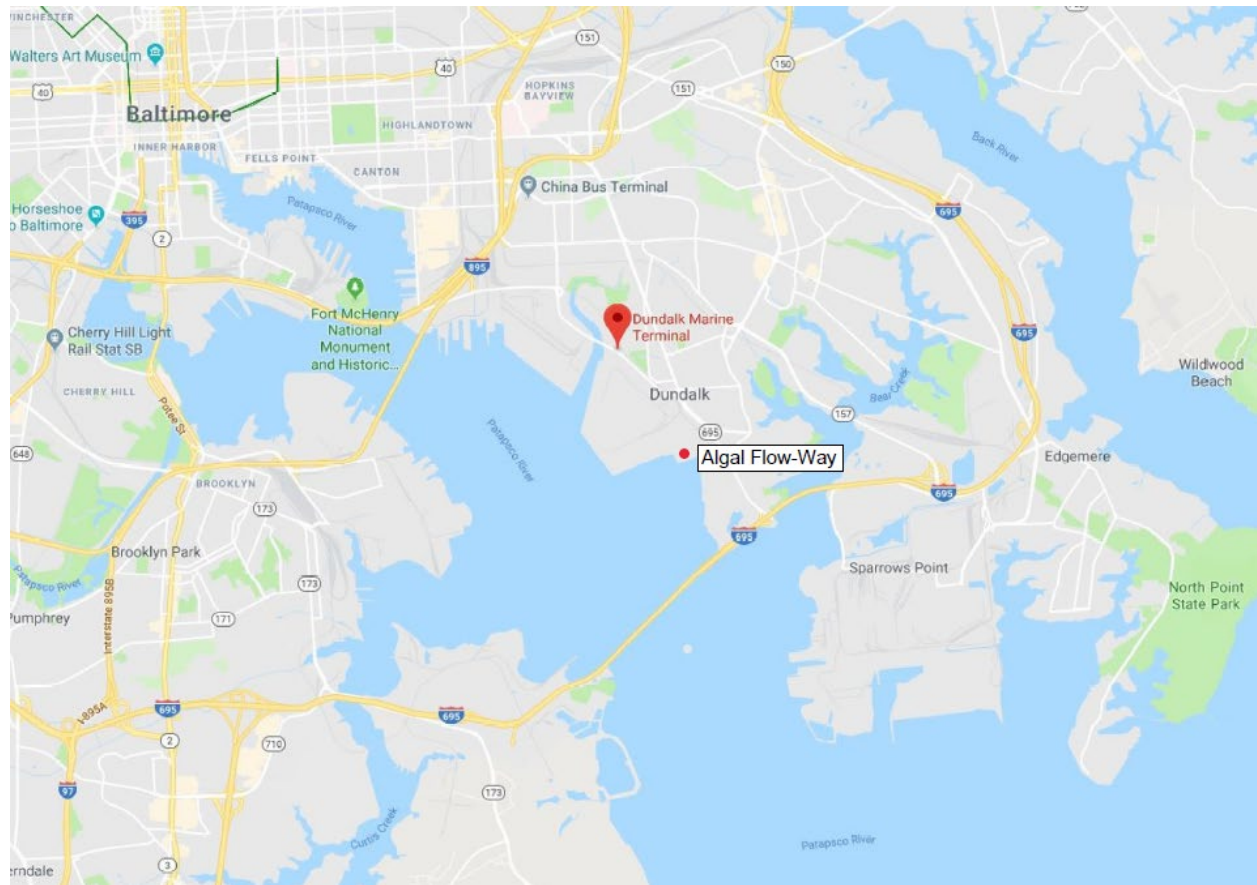
1.1 Project Objectives

The MDOT MPA algal flow-way is a linear raceway constructed at the DMT adjacent to the Patapsco River (Figure 1-1) that uses water from the Patapsco River to grow algae on a surface specifically designed to enhance algal growth. The algae biomass grown on the flow-way removes nitrogen and phosphorus from surface water, improving overall water quality.

The overall objective of the MARAD Phase 3 project was to study optimal operational conditions and biomass handling procedures that will maximize algal growth and recovery to achieve credit for TN, TP, and sediment removal from the Patapsco River. To achieve the overall project objective, the MARAD Phase 3 project focused on four approaches that were implemented concurrently throughout the project:

1. Testing how changes to operational conditions such as the water flow rate and the surface material of the flow-way influence total algal growth
2. Evaluating methods for harvesting and dewatering algal biomass to increase efficiencies for biomass recovery, handling, and transport
3. Calculating TN and TP removal based on the total algal biomass (productivity)
4. Optimizing operating conditions for an algal-based digester to produce and capture a consistent, high-quality biogas

Figure 1-1
Location of Algal Flow-Way at DMT



Basemap Source: Google Maps

1.2 Adaptive Management

Adaptive management is a systematic, iterative process used to improve decision-making by implementing lessons learned from experience and outcomes throughout the life of the project. An adaptive management strategy provides an opportunity to revise project goals and objectives as project conditions change. Additionally, the adaptive management process provides project stakeholders the opportunity to periodically review progress toward achieving the goals of the program, and to revise the program, if necessary, to reflect lessons learned during project implementation.

An adaptive management approach was necessary for the MARAD Phase 3 project to provide the flexibility to respond to changes in on-site conditions, to replace project components that were not effective in meeting the project objectives, to integrate new knowledge or new technologies, and to test alternative project hypotheses. Specifically, it was apparent early in the project that the originally

proposed dewatering approaches – the concrete dewatering pad and the evaporation bed – were insufficient to provide the dewatering capability required for the project given the dominance of filamentous diatoms. The project team worked on a weekly basis to design, discuss, and implement multiple new strategies for biomass handling that were based on observed site conditions and constraints, previous project experience from the DMT flow-way, expertise from operating algal flow-ways in other parts of the United States, and experience working with MDE’s regulatory framework. Additional dewatering strategies implemented blended engineering and scientific expertise and had the dual goals of enhancing the percent solids of algal biomass to make biomass handling easier and quantifying TN and TP concentrations to understand the potential for water quality improvements from flow-way operations. Additional dewatering methods implemented as a result of this adaptive management strategy are discussed in Section 3.1. Modifications to laboratory testing methods implemented after adaptive management discussions are summarized in Section 1.4.1.

1.3 Algal Flow-Way Operations

1.3.1 *Project History*

The first algal flow-way was constructed at DMT in 2013 to assess the potential for improving water quality by removing nutrient and sediment from the Patapsco River (Smith et al. 2013). An algal flow-way has operated each year from 2013 to 2017 at DMT, and each year improvements to the system design, method of operation, and biomass handling techniques were implemented (Smith et al. 2013, Smith et al. 2016, Selby et al. 2016, Selby et al. 2018). Previous versions of the flow-way experimented with various lengths of flow-way surface, different pump rates at which Patapsco River water was delivered to the flow-way, using tipping buckets to deliver Patapsco River water to the flow-way in a pulsed manner, operating for varying lengths of time and seasons, various manual harvest methods, transporting via vacuum truck, and air drying by evaporation in an open area. Dried algal biomass was periodically collected, weighed, and disposed of in a local landfill.

1.3.2 *MARAD Phase 3 Operations*

The MARAD Phase 3 project was designed as the culmination of previous design modifications into a single system that could be implemented as a large-scale operable facility. Algal biomass harvested from the flow-way each week was provided as feedstock for the digester system to produce biogas. The flow-way operated consistent with MDE’s guidance for operation of an alternative BMP that could be used to achieve nutrient credits for TN and TP removal. Therefore, flow-way operations targeted a full growing season from April through November 2018 to meet the 240 operating days specified in the Expert Panel Report (Bott et al. 2015).

In early March, the algal flow-way was reconstructed on a raised asphalt surface covered with a geomembrane liner that was overlain by a flexible low-profile nylon screen. The flow-way was 206

feet (ft) long and 6 ft wide with a slope of approximately 1 percent. The low-profile nylon screen was used to enhance algal growth by providing a suitable surface for the algae to attach. Water was pumped directly from the Patapsco River to the top of the flow-way, and a self-siphoning surge system controlled the flow by releasing water in pulses (Figure 1-2).

Phase 3 algal flow-way operations were initiated on April 23, 2018, and after allowing three weeks for an algal community to establish, the first harvest of algal biomass was conducted on May 17. An inflow pump failure over the July 4 holiday disrupted normal flow-way operations. Dried algal biomass was removed from the flow-way surface and the pump was replaced with a spare digester feed pump until repairs could be made. Once the pump was replaced, the algal flow-way operated for approximately two weeks to allow the algal community to reestablish and weekly harvests resumed on July 18. On August 27, the original inflow pump was put back in service. The algal flow-way was operated for a total of 218 days, and the last day of operations was November 29, 2018. Flow-way operations were discontinued once water temperatures started to drop and daily air temperatures were consistently near or below freezing, essentially halting substantial algal growth.

Figure 1-2
Surge System



The 2018 algal flow-way operations included the following:

- 1) Purchasing a new inflow pump and relocating the pump from next to the flow-way to outside the fence line and to a lower elevation closer to the Patapsco River to improve the

pump's operating efficiency and flow rate control. This relocation was anticipated to increase the pump's maximum flow rate to 120 gallons per minute (gpm) for a target of 20 gpm per linear foot (lf) of width. The reconfiguration of the pump and surge system provided access to manually change the flow rate for testing.

- 2) Purchasing an improved self-cleaning intake structure around the inflow pipe to prevent/reduce the effects of biofouling. In previous studies, substantial biofouling was identified as a major reason why the pump's inflow efficiency was reduced. MES purchased an 18-mesh self-cleaning intake screen for the pump that stabilized the pump and maintained the required depth of water for the intake while also protecting the pump from biofouling. The intake screen was attached to a concrete block anchor that was elevated above the river bottom. The self-cleaning unit had three jet nozzles inside the intake screen that would spray outward to prevent fouling on the mesh. The unit had veins inside the mesh to allow the entire screen segment to rotate, ensuring even cleaning across the intake surfaces. This self-cleaning was achieved by using pressurized water from a return line on the discharge side of the pump. A pressure gauge and gate valve allowed for throttling and monitoring of the return line.
- 3) Installing an ultrasonic flow meter to provide more accurate flow readings, including total flow. Previous flow meters were simple paddle wheel designs that were less accurate and prone to fouling. The ultrasonic meter allowed for flow and temperature measurement without a mechanical obstruction in the pipe. The new meter also had a flow totalizer, allowing for easier permit appropriation and discharge data collection.
- 4) Evaluating changes to the water flow rates and its impact total algal biomass production. Observations during previous studies indicated that higher flow rates seemed to favor the growth of filamentous green algae over filamentous diatoms. Filamentous green algae have a higher biomass and are easier to handle during harvest and drying, so testing was conducted to evaluate if increasing the flow rate could enhance the growth of a filamentous green algae community and increase algal growth.
- 5) Implementing a self-siphoning surge system, which replaced the tipping buckets that were used in previous years. While the use of the tipping buckets to generate a water pulse was initially successful, the system was inconsistent and broke down during long-term operations and was therefore not a feasible option for a larger system. The self-siphoning surge system's larger water capacity allowed for more control to pulse water onto the flow-way with each surge and the surge action was essentially maintenance free. The surge system was an open-top box with an air break that filled with Patapsco River water, and once the water level

reached a specific height within the surge box, water was released onto the flow-way in a single pulse.

- 6) Installing a concrete dewatering pad between two sump areas at the end of the flow-way. Previously, weekly harvests were captured in a simple single sump with concrete walls. The concrete dewatering pad was 8 inches above the sump, with 6:1 sloping sides into the two storage sumps. The two sumps were used for harvest collection and biomass dewatering experiments.
- 7) Testing different algal flow-way surface materials to evaluate the recommended material to enhance overall algal productivity for a larger flow-way system. If a larger flow-way system is constructed, additional cost-effective construction materials for the algal flow surface may be considered if those materials either have no effect on or enhance the total algal productivity. The 2018 algal flow-way included two 3-ft sections of roughened concrete – one bare and the other covered by the same low-profile nylon mesh – for comparison of algal biomass growth to the other sections of the flow-way. Both concrete sections were constructed within 100 ft of the surge system because higher algal growth rates were observed closer to the water source during previous flow-way operations.
- 8) Determining, if possible, the extent to which seasonal variability in water temperature influences total algal productivity.
- 9) Designing, constructing, and testing a sand filter to collect greenwater and to reduce turbidity in post-harvest water before discharge back to the Patapsco River.

1.4 Algal Flow-Way Harvests

Algal biomass was harvested from the flow-way weekly for the majority of the operating schedule (May – November), but when algal productivity rates decreased in November, harvests occurred on a biweekly basis (Table 1-1). Each week, the harvest process included the following:

- Ambient water quality data for the inflow water and the discharge water were collected at the top and bottom of the flow-way, including water temperature, pH, salinity, conductivity, and dissolved oxygen (Table B-1). In addition, starting in August, an inflow water sample was collected weekly to determine TN and TP concentrations. Data were downloaded from automated data loggers located at the top and bottom of the flow-way which recorded hourly water temperature and light intensity. The automatic data loggers were in use from April through September until they malfunctioned. Because only two months remained for the project, the data loggers were not replaced.

- All harvests were conducted as 'zero-flow harvests'. The inflow pump was turned off, and the flow-way was allowed to drain for approximately one hour prior to harvest.
- Once the flow-way was drained (no more visible water entering the sump), photographs were taken to document conditions.
- The outfall pipe from the sump area at the end of the flow-way was then blocked, and the algae were manually harvested by walking along the flow-way and pushing a squeegee attached to a broom handle from the top (near the surger) to the bottom (near the sump) of the flow-way. Harvested algal biomass was collected in the sump area.
- Samples were collected from the harvested biomass for analytical testing and for use in biomass handling/dewatering experiments (Section 3.1).
- Algae were vacuumed from the sump area at the bottom of the flow-way into a Vermeer vacuum truck, which was then driven to a scale and weighed. The wet weight of the harvest was calculated by subtracting the truck tare weight from the total weight. In cases where only a half harvest was collected by the vacuum truck, truck weights were multiplied by 2 to obtain the full harvest weight.
- Algae and water were then transferred from the Vermeer vacuum truck to decant tanks to feed the algal digester experiments (Attachment A).

**Table 1-1
2018 Dates of Algal Biomass Harvests**

Date
May 17 ¹ , 24 ¹ , 31
June 7, 14, 21, 28
July 18 ² , 26
August 2, 9, 16, 23, 30
September 6, 13, 20, 27
October 4, 12, 18, 25
November 1, 14, 29

Notes:

1. Samples from May 17 and May 24 arrived at the laboratory degraded due to shipping issues and therefore could not be analyzed.
2. An inflow pump failure over the July 4 holiday disrupted normal flow-way operations. Dried algal biomass was removed from the flow-way surface and the pump was replaced with a spare digester feed pump until repairs could be made. Once the pump was replaced, the algal flow-way operated for approximately two weeks to allow the algal community to reestablish and weekly harvests resumed on July 18, 2018.

Finding a consistent, cost efficient way to dewater the algal biomass harvested each week for the algal digester was a focus of the MARAD Phase 3 project. The initial dewatering plan included a dewatering pad and an evaporation bed, that were constructed and implemented as the primary methods for biomass dewatering. However, it was apparent early in the operations that neither the dewatering pad or the evaporation bed was a viable option for weekly management of the biomass produced (Section 3.1.1 and 3.1.2). An adaptive management strategy regarding the dewatering of the biomass was implemented. The team discussed, developed, implemented, and assessed multiple biomass dewatering options throughout the project. A summary of the dewatering methods evaluated during the 2018 project are summarized in Section 3.1. Successful dewatering strategies that are recommended for implementation in subsequent large-scale studies are discussed in detail in Section 5.2.

1.5 Nutrient Calculations

Throughout the project, harvested algal biomass samples were collected and tested for TN and TP concentrations to evaluate if the various dewatering methods tested had substantially different TN and TP removal efficiency.

1.5.1 Laboratory Analysis

Samples collected for the biomass handling portion of the MARAD Phase 3 project were analyzed by the TestAmerica laboratory in Pittsburgh, Pennsylvania. For the biogas production of the project, UMD conducted laboratory testing in-house (Attachment A).

Analytical testing of samples included:

- Percent solids (Standard Method (SM) 2540G) for biomass samples
- TN (SM 4500) for inflow water and biomass samples
- TP (SM 4500) for inflow water and biomass samples
- Total organic content (ASTM D2974) for biomass samples
- Total ash content (ASTM D2974) for biomass samples

As the project was adaptively managed to collect additional types of information needed to evaluate different biomass dewatering and handling techniques, additional analytical methods used to obtain data necessary to evaluate the success of each method were as follows:

- In August, the laboratory method selected for solids was changed from percent solids (%) to total solids (SM 2540B; on a volumetric basis; milligrams per liter) to be consistent with the analytical method employed for algal biomass analyses from past years (Yarberry 2018).

- In October, total suspended solids (SM 2540D) was added for water samples to measure solids recovered during the harvest and exclude dissolved solids present in the water that will be discharged or not recovered.

1.5.2 First Flush Samples

First flush samples are representative of the initial pulse of water that is released down the flow-way after harvest is completed and the inflow pump is turned back on. The process of harvesting algal biomass loosens solids (biomass and sediment) from the flow-way surface and a portion of that material is not collected as part of the manual harvest method. The first flush water rinses these solids from the flow-way surface.

First flush was evaluated to see if a downstream water management step was needed to reduce turbidity in discharge water. Options to manage water before direct discharge include a sand filter and/or a settling area (either an open-air pond or a decant tank). The samples from the first flush were used to evaluate the amount of biomass (including TN and TP) in these samples and to quantify the water volumes that would potentially be managed through a secondary process. Estimating the water volumes that may be sent to the sand filter and/or settling area will inform the design and sizing for a larger system. Some of the first flush samples were tested for TN and TP to evaluate how implementation of dewatering techniques may impact the quantity of TN and/or TP being removed by the algal flow-way.

Seven first flush samples were collected and analyzed for percent solids (May 31, September 6, September 13, September 20, September 27, October 4, and November 14). Two samples (September 20, and November 14) were analyzed for TN and TP. On September 27 and November 14, water samples were collected from first flush water every 30 seconds for 5 minutes to assess how total solids change over time.

From the time water flow was restored post-harvest, it took approximately 5 minutes for water to travel down the flow-way. Over the 5-minute flush period, turbidity during the first minute was substantially higher than the subsequent four minutes, and water clarity returned to normal less than 5 minutes of the flow being restored.

2 Algal Flow-Way Operations

The MARAD Phase 3 project was a pilot testing program with the goal of identifying the right combination of design elements and operational components that 1) maximize algal biomass productivity for the digester, 2) result in implementable options for large-scale construction, and 3) provide low-maintenance options for frequent reoccurring harvests. This section discusses the results of the design and operational modifications that were implemented during the MARAD Phase 3 project (Section 1.2)

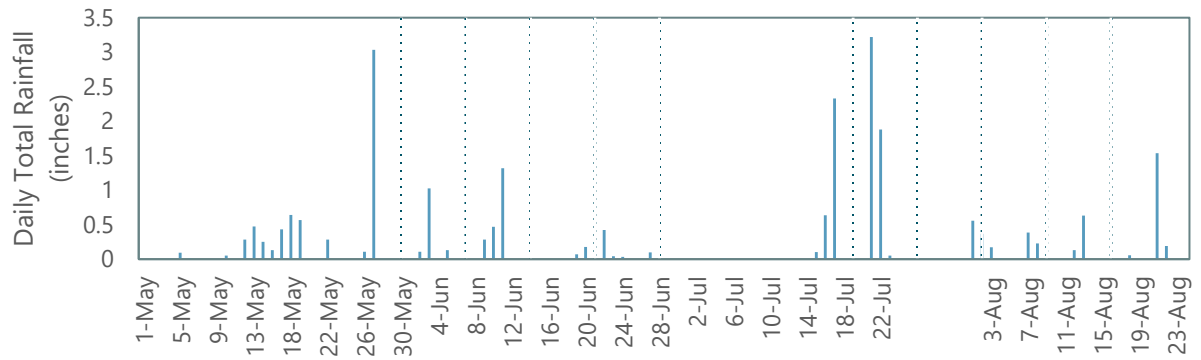
2.1 Environmental Conditions

It is important to note that algal growth is highly variable and susceptible to changes in a variety of ambient environmental conditions that cannot be controlled. Water temperature, light availability, and water quality conditions such as concentrations of available TN and TP and salinity are all important environmental conditions that influence algal growth and species composition, and these conditions are known to vary widely in the Patapsco River during planned flow-way operations (April to November). These environmental conditions were measured throughout the project testing program to provide information to interpret data and to evaluate if variability of one or more of these parameters impacted on algal growth. The intent of MARAD Phase 3 project was not to conduct a detailed study on algal biomass in response to environmental conditions, but to use environmental data as feasible to interpret data collected for algal biomass growth and total productivity.

Weather conditions in 2018 for the Baltimore region were unusual, as record-breaking precipitation occurred in the region. By the end of the year, Baltimore had received nearly 72 inches of precipitation, approximately twice the amount that occurs in a typical year. While not all of precipitation occurred during the testing period for the MARAD Phase 3 project, higher-than-normal amount of precipitation was recorded at DMT between April and November (Figure 2-1).

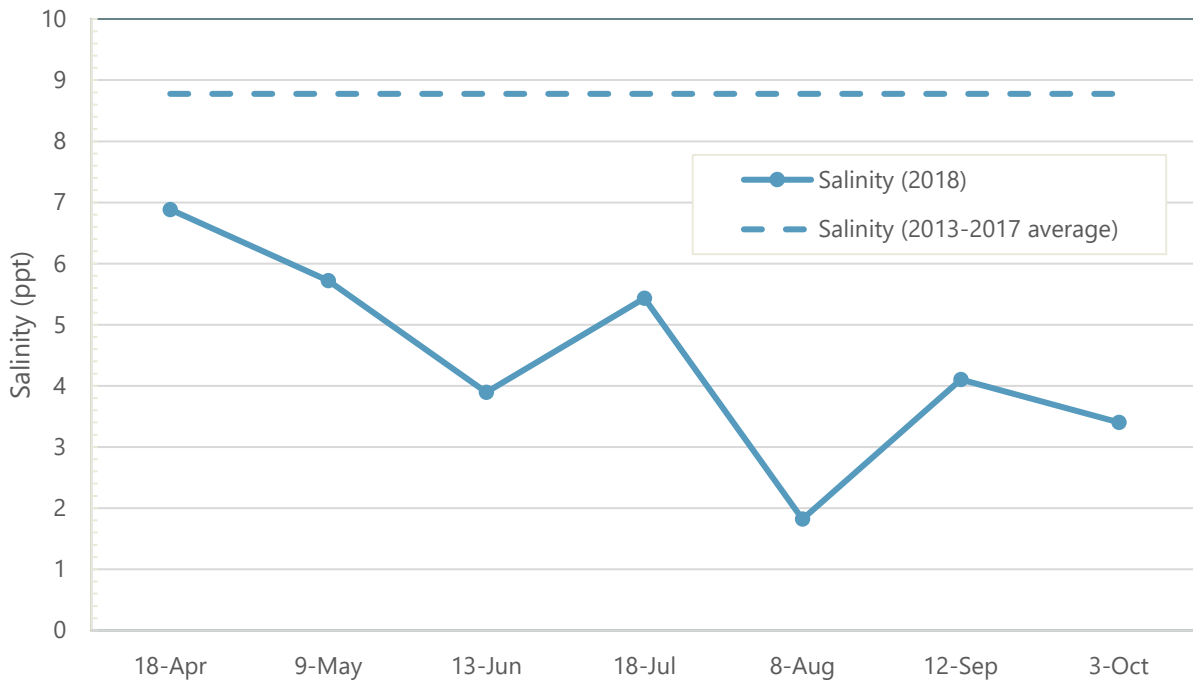
Overall, the unusually high precipitation in 2018 had at least two important influences on total algal growth along the flow-way. Cloudy, overcast conditions reduced the algae's daily light exposure and likely depressing total growth rates. More importantly, because of a near constant freshwater influx from storms and runoff, the salinity in the Patapsco River fell to oligohaline levels between 2 and 7 parts per thousand (ppt) (Figure 2-2), well below typical Patapsco River mesohaline levels of 9 to 12 ppt.

Figure 2-1
Daily Total Rainfall in 2018 at Dundalk Marine Terminal Weather Station



- Notes:
1. Historical Average Rainfall Per Day at Baltimore Washington International (BWI) Airport = 0.12 inches
 2. Data were unavailable for July 24 to July 31 and after August 24
 3. Dotted lines indicate dates of algal biomass harvests during the time period with rainfall data

Figure 2-2
Salinity in Baltimore Harbor in 2018

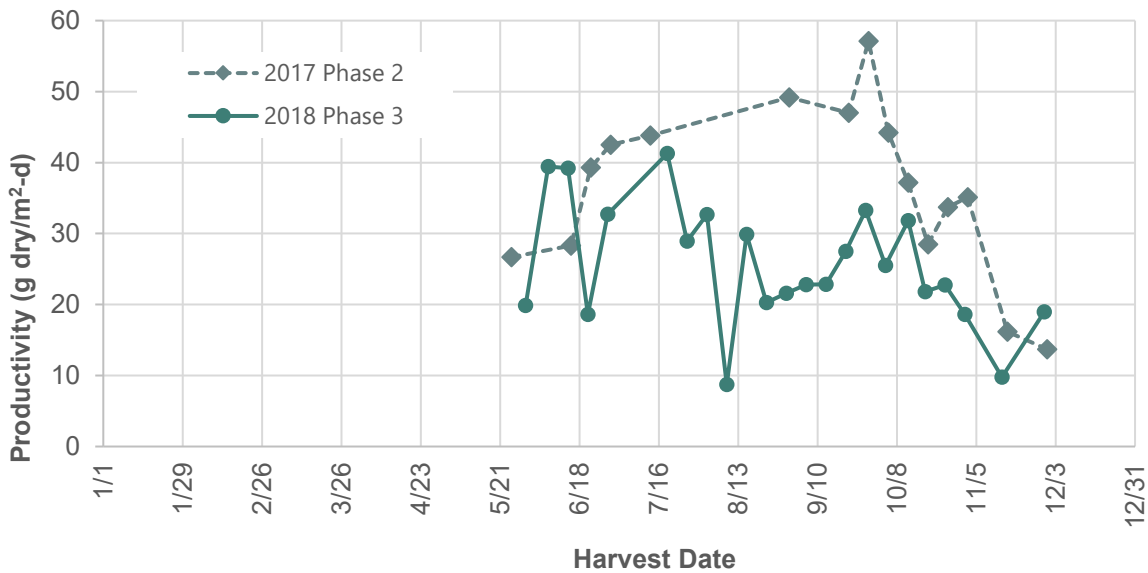


- Notes:
1. Data are for Mainstem B Station (BWB-PATMH-08) over the time period of flow-way operation.
 2. Data Source: Baltimore Harbor Water Alert (data available as of February 23, 2019)
- ppt: parts per thousand

For the flow-way, persistent lower-than-normal salinity conditions may have decreased overall algal biomass growth and influenced the algal community composition. In previous years, the start-up (April to early May) algal community was typically dominated by filamentous diatoms and by summer (usually mid-June), the community dominance shifted to filamentous green algae. Filamentous green algae provide more structure to the algal community on the flow-way, reducing sloughing during harvest and making biomass (solids) recovery during harvest more efficient. In 2018, the algal community was diatom-dominated for the entire project with limited filamentous green algae observed on the flow-way. Algal productivity was generally lower in 2018 compared to 2017 (Figure 2-3).

Therefore, the algal productivities achieved for the MARAD Phase 3 project likely represent conservative estimates of the potential algal productivity that could be achieved during operation of the flow-way. The low biomass productivity also made it difficult to quantify differences in the overall influence of some of the operational changes that were implemented for the project.

Figure 2-3
Algal Productivity from Algal Flow-Way at Dundalk Marine Terminal in 2017 and 2018



Note:
 Productivity was calculated based on algal biomass measured using the truck-weight measurement method.

2.2 Algal Flow-way Operational Changes in 2018

2.2.1 *Pump Relocation, Water Flow Rate and Biofouling*

Initially, the influence of the water flow rate on algal biomass and species dominance was to be tested by changing the flow rate every six weeks. Linear Hydraulic Loading Rate (LHLR) for the water flows were targeted at 12.5 gpm/lf (75 gpm) as the lower rate and 20 gpm/lf (120 gpm) as the higher rate.

During the 21-day start-up period from April 26 to May 17, the LHLR was 12 gpm/lf (72 gpm), essentially on target with the lower rate planned, and one harvest was collected during this time period (May 17). The LHLR was increased to 17.8 gpm/lf (107 gpm) for the 36-day period from May 17 to July 3, and six harvests were collected (May 24, May 31, June 7, June 14, June 21, and June 28). Following the inflow pump failure on July 3, flow to the system was restored on July 6 using a spare digester feed pump until repairs could be made to the inflow pump. The original inflow pump was reinstalled and operational on August 27. For the 146-day period from July 6 through November 29, the mean LHLR was 11.2 gpm/lf (67 gpm). Although the project team attempted to increase flow rate back to the 120 gpm design flow rate, the inflow pump never achieved the target high flow rate. The likely reason for the pumps' lower flow rate was because of biofouling on the intake screen. Biofouling was confirmed at the end of the season when the intake screen was pulled up for maintenance.

Therefore, for the 196-day period when the algal flow-way operated from May 17 to November 29, the LHLR on the flow-way was 12.7 gpm/lf (76 gpm) (Figure 2-4), achieving the target lower water flow rate for the project, but unable to maintain the higher flow rate. Comparisons of the influence of changes in water flow rate could not be completed because the project rarely achieved water flow rates different enough for a long enough period of time to attribute any observed differences in algal biomass to changes in flow rate.

In previous years of flow-way operation, a similar pattern of progressive reductions in LHLR occurred (Figure 2-5). Biofouling of the intake structure was noted as a potential challenge for the MARAD Phase 3 project, and although modifications to the intake were implemented for 2018 (Section 1.2), the result was similar. Because other algal flow-way sites have demonstrated that algal biomass production increases with higher LHLRs (M. Zivojnovich, personal communication), additional options to reduce the impact of biofouling will be considered for future project implementation.

Figure 2-4
Water Inflow Linear Hydraulic Loading Rate (LHLR)

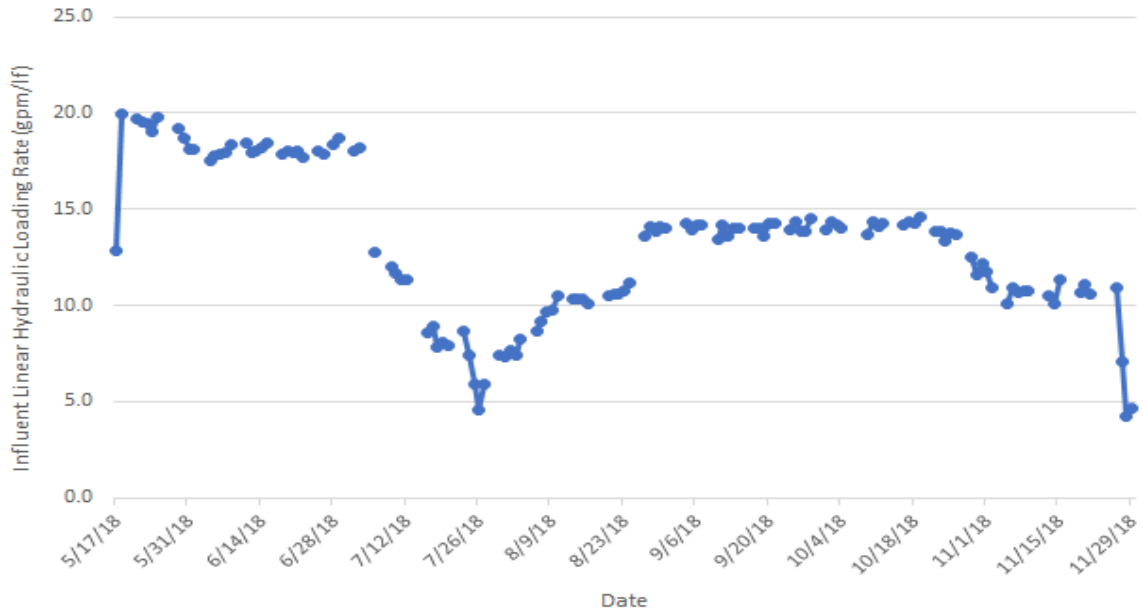
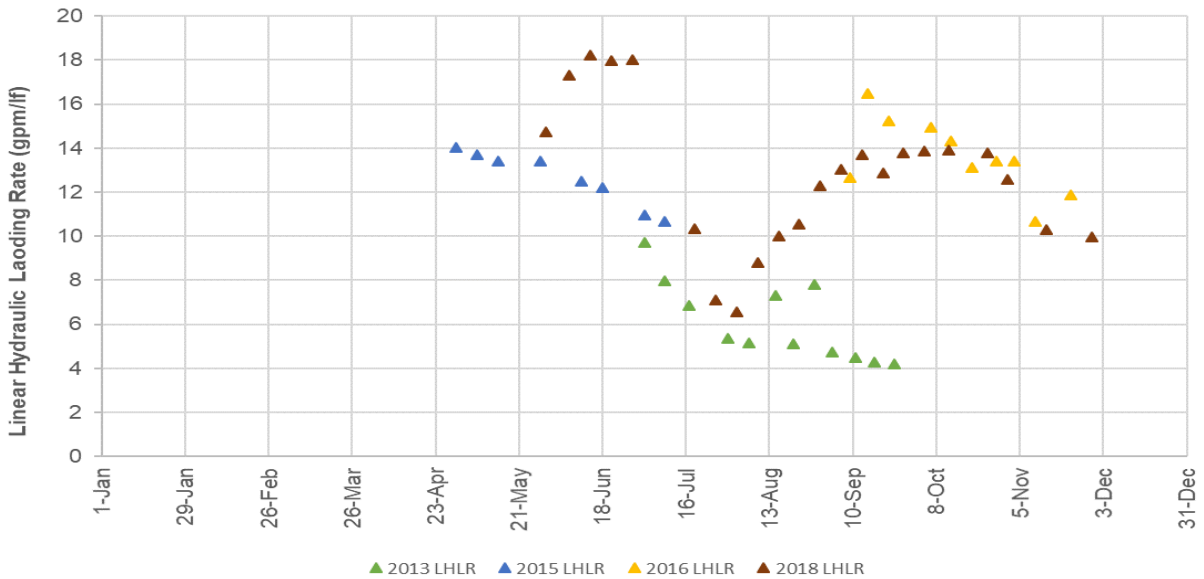


Figure 2-5
Linear Hydraulic Loading Rate (LHLR) for Algal Flow-way Operations



2.2.2 Self-Siphoning Surge System

Utilization of the self-siphoning surge system was successful, performing well throughout the project, with minimal biofouling and almost no maintenance during operations. The surge system allowed for larger water pulses to occur at a predictable frequency, as determined by the flow rate of the inflow pump.

Previous years of surge system testing at DMT flow-ways and experience at other algal flow-way sites have indicated (by observation) that algal growth is stimulated by pulses of water as compared to continuous flow operations. The original intent of the MARAD Phase 3 project was to evaluate if varying the rate of pulsing had a measurable impact on algal biomass along the length of the flow. For example, stronger, more frequent pulses of water that would result from an increased LHLR could create conditions for higher algal biomass growth along a longer section of the flow-way for an extended period, with the total impact being a higher biomass recovery during harvest. However, the impact of biofouling on the LHLR for the project (Section 2.2.1) meant that the inflow pump never achieved the target high LHLR, and therefore, a comparison of changes to algal biomass could not be completed.

2.2.3 Surface Material of the Flow-Way

The flow-way constructed at DMT consisted of an asphalt surface covered with an ethylene propylene diene terpolymer (EPDM) geomembrane liner that was overlain by a flexible low-profile nylon screen. The flow-way was manually harvested by pushing a squeegee over the surface by hand. Often, multiple passes over the length of the flow-way were conducted to maximize removal of algae. Manual harvests of the flow-way would be impractical for a large-scale system. For the utility-scale algal flow-way systems operated to date, harvests are conducted mechanically by running a small tractor fitted with a rubber blade over the flow-way surface. Other algal flow-way systems have employed both geomembrane with nylon screen and roughened concrete. Using this method, large flow-ways are harvested quickly and more efficiently.

For the MARAD Phase 3 project, two 3-foot sections of roughened concrete were added to the flow-way surface (Figure 2-6). One of the roughened concrete sections was left bare and the other was overlain by the same flexible low-profile nylon screen that was used on the remaining portions of the geomembrane lined flow-way (Figure 2-7). The nylon screen may create challenges for a large-scale harvest, but there was interest in attempting to quantify if providing the screen as an attachment surface substantially increased algal biomass productivity.

Algal growth varies along the length of the flow-way, with higher biomass at the top of the flow-way near the water inflow. Therefore, both concrete sections were constructed in the upper third of the flow-way to increase the likelihood that differences, if any, in algal biomass between the sections could be differentiated.

The approximate distances from the upstream end of the flow-way were as follows:

- Geomembrane liner with nylon screen: 0 to 37 ft
- Concrete with nylon screen (or grid): 37 to 40 ft
- Geomembrane liner with nylon screen: 40 to 50 ft
- Bare concrete: 50 to 53 ft
- Geomembrane liner with nylon screen: 53 to 206 ft

Throughout the operation of the flow-way, algal productivity for the roughened concrete sections was observed to be persistently lower compared to the sections with geomembrane and screen. This observation was noted regardless of LHLR, water temperature, or time of year.

Samples from the roughened concrete surfaces were collected four times, on May 31, August 23, October 12 and November 29, and analyzed for total solids. TN and TP were analyzed in the samples collected on May 31, October 12, and November 29 (Table C-4). There were too few data points collected to make a definitive conclusion and the limited algal species community observed in 2018 (diatom-dominated) limited the applicability of the results. Using roughened concrete as a surface may be a feasible option, but additional testing would be required before changing the algal flow-way surface to concrete-only.

2.2.4 Sand Filter

Design, installation and testing of a sand filter was implemented as an operational mode to recover fine algal solids (first flush water) in conjunction with scheduled harvests before flow-way harvest water is discharged to the Patapsco River. Sand filter operations do not influence overall algal biomass productivity. Testing of the sand filter was completed in conjunction with other biomass dewatering methods to test the effectiveness of options that could be implemented in sequence as part of an overall system. Therefore, results of the sand filter are discussed in Section 5.2.3.

Figure 2-6
Algal Flow-Way Design for Phase 3 Project

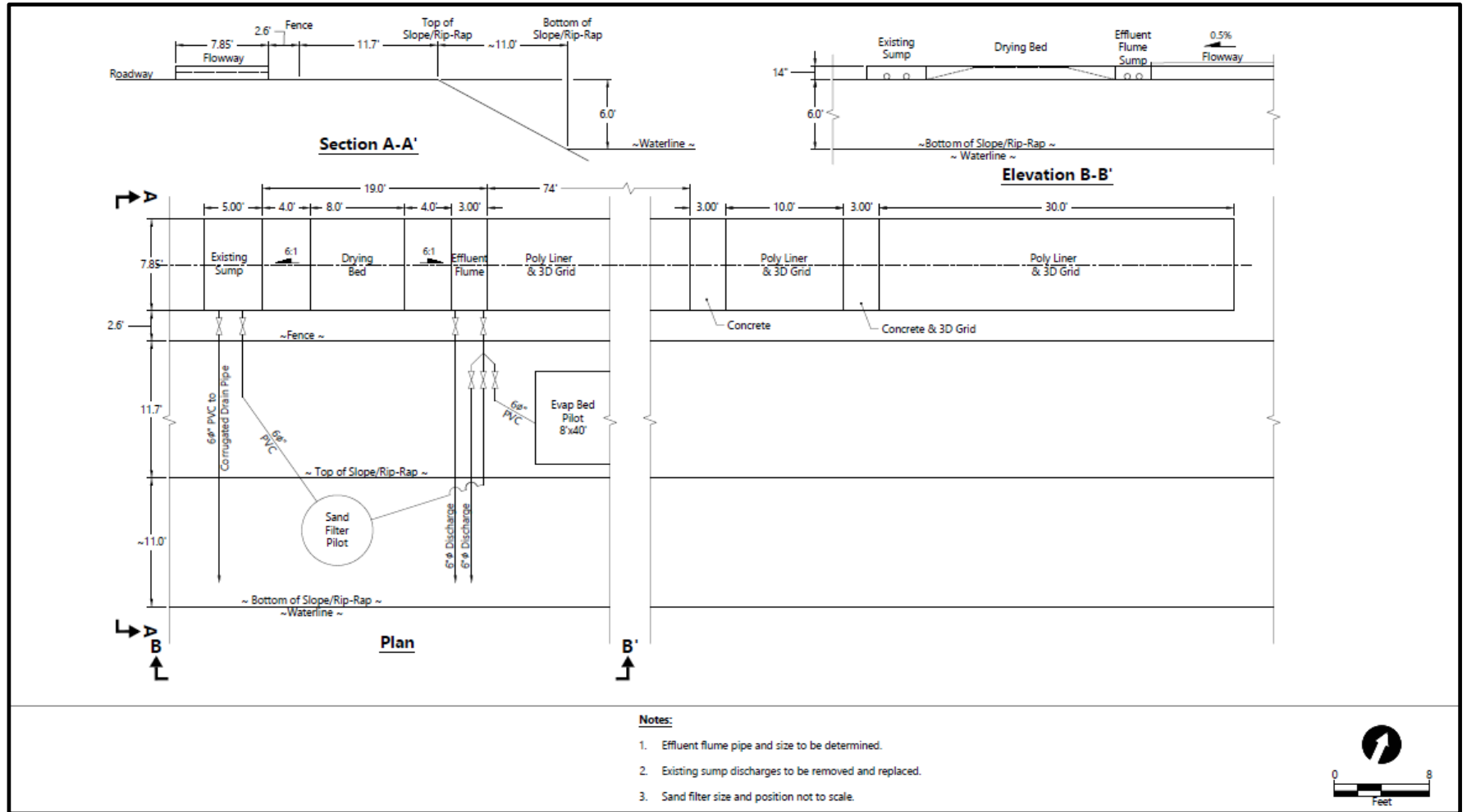


Figure 2-7
Two Algal Flow-way Sections with Roughened Concrete Surface



3 Biomass Recovery and Algae Dewatering Methods

One of the most important components of the MARAD Phase 3 project was determining an effective and time-efficient method for recovering and dewatering the harvested algal biomass to a consistency that could be easily (preferable mechanically) handled and transported off-site. Additionally, the dewatering portion of the project is important in determining when in the overall harvest process samples should be collected for TN and TP analysis for nutrient reduction calculations.

**Table 3-1
Dates for Testing of Dewatering Methods**

Harvest Date	Hanging Bag	Merit Tile	Wedge Wire Screen	Perpendicular Harvest	Sand Filter	Drying Subplots	Desktop Settling Test
Aug 2	X (series)						
Aug 23	X (parallel)	X					
Aug 30		X					
Sept 6		X					
Sept 13		X		X			
Sept 20		X					
Sept 27		X			X		
Oct 4		X			X		
Oct 12		X	X (field trials)		X		
Oct 18			X	X	X	X (no lab analysis)	
Oct 25			X	X	X	X	
Nov 1							
Nov 14			X	X	X	X	
Nov 27			X		X		X

Notes:

The evaporation bed was tested on May 31, June 7, and June 28. The dewatering pad was tested on May 31, June 7, and June 14. Both methods were discontinued after June because they did not function as intended.

Initially, a dewatering pad and an evaporation bed were constructed and tested as potential dewatering methods for harvested solids. The dewatering pad was designed for primary recovery of filamentous green algae prior to secondary recovery through the sand filter. As filamentous diatoms dominated throughout the year, the dewatering pad was not suitable. The evaporation bed employed in previous flow-way operations was tested and unable to adequately dewater the biomass without gravity drainage of free water. Through the adaptive management approach, the

dewatering bed concept was re-evaluated in conjunction with perpendicular harvest of the flow-way and a central harvest channel designed to function as a dewatering surface.

Over the course of the project, nine dewatering methods were discussed, several were tested either individually or in combination with other dewatering methods, and ultimately a combination of dewatering methods was the most effective (Table 3-1). Dewatering methods that are recommended for implementation and/or further study or both are discussed in more detail in Section 5.2.

3.1 Biomass Dewatering Methods

3.1.1 *Evaporation Bed*

The evaporation bed was constructed to allow for passive air drying of harvest biomass material. The evaporation bed was approximately 8 ft by 40 ft and sized to be able to stockpile a portion of the biomass from multiple weekly harvest events, with the intent that the biomass would be removed from the evaporation bed at the end of one month.

The evaporation bed at DMT was constructed adjacent to the flow-way, outside the fence line (Figures 3-1 and A-1). For weekly harvests in May and early June, a portion of the weekly harvest was directed through pipes from the flow-way sump area to the evaporation bed for drying. Initially, the weekly influx of additional harvest material re-wetted any biomass that started drying out. The weekly re-wetting of the material combined with high humidity and multiple rain events meant that the biomass never dried. Instead, the evaporation bed maintained a pool of standing water and none of biomass in the evaporation bed ever dried to the point of being able to be effectively handled. In addition, the site conditions resulted in the growth of a secondary algal bloom within the evaporation bed, and subsequent testing indicated that a portion of the algal growing within the evaporation bed included species that could potentially be toxic if allowed to flourish. Because the evaporation bed did not function as intended, its use was discontinued in June.

3.1.2 *Dewatering Pad*

A dewatering pad was constructed in the flow-way sump area that consisted of a slightly elevated concrete surface with inclined sides (Figure 3-2 and A-2). As initially conceived, algal biomass would be manually pushed up the incline to the top of the dewatering pad, and water would passively drain into the sump over several days, then the biomass would be collected.

The dewatering pad was tested in May and June. Because the algal community was dominated by filamentous diatoms, the weekly harvest material was typically mostly water and the filamentous diatoms did not have sufficient structure to remain on the concrete pad to passively dewater. Instead, the diatoms (and the rest of the biomass) immediately flowed off the dewatering pad and

**Figure 3-1
Evaporation Bed**



**Figure 3-2
Dewatering Pad**



back into the sump. Because the dewatering pad configuration was not suitable for the harvested biomass, its use was discontinued in mid-June. Because of the algal species that dominate the flow-way – filamentous diatoms and filamentous green algae - it is not anticipated that a dewatering pad will be an effective dewatering method for algal flow-ways using water from the Patapsco River.

3.1.3 *Hanging Bag*

Because the harvest material observed each week was mostly water and the dominant algae (filamentous diatoms) were small, a first stage biomass recovery system was needed to remove the biomass prior to the sand filter. The solids in the harvest material included algae and sediment, so the initial biomass recovery stage needed to include a mesh, filter fabric, or sieve material that could more effectively separate biomass from the sediment. Testing was conducted to identify a target pore size for potential screening material that could be effective in retaining the majority of the algae in each harvest.

Hanging bag tests were implemented to identify the size fraction of the solids present in the weekly harvest. The tests used filter fabric with variable pore sizes (600 micron (μm), 200 μm , 100 μm , 75 μm , and 25 μm) to separate the material of known size fractions. The filter fabric was shaped into bags, which were hung up and allowed to passively dewater after being filled with harvest material (Figure 3-3). The material retained in each filter material and the material that passed through the filter fabric were both retained and analyzed for percent moisture, percent solids, total solids, ash, total organic matter, nitrogen, and phosphorus.

Two rounds of hanging bag testing were completed:

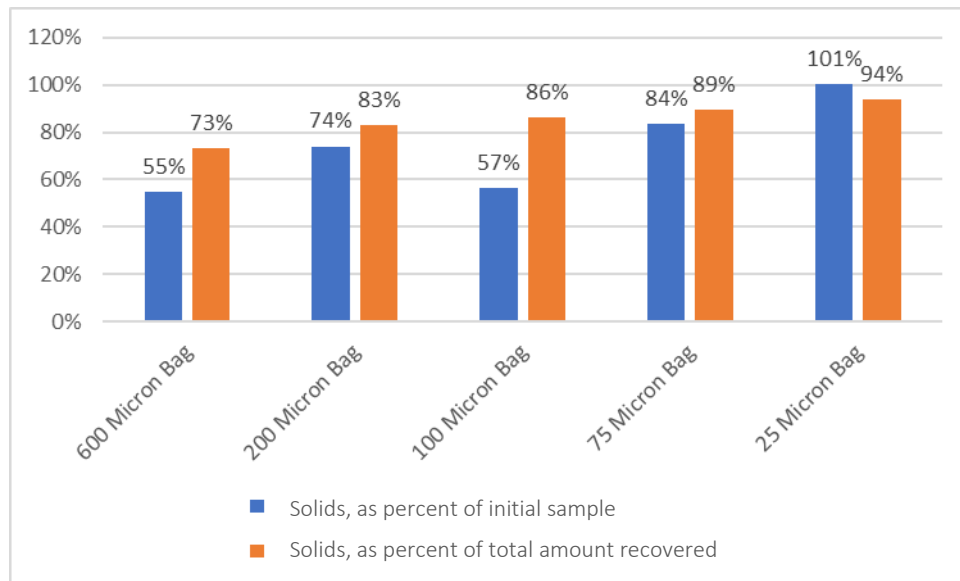
- **Series tests:** Whole harvest material is introduced into the bag with the largest pore size (600 μm) and allowed to passively dewater for 10 minutes or until the filtration was completed, whichever was longer. Material that passed through the 600 μm hanging bag was collected and then introduced into the bag of the next pore size in the series, 200 μm . This procedure was completed for each pore size in the series, until the smallest pore size (25 μm) was completed (Appendix A, Figure A-3).
- **Parallel tests:** Whole harvest material was introduced directly into a bag of each filter size and allowed to passively dewater (Appendix A, Figure A-4).

Based on the parallel tests, filtering the harvest with a screen size from 200 to 600 μm recovered between 55% to 83% of the harvested solids (Figure 3-3).

**Figure 3-3
Hanging Bag Testing**



**Figure 3-3
Solids Retained During Parallel Hanging Bags Tests**



3.1.4 Merit Tile

Once the hanging bag tests identified the target pore size of media that could be implemented for dewatering, Merit Filter Media was identified as one potential dewatering option. Merit Filter Media is a tile-like dewatering system made of polyurethane with 381- μm openings (Appendix A, Figure A-5). Tiles are approximately 1 square ft in size and could be combined together to create a large area with a hard surface that functions as a filter. The technology is used for the dewatering of polymer treated biosolids in wastewater, and the system is designed to allow for recovery of dewatered solids using a tractor mounted bucket.

Merit tile testing focused on evaluating the filter efficiency, as measured by hydraulic loading rate and solids loading rate of the tiles. Two assemblies were constructed using a single tile, and harvest material was loaded inside and allowed to passively dewater through the tile (Figure 3-4). Several rounds of testing were completed using the Merit tile, including slowly adding harvest material in aliquots, adding large quantities of harvest material at one time, allowing the harvest material to drain for prescribed time periods (up to 48 hours), and allowing for long-term dewatering (up to one week).

Figure 3-4
Merit Tile Testing



Results from field testing were limited by the use of a single tile to represent a larger-scale system. The tile generally performed best when algal harvest material was loaded slowly onto one half of the tile while maintaining a clear area on the tile surface for water to separate from the algal solids and drain quickly. Once the tile was covered by solid material, the dewatering rate decreased substantially. As dewatering slowed, the tiles also clogged quickly with dried algae underneath which further prevented draining. Overall, the Merit tiles were abandoned as an effective large-scale dewatering method because the pore size was too small to allow for initial dewatering before getting clogged and maintenance to prevent the tiles from clogging underneath was an expected concern.

One of the important conclusions from the Merit tile testing was that recovery of harvest material for the DMT flow-way was possible using a first stage method that separated the solids (algae and sediment) from the water and then two-step dewatering process to effectively capture the algal biomass and dewater it to a consistency that can be easily handled.

3.1.5 *Wedge Wire Screen*

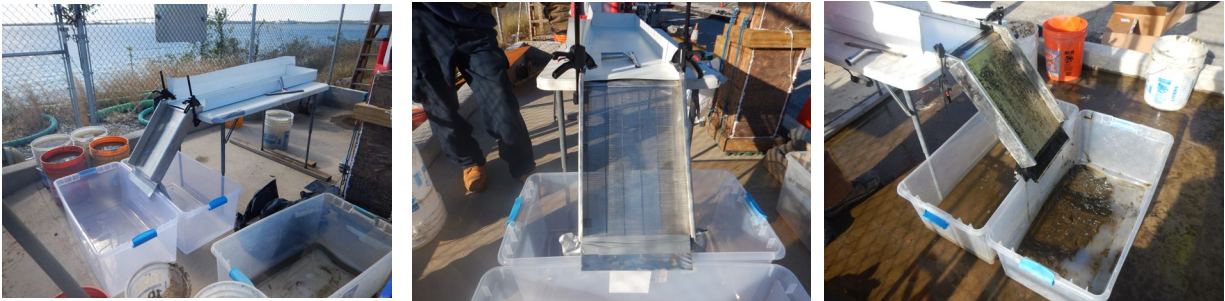
Another technology tested to separate the solids from the water was a wedge wire screen. A wedge wire screen is a slotted and welded self-cleaning screen used for in-line filtration in systems that have constant water flows. Wedge wire screen tests were conducted to quantify performance and inform design options as to inclusion of a wedge wire screen as the first stage method to separate the solids (algae and sediment) from the water. It should be noted that wedge wire screens are used on all HydroMentia pilot systems as a means of recovering sloughed solids greater than 500 μm . for solids recovery either in coordination with 1) a parallel-to-flow harvest and effluent flume design or 2) a perpendicular harvest with central channel/dewatering bed design as discussed in Section 3.1.6.

In August, harvested algal biomass was delivered to Kason Corporation in New Jersey for preliminary external testing using a wedge wire screen to evaluate if using a wedge wire screen to dewater harvest material was a feasible option. Initial testing using a Kason model CF2430SS, 24" wide x 30" long Cross Flo Static Sieve equipped with a 0.03" (762 μm) effectively separated the harvest material, into approximately 21% wet solids and 79% liquid, indicating that the wedge wire screen could be effective as a first-stage separation method and that field testing was warranted. In October, on-site field testing was initiated with a 4-foot long wedge wire screen flume, with a 12" wide by 12" long 500- μm wedge wire as manufactured by HydroScreen installed at approximately a 45-degree incline.

Multiple rounds of tests were conducted with the wedge wire screen in October and November by running harvest material, including full harvest material and harvest fractions that had been allowed to separate (pushed solids) over the screen (Figure 3-5 and A-6). The percent solids of the harvested material introduced to the wedge wire screen was approximately 3%. The 500- μm field wedge wire screen tests produced a recovered algal material that was about 8 to 10% solids with approximately 52% of the total solids separated from the liquid fraction. Results of the wedge wire screen testing were generally consistent with the percentage of solids retained in the 600 μm hanging bag test. The shorter length of the HydroScreen when compared to the Kason wedge wire screen likely resulted in relatively slightly lower solids recovery numbers in the field tests.

As confirmed through testing, the wedge wire screen allows for simple recovery of solids and may be implemented as part of the biomass handling procedures for future algal flow-way designs (Section 3.2).

Figure 3-5
Wedge Wire Screen Testing



3.1.6 *Perpendicular Harvest + Side Channel*

Harvests were conducted by manually pushing a squeegee downgradient along the surface of the flow-way starting at the surge and ending at the sump. Testing with the Merit tiles and wedge wire screens demonstrated that both methods would be most effective if the amount of water passing over the tile or screen could be decreased. To accomplish this, the harvest strategy was modified to a perpendicular harvest + side channel approach, which involved pushing the harvest material perpendicular to the direction of water flow into a side dewatering channel (Figure 3-6 and Appendix A, Figure A-7). The side channel was temporarily isolated and allowed to drain into the sump.

Figure 3-6
Perpendicular Harvest and Side Channel



The perpendicular harvest was completed manually in two passes. The first pass pushed the majority of the harvest material to the side channel, and the material was allowed to gravity drain for about 10 minutes. Then a second pass was completed along the length of the flow-way to ensure a complete harvest. After draining for another 30 minutes, the water that drained to the sump area ('free water') was collected and analyzed for total solids. The remaining material in the side channel

('pushed solids') was then pushed down to the flow-way sump area, and collected separately analyzed for total solids.

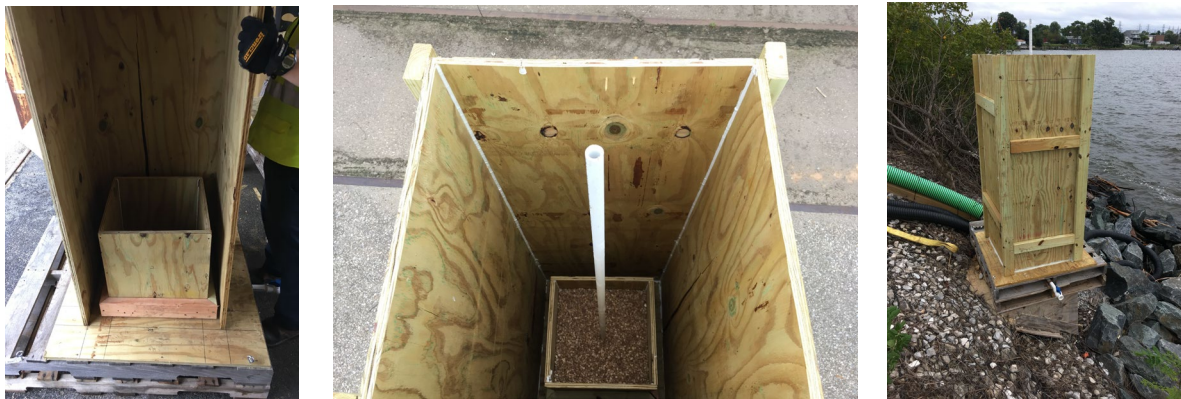
Total solids in the typical harvest dominated by filamentous diatoms was approximately 3 to 4% solids. During the perpendicular harvest testing, the dewatered harvest material ranged from 3% to 6% solids and the water that drained was 0.5 to 1% solids. Based on this separation achieved during the perpendicular harvest, the dewatered material included between 84% to 94% solids and the water fraction contained between 6% to 16% solids. The testing conducted indicated that this perpendicular harvest + side channel approach may be an effective first stage solid recovery and dewatering method.

A side channel was used in the MARAD Phase 3 project because it was easily implementable, given the constraints of the flow-way constructed for the 2018 testing. However, a central dewatering channel may also be an effective approach for the larger flow-way. Either option would include another technology to separate the solids before the sump area. For the last few weeks of the harvest testing, harvest material collected using a perpendicular harvest was then passed over the 500- μ m wedge wire screen to quantify additional solids recovery Appendix C, Tables C-15 through C-20).

3.1.7 *Sand Filter*

After harvest material was processed using the perpendicular harvest + side channel approach (first stage) followed by the wedge wire screen (second stage), the remaining liquid fraction still contained visible solids (a combination of biomass and sediment). To further separate the solids and decrease the turbidity of discharge water below discharge standards, a sand filter was used. To test sand filter operation, a sand filter assembly was designed and constructed on-site in October (Figure 3-7 and Appendix A, Figure A-8). The sand filter was used to treat harvest water that had already been processed through other dewatering methods, such as the Merit tile and wedge wire screen.

Figure 3-7
Sand Filter Testing



Over two months, the sand filter was loaded with about 138 gallons ranging in total solids from about 0.5% to 4.0%. After the first two weeks of operation, incoming TSS ranged from 450 to 28,000 milligrams per liter (mg/L) and outgoing TSS was 12 to 130 mg/L. Turbidity meter readings of the sand filter effluent were typically less than 50 nephelometric turbidity units (NTU) and as low as 2 to 10 NTU, well below the typical discharge limit of 150 NTU above background in the receiving surface water after mixing.

The solids retained on the sand filter were collected twice (November 1 and November 29) and analyzed for total solids and for TN and TP to investigate the composition of the solid material. There were not enough samples collected to produce a reliable estimate on overall proportions, but the testing showed that the material in the samples was predominantly sediment and salts, and the portion of algal biomass was low.

Overall, the sand filter was an effective third step in separating the solid material from the harvest from the water. To effectively implement a sand filter as part of an algal flow-way, maximizing the separation effectiveness of the previous two steps (perpendicular harvest and wedge wire screen) to minimize the long-term loading to the sand filter.

3.1.8 *Small-Scale Dewatering Tests*

As the 2018 dewatering tests progressed, several additional small-scale informal dewatering tests were conducted on-site to evaluate the behavior of the harvest material.

3.1.8.1 **Subplots of Dried Material**

During October and November, a mock test area was set-up on a concrete pad to observe the natural drying of algae harvest material over one or two weeks to simulate the behavior of harvested

solids in a side or central dewatering channel. Two subplots were created and allowed to air dry. One subplot was representative of the solids retained the side channel after the perpendicular harvest and other subplot was representative of the solids retained on the wedge wire screen.

Percent solids increased from approximately 6% to 20% solids over 7 days and from approximately 3% to 24% over 15 days. Based on these limited findings, passive dewatering via evaporation while the harvest material is in a side or central dewatering channel may substantially increase the percent solids of biomass and improve overall handling efficiency.

Nutrient content analysis was performed during the drying tests to assess the impact of passive air drying on nutrient concentrations. TN analyses were conducted for the dried material from the side or central dewatering channel and TN decreased by 48%. For the dried material from the wedge wire screen, the TN concentration increased by 62%. These widely variable results were inconclusive, and additional testing would be needed to fully assess the impact of drying on TN concentrations.

3.1.8.2 Settling Test

During testing throughout 2018, it was observed that if the harvest material was allowed to settle, a substantial amount of separation was achieved in a short period of time (over several hours). Settling was considered as a separation method in earlier testing, but because of the small particle size of the filamentous diatom-dominated algal biomass harvest a method to capture and recover fine solids more frequently supported the recommendation of the sand filter. However, based on the rapid settling of solids as observed, a settling test was recommended to better understand solids settling behavior.

Two samples of harvest material, one representative of the water outflow from the dewatering channel and other representative of the material that passed through the wedge wire screen were collected from the last harvest on November 29, 2018. These samples were placed in 0.95 L jars, placed on a tabletop indoors, and passive settling was monitored for a 6-day period (Figure 3-8). The settling jars were sealed, and the solids turned black after approximately 74 hours, likely from degradation of the biological material, impacting the results of the test. Turbidity was measured in the sample jars multiple times per day over the 6-day monitoring period to evaluate water clarity via gravity settling (Figures A-9 and A-10). At 24 hours, turbidity levels at the surface decreased to approximately 600 NTUs and in 50 hours to approximately 200 NTUs.

Figure 3-8
Wedge Wire Screen Effluent After 24 Hours of Settling



3.2 Recommended Algal Solids Recovery and Dewatering Method

Because harvest material for the flow-way was comprised predominantly of small filamentous diatoms that break apart during harvest and fine-grained silts suspended in the water, a multi-step dewatering process was required to effectively capture and dewater biomass for efficient on-site handling. Based on the results of the MARAD Phase 3 project, the following multi-step process is recommended for harvest material dewatering and biomass recovery:

1. Perpendicular harvest + side or central dewatering channel
2. Wedge wire screen for material that flows freely from the dewatering channel
3. Sand filter (with a weir discharge option) as a final solids retention step

The effluent flume at the end of the algal flow-way remains a component of the system design and therefore the option to harvest parallel to the flow path will remain.

4 Algal Digester Testing

The MARAD Phase 3 project included experiments to determine the effectiveness of an anaerobic digestion (AD) system capable of producing renewable energy from the algae harvested from the algal flow-way. Batch-scale experiments in Phase 1 concluded that anaerobic digestion of the harvested algae could successfully produce biogas and support the design of a system for collecting the expected biogas production. In Phase 2, the process was scaled up to a pilot-scale AD unit, which was installed at DMT in 2017. The pilot system consisted of three digesters in series. Digesters 1 and 2 (D1 and D2) each had an effective digestion capacity of 1,700 liters (L), and Digester 3 (D3) had a capacity of 500 L. For Phase 2 testing, the three digesters were connected in series and operated as a single continuous unit. Results from the Phase 2 testing indicated that the overall hydraulic retention time (HRT) for the algae digestion system was high and that running the system as a single sequence connected in series limited the potential for collecting replicate data.

For the Phase 3 project, the pilot-scale AD system was modified to improve the anaerobic digestion process and increase methane output. To achieve replicability within the system, D1 was disconnected from the other digesters and operated as its own system. Digesters D2 and D3 remained connected and were operated in series as a second system. The D1 system was run in parallel with the D2+D3 system, providing replicate data and testing the effect of two HRTs on the production of methane-enriched biogas. Results of the Phase 3 algal digester operations are summarized below and detailed in Attachment A.

4.1 Algal Digester Operation

Phase 3 operations for the algal digesters were conducted from July 23, 2018 through November 21, 2018 (18 weeks). Manure inoculum was loaded into the system on July 23, 2018, followed by the first algal addition on July 25, 2018. Harvested algal biomass was added to the digesters according to the following schedule:

- Algal harvest was pumped into the AD decant tank every Thursday
- Digesters were fed algae according to schedule in Table 4-1
- Digesters were sampled Monday, Wednesday, and Friday until September 7, 2018, and then Wednesday and Friday until digester shutdown on November 12, 2018
- Laboratory analysis of biogas, algal influent, and AD effluent samples was conducted on a weekly basis

A new heating system was installed in D1 and D2 to provide external heat so the system would not solely rely on ambient air temperatures and could continue in the fall and winter once air temperatures started to drop. Construction on the new recirculating heating system was performed in July 2019, but delivery delay for required components delayed operation of the heating system

until October 2018. Start-up tests to maintain optimal algal digester temperature of 80-100°F were successful and the heating system was initiated, but the pumps used to recirculate the digestate were too strong and an excessive draw-down of the digester fluid occurred creating a vacuum within D1 and D2 that nearly led to digester rupture via inflation. Emergency shut-down procedures were implemented and the digester headspace gas was evacuated, but the loss of an anaerobic environment destabilized the two digesters for the remainder of the study. While the start-up tests showed that a heating system may be successful to maintain digester operations year-round, a new design is required to maintain safe operations and to maintain a stable digestion temperature.

During Phase 3 operation the supply of algae to feed the digesters was lower than planned because the volume of algae harvested from the algal flow-way was dominated by filamentous diatoms (Section 2.1). Overall, the algal biomass produced by the flow-way was approximately 30% lower than the biomass that was produced during the Phase 2 testing.

**Table 4-1
Quantity of Algae Fed to the Digesters**

Week	Feeding Schedule	Digester 1 Feed (liters)	Digester 2 + 3 Feed (liters)	Total Feed (liters)	Hydraulic Retention Time of Digester 1 (days)	Hydraulic Retention Time of Digester 2+3 (days)
1	W-F	568	568	1,136	21.0	27.1
2	M-W-F	386	371	757	30.8	41.5
3	M-W-F	308	312	620	38.6	49.4
4	M-W-F	293	292	585	40.6	52.8
5	M-W-F	166	189	355	71.7	81.3
6	M-F	198	196	394	60.0	78.7
7	Tu-F	265	248	513	44.8	62.1
8	M-W-F	187	161	349	63.5	95.5
9	M-W-F	185	207	392	64.4	74.3
10	M-W-F	284	284	568	41.9	54.2
11	M-W-F	259	259	517	46.0	59.6
12	M-W-F	206	206	411	57.9	74.9
13	M-W-F	163	166	329	73.0	92.8
14	M-F	146	148	294	81.3	104.0
15	M-W-F	198	169	366	60.2	91.3
16	M-F	52	52	105	227.0	293.8
17	F	291	291	582	40.9	52.9
Total	--	4,156	4,119	8,275	1,060	1,390
Average	--	244	242	487	62.6	81.5

4.2 Biogas Production

Stable digester operations were maintained for 13 weeks, from July 25 through October 19, 2018. During this period, D1 and the D2-D3 system produced 1,840 and 2,461 L of biogas consisting of 1,290 and 1,620 L of methane, respectively (Figures 4-1 through 4-3). Overall, there was an average methane production of 107 ± 20 L methane per week for D1 and 135 ± 19 L methane per week for the D2-D3 system.

Chemical composition of biogas in digester headspace was measured during each day of feeding using a Landtec Biogas 5000+ gas meter via a sampling port connected to the top of each digester bag's gas removal system. Measurements were averaged on a weekly basis to determine the mean percent composition of four primary gas components, methane, carbon dioxide (CO₂), oxygen (O₂), and balance gas (N₂), in each digester during each week of study (Table 4-2).

Table 4-2
Biogas Production and Composition, Weeks 1-13

Source	Total Biogas (L)	Methane (%)	Carbon Dioxide (%)	Oxygen (%)	Nitrogen (%)
D1	1840	73.0 ± 1.57	16.7 ± 0.45	0.25 ± 0.05	10.2 ± 1.69
D2	1781	68.9 ± 3.42	16.7 ± 0.45	0.34 ± 0.15	14.1 ± 3.6
D3	680	69.2 ± 2.81	13.5 ± 0.48	0.20 ± 0.01	17.2 ± 3.11

Notes:

Data from Weeks 14-18 omitted due to instability in D1 and D2 starting in Week 14

The percentage of methane in the digester headspace gas rose steadily in all three digesters during the startup period in Weeks 1 through 3. Production remained steady between, with 70-80% methane in the biogas of Digesters 1 and 2 until the system malfunction in Week 14 (Section 4.1). The heating and recirculation systems were completely shut down during Week 15, and the composition of the headspace gas began returning to expected levels of methane.

Digester 3 was unaffected by the system malfunction because it was being run as a separate system. Digester 3 maintained biogas production throughout the study at 70-80% methane, except for a small decrease in percent methane in Week 8 due to a leak.

Similar to the results observed in Phase 2, the concentration of methane measured during optimal digester operations in Phase 3 testing was greater than the methane concentrations that were predicted in the Phase 1 experiments.

Figure 4-1
Total Biogas Production from Algal Digestion

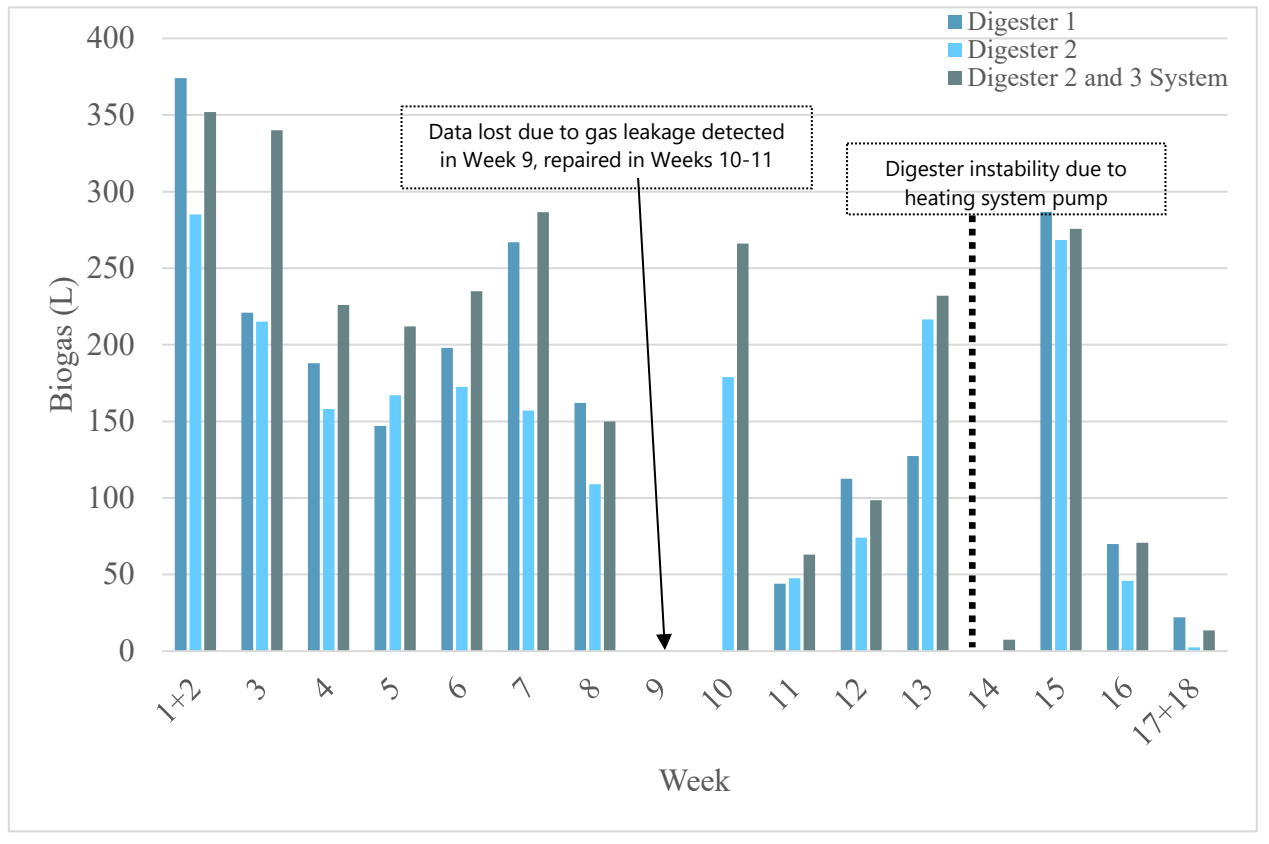


Figure 4-2
Total Methane Production from Algal Digestion

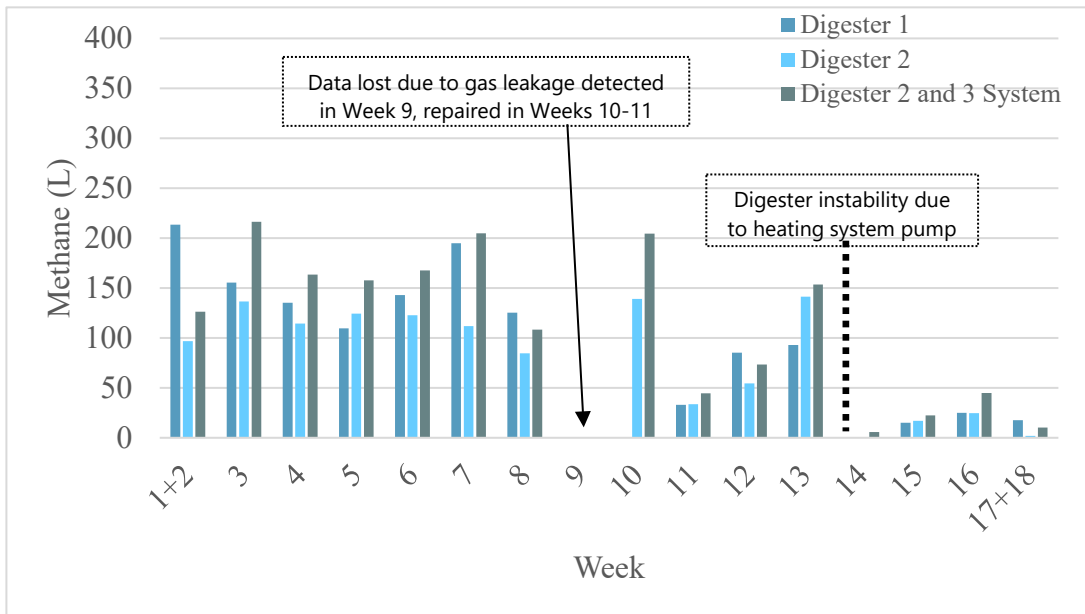
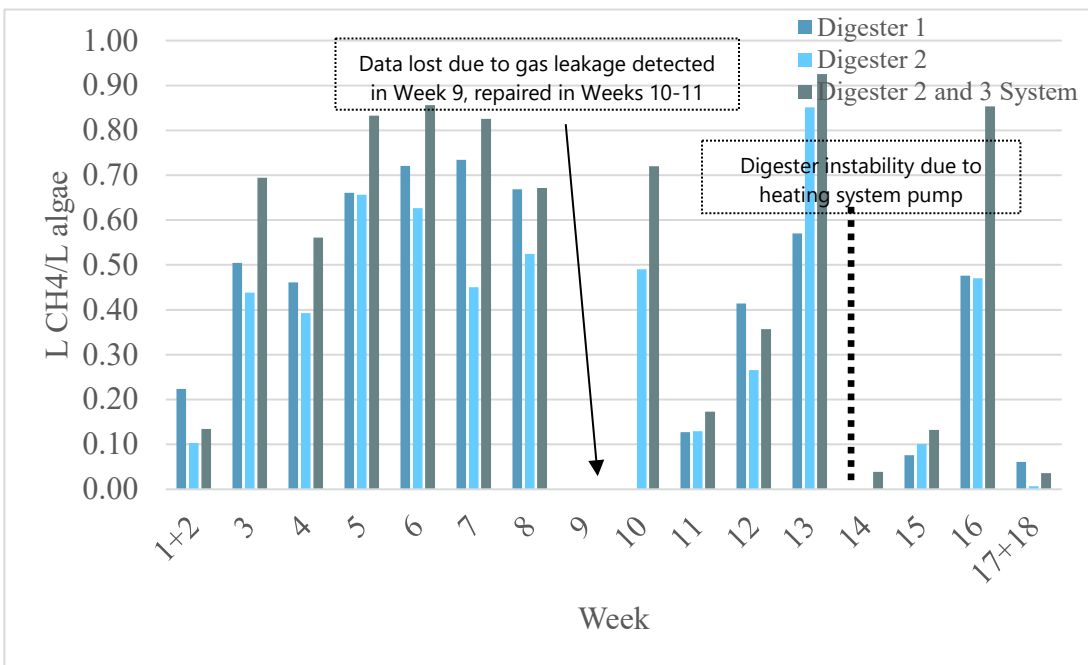


Figure 4-3
Methane Production Normalized by Algae Fed



4.3 Summary of Algal Digester Testing

For Phase 3, the design of the algal digester system was modified to run 2 parallel systems that would allow for data replication – D1 was run as a single system and digesters D2 and D3 were connected and run a single system. Phase 3 testing of the algal digesters was limited because of several project challenges, including a delay in initiation of the system until late July which shortened the operational window to late July to late November, a delay in the implementation of the heating system until October, and a malfunction in the heating system that impacted operations once ambient air temperatures decreased. In addition to these operational challenges, the algal-flow biomass production was approximately 30% lower than in Phase 2, so there was a lower quantity of organic feedstock available.

Overall, lower methane production was observed in Phase 3 compared to Phase 2. The single 3-unit series digester used in Phase 2 produced 588 ± 68 liters of methane per week, while the production in Phase 3 was 107 ± 20 liters of methane per week for D1 and 135 ± 19 liters of methane per week for the D2-D3 system. Combined, the algal digester units produced an average of 242 ± 34 liters of methane per week in Phase 3 over the thirteen weeks of stable production, which was a decline in production of 59% compared to Phase 2. The biogas that was produced contained low amounts of hydrogen sulfide, which suggested that the biogas could be used in a fuel cell with only minimal processing.

While the decreased quantity of algae available to feed the digester system likely contributed to the reduction in the production of methane, the total decrease in methane production likely resulted from a combination of low biomass production, changes to the operating design, and operational challenges. The potential impact of each project component will be reevaluated and changes may be implemented during future pilot testing.

4.4 Feasibility of Fuel Cell Use at Dundalk Marine Terminal

When high-quality biogas is successfully produced from an algal digester system, the biogas could be used to power a fuel cell, using a cleaner fuel source to reduce dependence on the existing electrical grid. The proposed system - growing algae on a flow-way, using a digester to breakdown the algae and create biogas, and using the biogas to feed a fuel cell – creates a closed energy loop to produce on-site electricity. The Phase 2 project completed in 2017 used biogas generated from the algal digesters as supplemental fuel to natural gas and achieved a steady power output of 300 watts (Anchor QEA 2018).

The fuel cell operated in Phase 2 was a demonstration project and was not used to power existing equipment or systems at DMT. While the Phase 2 project demonstrated that a fuel cell could be successfully operated using the algal biomass produced by the DMT algal flow-way, the Phase 3 project (2018) did not include additional fuel cell testing. For the Phase 3 study, MDOT MPA

coordinated with an Environmental Defense Fund Climate Corps fellow to study the feasibility of using a fuel cell to power buildings at DMT (Attachment B). Use of fuel cell technology could facilitate a shift away from fossil fuel-based power production and the emissions generated by this process toward a process that generates clean electricity through electrochemical reactions. The maritime industry is actively involved in identifying viable alternatives to fossil fuel-based power production to reduce emissions at ports throughout the United States.

To manage these challenges, renewable power options that can be reliably and resiliently operated without significant battery power or energy management systems are being increasingly investigated to determine if they could be utilized on a wide scale. Fuel cells are one renewable power option being evaluated to measure potential the overall reliability and resiliency of these systems when employed in real-world settings. Fuel cells are currently being used for primary or backup power as well as portable and emergency backup power scenarios ranging from heat and electricity for homes, material handling, passenger vehicles, buses and consumer electronics. As ports continue to expand and invest in additional infrastructure development, there are wide-ranging opportunities to incorporate renewable power sources, including fuel cells, as a clean energy option. Commercial viability of fuel cell technology is expanding, and the annual production of electricity by fuel cells is growing rapidly, with an estimated 30% year-over-year increase over the last decade.

The overall objective of the Phase 3 project for DMT was to perform an in-depth energy audit on a subset of buildings at DMT to evaluate the energy demand loads that could be offset using the existing fuel cell owned by MDOT MPA. The goal of this project was to repurpose the fuel cell already owned by MDOT MPA to provide power to one of the existing buildings. After performing an internal energy audit on four buildings and consulting fuel cell vendors and Baltimore Gas and Electric (BGE, the regional utility,) four fuel cell deployment options were evaluated for power co-generation with the existing electrical grid. These options included solid oxide fuel cells (SOFCs) from two different manufacturers capable of producing 0.5 kilowatts (kW), 1.5 kW, 5.5 kW, and 200 kW.

4.4.1 Description of Fuel Cell Technology

Fuel cells are electrochemical materials that convert the chemical energy of fuels directly into electrical energy. By means of two oppositely charged electrodes, ions are passed through an electrolyte using two oppositely charged electrodes, resulting in a reaction that produces electricity and heat at efficiencies of up to 90%. There are six dominant fuel cell technologies available on the market today: alkaline, direct methanol, phosphoric acid, molten carbonate, proton exchange membrane, and solid oxide. For this project, the proton exchange membrane and solid oxide were the only fuel cell types considered because of the commercial availability to MDOT MPA, the broad range in power rating, and the fuels needed to power them (hydrogen and methane, respectively).

Proton exchange membrane fuel cells are designed to be fueled by pure hydrogen, which results in a low operating temperature and no carbon emissions. However, operation of Proton exchange membrane fuel cells is limited by the availability of hydrogen which limits the geographic extent of where these fuel cells can be operationally deployed. Because of this reason, proton exchange membrane fuel cells are not a feasible option for implementation at MDOT MPA at this time.

Solid oxide fuel cells result in clean and efficient power production but have a wide range of fuel flexibility that includes gaseous fuels, liquids, and solid materials such as carbon, untreated coal and biomass. Most commonly, solid oxide fuel cells oxidize methane to produce waste heat which can then be utilized for power generation. Solid oxide fuel cells are the lowest emitting self-generation technology that can capture the benefits of combined heat and power generation. Gases with a high sulfur content will cause rapid degradation in electrode performance, which can be managed by installing purge traps within the system, upstream of the fuel cell. Solid oxide fuel cells are modular and available in a broad range of sizes that can be modified based on the needs of the project. Therefore, solid oxide fuel cells are the most likely option for implementation at MDOT MPA, based on the current state of the technology.

4.4.2 Operational Considerations

Four options for fuel cell operation modes were considered for MDOT MPA:

- 1) Baseload power generation: to provide a constant, steady supply of clean power at some value below the minimum energy usage
- 2) Variable power supply: a daily production profile with seasonal adjustment to provide energy use during the day and idling or shutting off at night
- 3) Constant fuel cell operation and variable power output: achieved with the addition of a battery pack, which discharges for extra demand during the day and recharged by fuel cells at night
- 4) A combined heat and power solid oxide fuel cell: waste heat is cooled providing hot water or sensible heat for indoor air

Using a fuel cell for baseload power generation while connected to the electrical grid (Option #1) was the operation mode that was used for the emissions analyses and economic assessments (Attachment 2). For solid oxide fuel cells, supplying a baseload demand is most advantageous because the high operational temperatures discourage a start/stop cycle. Stack damage from thermal stress can occur under circumstances of variable operation, which is why idling/standby features are normally included. Idling is recommended because relatively large amount of energy is

required to raise the core to the desired temperature before the fuel cell can sustain itself in normal active mode.

To identify the most effective system for MDOT MPA to implement at Dundalk Marine Terming, buildings compatible with a baseload operation mode proximity to preexisting natural gas pipeline termination points were identified - Buildings 1702, 91A, 91B, and 91C (Attachment 2). These four buildings were compatible with baseload operation because operate for 16 hours every day, maximizing the onsite benefits of a fuel cell system. Because Buildings 91 A, B, and C are clustered together, and their daily energy usage can sum to a near 100 kW, they were identified as the most feasible location to implement a fuel cell. Powering Buildings 91A, B, and C with one fuel was initially considered, but since no commercially available 100 kW solid oxide fuel cells modules were identified, it is more likely that a smaller fuel cell system could be used to power a portion of one of the buildings.

4.4.3 Emissions and Economic Analysis

Four fuel cells with ratings of 0.5 kW, 1.5 kW, 5 kW, and 200 kW were selected for emissions and economic analysis. Because of the solid oxide fuel cell technology’s high efficiency (almost triple that of coal power plants), potential reductions in greenhouse gas emissions differences were all positive and indicated that fuel cell implementation would result in an overall reduction of emissions.

**Table 4-3
Greenhouse Gas Emission Reductions for Deployment Options**

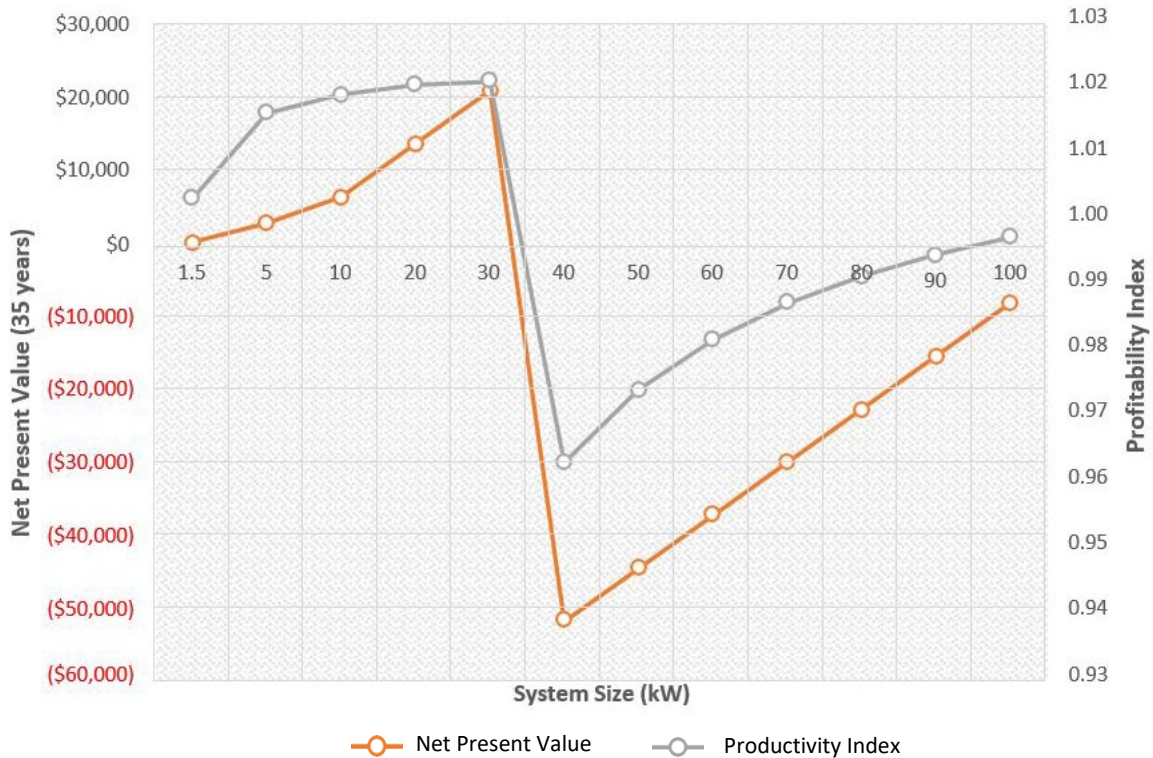
Project Option	Annual GHG Emission Reduction (MT CO ₂ eq)	GHG Emission Reduction Over System Lifetime of 35 Years (MT CO ₂ eq)
0.5 kW solid oxide fuel cell	2.16	75.6
1.5 kW solid oxide fuel cell	6.47	226.45
5.5 kW solid oxide fuel cell	23.71	829.85
200 kW solid oxide fuel cell	862.04	30,171.4

The economic analysis evaluated the lifetime value and performance of each of the four fuel cells. Two key financial metrics to assess the feasibility these systems were calculated (Figure 4-4:

- 1) Net present value
- 2) Profitability index: present value of future cash flows divided by the initial investment:

$$\text{Profitability index} = \frac{\text{total operating saving and income}}{\text{capital expense}}$$

Figure 4-4
Performance Regression Model for a Variety of Fuel Cell System Sizes



The cost-benefit analysis indicated that the best option for fuel cell implementation at Dundalk Marine Terminal is a 0.5 kW fuel cell system that could be connected to the electrical grid and operated nonstop off pipeline natural gas. This approach could effectively offset the energy demand from a single building. MDOT MPA has 0.5 kw fuel cell at DMT which could be installed by itself or in combination with larger fuel cells to benefit on-site operations.

5 Project Recommendations

Results from the MARAD Phase 3 project were used to identify methods to optimize the design and operation of algal flow-way system and potential scale-up at the Port of Baltimore. To optimize the algal flow-way, design considerations must balance enhancing biomass productivity (and subsequent nutrient removal) with operational and cost efficiency.

5.1 Biomass Productivity

5.1.1 *Flow-Way Surface Material*

The flow-way surface material impacts algal growth rate, algal species dominance, capital costs, and operating costs. The existing approach - an asphalt surface covered with an ethylene propylene diene terpolymer (EPDM) geomembrane liner that was overlain by a flexible low-profile nylon screen – is effective in supporting algal growth. This approach hinders the ability to mechanically harvest the biomass which would be required for large-scale implementation.

Concrete is one viable construction material for the flow-way that might be mechanically harvested, however using concrete as a surface may impact total algal biomass growth and could potentially increase long-term operational maintenance cost. Additional testing is recommended to quantify the potential impact of using concrete as a flow-way surface on algal biomass growth. Additional testing may include installing concrete sections larger than 3-ft and using a rougher concrete surface to increase surface area for algae to attach.

5.1.2 *Biofouling and the Linear Hydraulic Loading Rate*

The impact of biofouling on the LHRL was observed in 2018, even though modifications to the inflow pump were implemented prior to the start of flow-way. Because LHRL is known to affect the growth rate and algal species on the flow-way, additional strategies are recommended to be developed to address biofouling of the intake pump so a consistent, higher LHRL can be maintained for the duration of the testing period.

5.1.3 *Surge/Pulsed Flow*

Surge or pulsed flow is used in many algal flow-way systems because it has been documented to enhance algal growth under those site-specific conditions. However, the addition of surge increases both capital and operating costs and there are limited long term data comparing the performance of surge systems to a system where the water is delivered as a continuous flow. The surge approach was successful in the MARAD Phase 3 study, but it is recommended that additional testing be performed to directly compare the algal biomass growth and algal species dominance between a surge system and a continuous flow system. The system should be designed so that the two

methods are conducted concurrently, under the same operating conditions for a minimum of 120 days.

5.1.4 Water Quality Monitoring

Water quality, including nitrogen and phosphorus concentrations as well as salinity and water temperature, impacts algal biomass growth. If additional testing with the algal flow-way is conducted, it is recommended that a focused water quality testing program for the inflow water be implemented. These additional data will be useful for understanding the algal biomass growth relative to water quality and for comparing site conditions to historical data.

Water quality conditions in 2018 were unusual relative to historical trends because of the record rainfall in the region. Additional testing of the algal flow-way would be an opportunity to capture water quality data that represents typical water quality conditions, which may be useful in understanding the potential algal biomass growth that the algal flow-way could support.

5.2 Algal Flow-Way Design

A multi-step dewatering process is required to effectively capture and dewater biomass for efficient on-site handling. Based on the results of the 2018 testing, the combination of the following methods is recommended:

1. Perpendicular harvest + side or central dewatering channel
2. Wedge wire screen for material that flows freely from the dewatering channel
3. Sand filter (with a weir discharge option) as a final solids retention step

5.2.1 Perpendicular Harvest and Side Channel Dewatering

Results of the 2018 testing demonstrated that algal solids harvested perpendicular to flow into a side and/or central channel dewatered substantially so that between 84 to 94% of solids remained in the dewatering channel. This method recovered a substantially larger proportion of solids more efficient than other methods investigated.

Because the initial design of the flow-way used in 2018 did not include a side or central channel, implementation and testing of this approach was constrained to modifications of the existing design. It is highly recommended that this dewatering approach be replicated multiple times to confirm the results. Recommended testing would include a design that hydraulically isolates the dewatering channel from the operating flow-way so that dewatering measurements can be taken over various time periods, from several hours up to 7 days. Collecting data to document harvest material behavior during variable weather conditions (e.g., rain) is valuable to inform the design. Data from this effort will also provide insight into use and design of a wedge wire screen that would be implemented to manage the outflow from the side or central dewatering channel.

5.2.2 *Wedge Wire*

The self-cleaning wedge wire screen effectively captured harvest material larger than the 500- μ m opening. Additional testing recommended include methods to effectively incorporate a wedge wire screen so that outflow from the dewatering channel is directed across the screen. These data would allow further evaluation as to performance with dewatered algal solids in the harvest channel as well as potentially evaluating the recovery of solids which may be associated with rain-induced runoff from the dewatering channel.

5.2.3 *Sand Filter*

The sand filter is an important final step in retaining solids to ensure that the water is below the turbidity requirements for discharge. The sand filter was tested for only a few weeks in combination with the dewatering channel and wedge wire screen, so additional testing is recommended to assess the performance of the sand filter over time, specifically focused on filtration capacity and long-term maintenance costs.

5.3 *Algal Digesters*

The algal digester system did produce high-quality biogas (high methane content, low hydrogen sulfide content) even though the total quantity of biogas produced in Phase 3 was lower than for Phase 2. Additional testing of the system is recommended to allow for modification the system design to include a more efficient recirculation system to completely mix the digestate and enhance full digestion of nutrients and to install and operate a heating system to maintain internal temperatures during a full operating season. Future testing may also include a system redesign to identify the optimal configuration - such as the number of digesters, running single digester units, running multiple digesters connected in series, and/or the type of digester units to use - to achieve maximum biogas production.

6 References

- Anchor QEA, LLC, 2018. *Integrated Algal Flow-Way, Digester, and Fuel Cell Demonstration Project*. Prepared for U.S. Department of Maritime Administration, Maryland Department of Transportation Maryland Port Administration, and Maryland Environmental Service. April 2018.
- Bott et al., 2015. *Nutrient and Sediment Reductions from Algal Flow-way Technologies: Recommendations to the Chesapeake Bay Program's Water Quality Goal Implementation Team from the Algal Flow-way Technologies BMP Expert Panel*. October 21, 2015.
- MDE, 2014. *Accounting for Stormwater Wasteload Allocations and Impervious Acres Treated, Guidance for National Pollutant Discharge Elimination System Stormwater Permits*. August 2014.
- Richardson, Bill, 2018. Regarding: FW Port Data. Email to: Paul Nevenglosky (NMP), Karin Olsen (Anchor QEA), and Jamie Scheerer (MES). October 4, 2018.
- Selby, B., P. Kangas, P. May, W. Mulbry, and S. Calahan, 2016. *Algal Biomass Productivity at the Port of Baltimore Algal Turf Scrubber: Fall 2016*. First draft: December 6, 2016. Submitted to MES.
- Selby, B., P. May, S. Calahan, A. Blair, and P. Kangas, 2018. *Algal Biomass Productivity at the Port of Baltimore Algal Turf Scrubber: 2017*. First draft: January 12, 2018.
- Smith, J., B. Selby, P. Kangas, and P. May, 2013. *Progress Report on the Port of Baltimore Algal Turf Scrubber Project*. Unpublished report. December 2013.
- Smith, J., B. Selby, P. Kangas, P. May, and W. Mulbry, 2016. *2015 Final Progress Report on the Port of Baltimore Algal Turf Scrubber Project*. Unpublished draft report to the Maryland Port Administration. March 27, 2016.
- Yarberry, Annie, 2018. Regarding: Algae drying method. Email to: Karin Olsen (Anchor QEA). June 5, 2018.

Appendix A
Project Photographs

Appendix B

Field Data Tables

Appendix C

Analytical Data for Algal Flow-Way Testing

Attachment A
Algal Digester Report
University of Maryland

Attachment B

Feasibility of Fuel Cell Use at Ports

Environmental Defense Fund Report

Appendix A
Project Photographs

Evaporation Bed



Post construction



Post construction inflow side



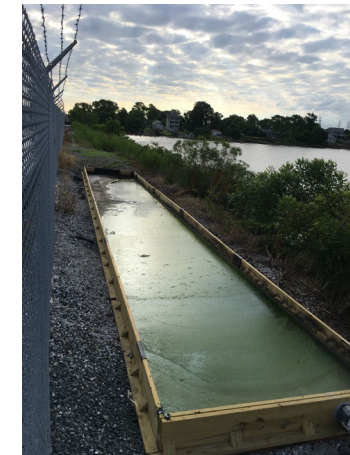
Inflow pipe and drain pipe



Secondary algal growth on surface



Settled solids



Secondary algal growth on surface

Dewatering Pad



Dewatering pad overview



Drains in normal operation



Secondary sump drain layout



Drying pad with harvest



Drying pad with harvest



1-week drying on pad and sump

Hanging Bag Test - Series



1,587micron pre-screen



Filter bag setup



Filter bag setup



Pre-screen



600 micron



200 micron

Hanging Bag Test - Series



Algae in filter bag



25 micron



Squeeze sample

Hanging Bag Test - Parallel



Overview of bags



Solids captured



600-micron



200-micron with effluent



Harvest to be added



Adding harvest sample to filter bag

Merit Tile



Merit Tile 1



Merit draining



Tile surface detail



Clean tile



Merit 2 8-30-18 three hours drain



Dewatering tile

Merit Tile



Merit 2 and 1 covered from rain



Merit 2 holding water 24hrs

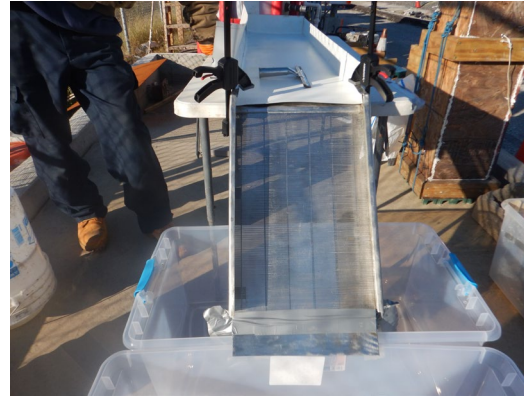


Effluent clarity

Wedge Wire Screen



Wedge wire setup



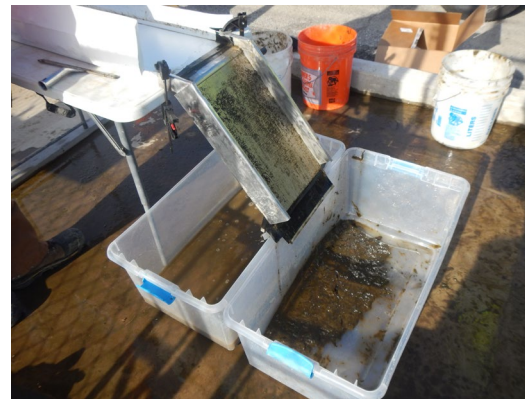
Wedge wire flume



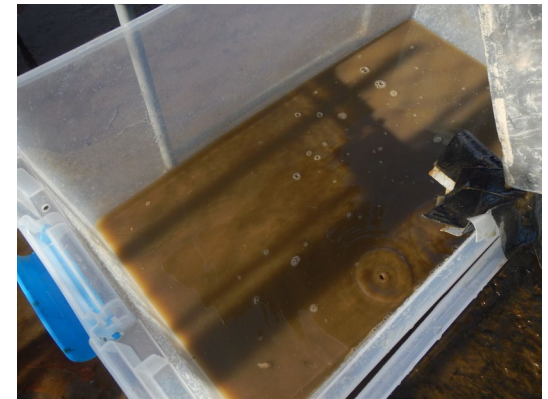
Pushed solids and effluent tubs



Screened solids



Wedge wire separation



Effluent

Perpendicular Harvest



Moving harvest and fire hose berm



Completed harvest draining



Harvest detail



Harvest depth



Harvest detail



Harvest detail

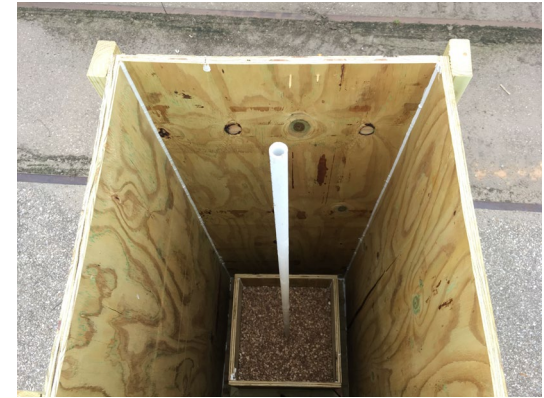
Sand Filter



Internal Construction



Drain and air break PVC



Pea gravel layer



Final and in place



First addition



Draining with typical effluent

Sand Filter



Final Crust



Final crust sample



7.39NTU Effluent

Appendix B

Field Data Tables

Table B-1**Water Quality Data Collected at the Top and Bottom of the Algal Flow-Way**

Date	Top of Flow-Way						Bottom of Flow-Way					
	pH	Conductivity (mS)	Salinity (ppt)	Temperature (°C)	DO (mg/L)	DO %	pH	Conductivity (mS)	Salinity (ppt)	Temperature (°C)	DO (mg/L)	DO %
4/26/2018	8.30	5.15/4129µS	3.7	13.5	9.97	99.4%	8.27	5.25/4143µS	3.7	14.0	10.70	106.2%
5/4/2018	8.90	8.12/6.17	5.5	17.0	8.48	90.7%	8.87	8.37/6.15	5.3	19.0	12.95	145.5%
5/11/2018	9.40	4.56/6.73	3.8	21.3	9.29	108.5%	9.38	4.58/6.41	3.8	22.4	9.46	109.8%
5/17/2018	8.96	8.12/5.85	5.0	20.3	8.23	94.5%	8.83	7.95/5.78	4.9	20.0	8.08	92.1%
5/24/2018	9.02	5.61/4024µS	3.3	20.6	8.32	95.0%	8.95	5.57/4016µS	3.3	20.5	10.95	124.5%
5/30/2018 ^a	7.74	4984/3427µS	2.7	23.8	6.51	79.7%	8.30	5.01/3442µS	2.8	23.9	8.20	99.2%
6/7/2018	7.66	7.36/5.27	4.4	20.8	8.25	93.1%	8.36	7.40/5.31	4.5	20.5	10.15	115.7%
6/14/2018	8.32	6.14/4243µS	3.5	23.5	7.29	87.6%	8.18 ^b	6.02/4198µS	3.5	22.8	10.07	122.1%
6/21/2018	9.03	7.58/5.13	4.2	25.0	8.70	108.8%	8.83	7.54/5.12	4.2	24.7	7.14	89.3%
6/28/2018	8.08	8.62/5.88	4.9	24.1	7.46	90.9%	8.47	8.67/5.94	4.9	24.2	8.75	107.7%
7/12/2018	7.39	10.86/7.32	6.1	25.5	5.06	65.0%	8.35	10.74/7.29	6.1	24.6	9.58	119.7%
7/19/2018	7.42	11.00/7.39	6.2	25.7	4.56	57.8%	7.71	10.68/7.32	6.2	24.2	11.33	143.1%
7/26/2018	7.18	6.04/4101µS	3.3	24.8	4.20	52.8%	7.53	5.93/4034µS	3.2	24.5	10.68	135.1%
8/2/2018	7.80	4520us/2996µS	2.3	26.5	6.05	80.1%	8.31	4498us/2985µS	2.3	26.8	9.30	120.8%
8/9/2018	7.80	3581/2576µS	1.9	29.2	5.78	77.4%	8.37	3900/2534µS	1.9	27.5	8.79	116.2%
8/16/2018	6.93	5.70/3231µS	3.0	26.9	5.36	69.5%	7.61	5.63/3755	3.0	26.4	7.15	91.3%
8/23/2018	7.45	4519/3032µS	2.2	24.8	5.90	73.9%	8.15	4363/3030µS	2.4	23.1	9.16	105.9%
8/30/2018	0.33	5.24/3399µS	2.6	28.4	6.70	89.0%	8.21	5.09/3375µS	2.6	27.0	7.11	92.8%
9/6/2018	7.98	4757us/2931µS	2.0	30.3	5.50	75.9%	7.97	4646/3010µS	2.3	29.3	6.75	91.1%
9/13/2018	7.16	6.08/4168µS	3.4	24.0	5.81	70.8%	7.44	6.06/4168µS	3.4	23.8	6.58	80.1%
9/20/2018	6.97	6.27/4304µS	3.4	23.9	6.52	78.3%	7.34	6.22/4316µS	3.5	23.1	6.72	80.8%
9/27/2018	7.22	7.07/5.07	4.3	23.3	6.67	79.8%	7.85	7.17/5.04	4.2	21.2	8.14	95.7%
10/4/2018	7.54	3945/2477µS	2.1	23.4	7.24	87.1%	7.60	3905/2719	2.2	22.9	6.71	80.4%
10/11/2018	6.91	3411uS/2332µS	1.8	24.2	7.43	92.8%	6.95	31.2µS/21.3µS	0.0	23.8	7.46	91.4%
10/18/2018	7.45	8.25/6.08	5.3	18.7	7.92	87.6%	7.74	7.89/5.99	5.3	16.6	8.76	92.3%
10/25/2018	7.51	9.59/7.38	6.7	15.9	8.44	87.6%	7.69	9.34/7.31	6.7	14.7	9.78	99.1%
11/1/2018	8.04	4133/3302µS	2.9	13.1	10.73	105%	7.87	3922/3155µS	2.8	12.7	10.13	98.6%

Table B-1**Water Quality Data Collected at the Top and Bottom of the Algal Flow-Way**

	Top of Flow-Way						Bottom of Flow-Way					
11/8/2018	7.39	3852/3062 μ S	2.7	13.5	9.36	93%	8.44 ^b	3753/3009 μ S	2.6	12.9	15.32	151.0%
11/14/2018	7.50	4376/3655 μ S	3.3	10.3	9.83	91%	8.00 ^b	4103/3540 μ S	3.3	8.3	14.55	129.9%
11/29/2018	7.90	5.57/4.91	4.9	5.7	10.15	88%	8.19	4905/4679 μ S	4.8	1.2	15.21	118.6%

Notes:

a. Measurements were taken the day before the algal biomass harvest.

b. Mixing zone reading

°C: degrees Centigrade

μ S: microsiemen

mg/L: milligrams per liter

mS: millisiemen

ppt: parts per thousand

Appendix C

Analytical Data for Algal Flow-Way Testing

Table C-1
Analytical Data for Weekly Harvest Samples

Sample Name	Description	Sample Collection Date	Percent Moisture (%)	Percent Solids (%)	Total Solids (mg/L)	Total Suspended Solids (mg/L)	Ash Content (%)	Nitrate Nitrite as N (mg/kg dry)	Total Kjeldahl Nitrogen (mg/kg dry)	Total Nitrogen (mg/kg dry)	Phosphorus (mg/kg dry)	Total Organic Matter (%)
AF18-	Weekly harvest	5/31/18	86.9	13.1			69.0	15	21,000	21,000	2,200	
AF18-	Weekly harvest	6/7/18	85.5	14.5								
AF18-	Weekly harvest	6/14/18	84.6	15.4			68.6	8.9	19,000	19,000	1,600	31.4
AF18-	Weekly harvest	6/21/18	85.6	14.4								
AF18-	Weekly harvest	6/28/18	90.8	9.2			69.5	16 B	33,000	33,000	2,500	30.5
AF18-	Weekly harvest	6/28/18					69.6					30.4
AF18-	Weekly harvest	7/18/18			53,000 H							
AF18-	Weekly harvest	7/18/18			52,400							
AF18-	Weekly harvest	7/26/18	84.3	15.7			78.0	7.8 B	15,000	15,000	1,200	22.0
AF18-	Weekly harvest	7/26/18	84.5	15.5			77.7					22.3
AF18-	Weekly harvest	8/2/18			48,000 H,E		76.2	0.67 JB	2,400	2,400	200B	23.8
AF18-	Weekly harvest	8/2/18					75.6					24.4
AF18-	Weekly harvest	8/9/18			13,000 H							
AF18-	Weekly harvest	8/16/18			49,000							
AF18-	Weekly harvest	8/23/18	1.6	98.4	41,000 E		76.5	6.5 B	14,000	14,000	1100B	23.5
AF18-	Weekly harvest	8/30/18			34,000 E			27	16,000	16,000		
AF18-	Weekly harvest	9/6/18			43,000 E			49	18,000	18,000		
AF18-	Weekly harvest	9/13/18			48,000 E		78.4	44	14,000	14,000	1,700	21.6
AF18-	Weekly harvest	9/20/18			44000 H,E		81.2	30 B	9,500	9,500	1,500	18.8
AF18-	Weekly harvest	9/27/18			41,000 E		77.1	200 B	13,000	13,000	1,700	22.9
AF18-	Weekly harvest	10/4/18			39,000 E	27,000	83.0	32 B	16,000	16,000	1,600	17.0
AF18-	Weekly harvest	10/4/18			38,300 E							
AF18-	Weekly harvest	10/12/18			50,000 E	40,000	75.1	160	14,000	14,000	1,600	24.9
AF18-	Weekly harvest	10/12/18			45,900 E							
AF18-	"Free water"	10/18/18			6,600 H,E	840 H			3,000			
AF18-	"Free water"	10/18/18			6,680 H, E							
AF18-	"Pushed solids"	10/18/18			64,000 H,E	53,000 H	76.9	97	14,000	14,000	1,700	23.1
AF18-	"Free water"	10/25/18			7,700 E	610			1,700			
AF18-	"Pushed solids"	10/25/18			64,000 E	49,000	77.3	44	13,000	13,000	150	22.7
AF18-	"Pushed solids"	10/25/18			64,440 E							
AF18-	Weekly harvest	11/1/18			33,000 E	19,000	75.1	40	9,300	9,300	1,800	24.9
AF18-	Weekly harvest	11/1/18			33,500 E		75.8					24.2
AF18-	Free water	11/14/18			9,900 E	2,800			13,000		1300B	
AF18-HAR-	Free water	11/14/18			9,240 E							
AF18-	Pushed solids	11/14/18	97.4	2.6			73.6	380	29,000	29,000	8,000	26.4
AF18-	Harvest material	11/29/18			30,000 E	28,000	78.2	13B	14,000	14,000	1500B	21.8
AF18-	Harvest material	11/29/18			30,500 E							

Notes:

Shaded cells indicate that no data was collected for these samples

a. Results for these two samples together represent the weekly harvest sample

kg: kilogram

B: compound was found in the blank and sample

L: liter

E: result exceeded calibration range;

mg: milligram

H: sample was prepped or analyzed beyond the specified holding time;

J: result is less than the RL but greater than or equal to the MDL and the concentration is an approximate value

Table C-2
Analytical Data for Drying Pad Samples

Sample Name	Description	Sample Collection Date	Percent Moisture (%)	Percent Solids (%)	Ash Content (%)	Nitrate Nitrite as N (mg/kg dry)	Total Kjeldahl Nitrogen (mg/kg dry)	Total Nitrogen (mg/kg dry)	Phosphorus (mg/kg dry)	Total Organic Matter (%)
AF18-SP-DP-WK6 (1)	Drying pad sample after one week drying	5/31/18	80.2	19.8	ND	ND	ND	ND	ND	ND
AF18-SP-DP-WK6 (2)	Drying pad sample after one week drying	5/31/18	7.3	92.7	ND	ND	ND	ND	ND	ND
AF18-SP-DP-WK7	Drying pad sample after one week drying	6/7/18	87.2	12.8	69.7	17	20,000	20,000	2,700 B	30.3
AF18-SP-DP-WK7 (2)	Drying pad sample after one week drying	6/7/18	83.4	16.6	75.8	24	51,000	51,000	4,700 B	24.2
DRYING PAD-HAR 4	Drying pad sample after one week drying	6/14/18	85.4	14.6	73.5	7.7	15,000	15,000	1,900 B	26.5

Notes:

ND = no data collected for these samples

B: compound was found in the blank and sample

Table C-3
Analytical Data for Evaporation Bed Samples

Sample Name	Description	Sample Collection Date	Percent Moisture (%)	Percent Solids (%)	Ash Content (%)	Nitrate Nitrite as N (mg/kg dry)	Total Kjeldahl Nitrogen (mg/kg dry)	Total Nitrogen (mg/kg dry)	Phosphorus (mg/kg dry)	Total Organic Matter (%)
AF18-MAY	Two half harvests added	5/31/18	87.7	12.3	71.4	8.4	20,000	20,000	1,400	ND
EVAP BED	Three half-harvests added	6/7/18	85.5	14.5	75	11	16,000	16,000	2,100 B	25.0
AF18-JUN	Four half harvests added	6/28/18	84.1	15.9	72.4	12 B	19,000	19,000	1,700	27.6

Notes:

ND = no data collected for these samples

B: compound was found in the blank and sample

Table C-4

Analytical Data for Flow-Way Surface Samples

Sample Name ^a	Description	Distance from Top of Flow-Way (ft)	Sample Collection Date	Percent Moisture (%)	Percent Solids (%)	Total Solids (mg/L)	Nitrate Nitrite as N (mg/kg dry)	Total Kjeldahl Nitrogen (mg/kg dry)	Total Nitrogen (mg/kg dry)	Phosphorus (mg/kg dry)	Ash Content (%)	Nitrate Nitrite as N (mg/kg dry)	Total Kjeldahl Nitrogen (mg/kg dry)	Total Nitrogen (mg/kg dry)	Phosphorus (mg/kg dry)	Total Organic Matter (%)
AF18-SP-C-WK6	Just concrete	50 to 53	5/31/18	86.0	14.0	ND	ND	ND	ND	ND	ND	12	18,000	18,000	2,100	ND
AF18-SP-LM-WK6	Middle flow way	100	5/31/18	87.0	13.0	ND	ND	ND	ND	ND	ND	12	20,000	20,000	1,800	ND
AF18-SP-LT-WK6	Top flow way	20	5/31/18	80.0	20.0	ND	ND	ND	ND	ND	ND	14	16,000	16,000	1,700	ND
AF18-SU2-C	Just concrete	50 to 53	8/23/18	ND	ND	73,000	ND	ND	ND	ND	ND	ND	ND	ND	ND	ND
AF18-SU2-CG	Concrete with grid	37 to 40	8/23/18	ND	ND	48,000	ND	ND	ND	ND	ND	ND	ND	ND	ND	ND
AF18-SU2-LM	Middle flow way	100	8/23/18	ND	ND	42,000	ND	ND	ND	ND	ND	ND	ND	ND	ND	ND
AF18-SU2-LT	Top flow way	20	8/23/18	ND	ND	13,000	ND	ND	ND	ND	ND	ND	ND	ND	ND	ND
AF18-FA1-C	Just concrete	50 to 53	10/12/18	ND	ND	45,000 E	11	510	520	49	ND	ND	ND	ND	ND	ND
AF18-FA1-CG	Concrete with grid	37 to 40	10/12/18	ND	ND	89,000 E	7.0	70	77	15	ND	ND	ND	ND	ND	ND
AF18-FA1-LM	Middle flow way	100	10/12/18	ND	ND	42,000 E	0.35	40	40	3.9	ND	ND	ND	ND	ND	ND
AF18-FA1-LT	Top flow way	20	10/12/18	ND	ND	66,000 E	1.0	62	63	9.3	ND	ND	ND	ND	ND	ND
CONCRETE	Just concrete	50 to 53	11/29/18	96.7	3.3	ND	ND	ND	ND	ND	77.2	15 J	25,000	25,000	1,600	22.8
CONCRETE WITH GRID	Concrete with grid	37 to 40	11/29/18	95.1	4.9	ND	ND	ND	ND	ND	78.8	50	22,000	22,000	2,500	21.2
CONCRETE WITH GRID DUP	Concrete with grid	37 to 40	11/29/18	95.3	4.7	ND	ND	ND	ND	ND	ND	ND	ND	ND	ND	ND
MIDDLE FLOW WAY	Middle flow way	100	11/29/18	97.9	2.1	ND	ND	ND	ND	ND	74.1	190	9,900	10,000	1,000	25.9

Notes:

a. C - concrete surface with mesh; LM - middle section of flow-way with mesh liner; LT - top section of flow-way with mesh liner

b. Subplots were 1 meter square plots harvested with a squeegee and pan

ND = no data collected for these samples

E: result exceeded calibration range

Table C-5
Analytical Data for Hanging Bag Test (in Series) on August 2, 2018

Sample Name	Description	Percent Moisture (%)	Percent Solids (%)	Total Solids ^a	Ash Content (%)	Nitrate Nitrite as N (mg/kg dry)	Total Kjeldahl Nitrogen (mg/kg dry)	Total Nitrogen (mg/kg dry)	Phosphorus (mg/kg dry)	Total Organic Matter (%)
Initial Sample	Harvest sample before treatment	ND	ND	44000 HE	72.5	0.58 JB	2,200	2,200	170 B	27.5
1500 Greenwater	1500u sheet metal effluent water	ND	ND	33000 HE	77.2	0.65 JB	2,200	2,200	170 B	22.8
1500 solids	1500u sheet metal solids on top	89.8	10.2	ND	72.3	8.1 JB	18,000	18,000	910 B	27.7
1500 solids dup	1500u sheet metal solids on top	89.7	10.3	ND	74.1	ND	ND	ND	ND	25.9
600 Effluent	600u hanging bag effluent	ND	ND	22000 HE	78.3	0.67 JB	2,000	2,000	180 B	21.7
600 solids	600u hanging bag captured solids.	93.9	6.1	ND	83.1	8.9 JB	15,000	15,000	1200 B	16.9
600 Squeezed solids	Solids after squeezing bag	86	14	ND	76.1	8.4 B	17,000	17,000	1100 B	23.9
600 Squeezed effluent	effluent while squeezing bag	ND	ND	40000 HE	77.0	0.71 JB	2,100	2,100	180 B	23.0
200 solids	200u solids remaining	95	5	ND	77.8	13 JB	15,000	15,000	1600 B	22.2
200 Effluent	200u effluent	ND	ND	14000 HE	78.4	0.66 JB	1,900	1,900	150 B	21.6
200 squeezed solids	200u solids after squeezing	84.7	15.3	ND	77.4	6.4 JB	15,000	15,000	1100 B	22.6
200 squeezed effluent	effluent while squeezing bag	ND	ND	19000 HE	77.5	0.69 JB	1,900	1,900	160 B	22.5
100 solids	100u solids in bag	95.7	4.3	ND	76.2	22 JB	23,000	23,000	2100 B	23.8
100 effluent	100u effluent	ND	ND	5700 HE	ND	2.3 JB	1,600	ND	ND	ND
100 squeezed solids	100u solids after squeezing	73.7	26.3	ND	77.6	3.1 JB	14,000	14,000	950 B	22.4
100 squeezed effluent	effluent while squeezing	ND	ND	6300 HE	ND	ND	1,100	ND	ND	ND
75 solids	75u solids in bag	87	13	ND	ND	ND	11,000	ND	ND	ND
75 effluent	75u effluent	ND	ND	4600 HE	ND	1.3 JB	1,300	ND	ND	ND
25 solids	25u solids in bag	99.1	0.9	ND	66.7	46 JB	9,900 J	9,900	370 B	33.3
25 effluent	25u effluent	ND	ND	3100 HE	ND	ND	570	ND	ND	ND
25 squeezed solids	25u solids after squeezing	74.2	25.8	ND	ND	ND	10,000	ND	ND	ND
25 squeezed effluent	25u effluent while squeezing	ND	ND	3,000 HE	ND	ND	790	ND	ND	ND

Notes:

a. Samples were analyzed per client's specific method modification request. results may be biased high.

ND = no data collected for these samples

B: compound was found in the blank and sample

E: result exceeded calibration range;

J: result is less than the RL but greater than or equal to the MDL and the concentration is an approximate value

H: sample was prepped or analyzed beyond the specified holding time;

Table C-6

Analytical Data for Hanging Bag (in Parallel) and Merit Tile Tests on August 23 and 24, 2018

Sample Name	Description	Volumetric Solids (mg/L)	Percent Moisture (%)	Percent Solids (%)	Nitrate Nitrite as N (mg/kg dry)	Nitrogen, Kjeldahl (mg/kg dry)	Total Nitrogen on Solids (mg/kg dry)	Total Phosphorus on Solids (mg/kg dry)
Hanging Bag								
HW-1	Harvest Water Bucket #1	40,000 E	ND	ND	ND	ND	ND	ND
HW-2	Harvest Water Bucket #2	40,000 E	ND	ND	ND	ND	ND	ND
HW-3	Harvest Water Bucket #3	38,000 E	ND	ND	ND	ND	ND	ND
Dec-Top	Top "fluid" portion from decant test	3,100 E	ND	ND	ND	ND	ND	ND
Dec-Bot	Bottom "solids" portion from decant test	77,000 E	ND	ND	ND	ND	ND	ND
Merit Tile								
Merit-Eff	Merit Filter Tile (380 micron) effluent	7,300 E	ND	ND	ND	ND	ND	ND
600m-Eff	600 micron bag effluent	10,000 E	ND	ND	ND	ND	ND	ND
200m-Eff	200 micron bag effluent	7,700 E	ND	ND	ND	ND	ND	ND
100m-Eff	100 micron bag effluent	4,800 E	ND	ND	ND	ND	ND	ND
75m-Eff	75 micron bag effluent	4,700 E	ND	ND	ND	ND	ND	ND
25m-Eff	25 micron bag effluent	3,400 E	ND	ND	ND	ND	ND	ND
Merit-Sol	Solids captured on Merit Filter Tile (380 micron)	ND	88.5	11.5	7.5	16,000	16,000	1,400 B
600m-Sol	Solids captured in 600 micron bag	ND	79.2	20.8	5.1 B	18,000	18,000	1,100 B
200m-Sol	Solids captured in 200 micron bag	ND	82.7	17.3	6.3 B	18,000	18,000	1,400 B
100m-Sol	Solids captured in 100 micron bag	ND	83.9	16.1	7 B	19,000	19,000	1,400 B
75m-Sol	Solids captured in 75 micron bag	ND	84.3	15.7	7.2 B	18,000	18,000	1,600 B
25m-Sol	Solids captured in 25 micron bag	ND	83.3	16.7	6 B	17,000	17,000	1,300 B

Notes:

Table C-7
Analytical Data for Merit Tile Tests on August 30, 2018

Sample Name	Description	Volumetric Solids (mg/l)	Percent Moisture (%)	Percent Solids (%)	Ash Content (%)	Nitrate Nitrite as N (mg/kg dry)	Nitrogen, Kjeldahl (mg/kg dry)	Total Nitrogen on Solids (mg/kg dry)	Total Phosphorus on Solids (mg/kg dry)	Total Organic Matter (%)
HW-1A	Harvest Water Bucket #1A	ND	98.6	1.4	ND	ND	ND	ND	ND	ND
HW-2A	Harvest Water Bucket #2A	ND	98.3	1.7	ND	ND	ND	ND	ND	ND
Merit2-Eff	Merit Assembly 2 effluent	4,400 E	ND	ND	ND	ND	ND	ND	ND	ND
Merit1-Eff	Merit Assembly 1 effluent	4,700 E	ND	ND	ND	ND	ND	ND	ND	ND
Merit2-Sol-A	Solids captured on Merit Assembly 2	ND	88.1	11.9	69.2	8.3 JB	16,000	16,000	1,300 B	30.8
Merit1-Sol-A	Solids captured on Merit Assembly 1	ND	88.4	11.6	75.4	8 JB	17,000	17,000	1,100 B	24.6
Merit2-Sol-B	Solids captured on Merit Assembly 2	ND	ND	ND	ND	ND	ND	ND	ND	ND
Merit1-Sol-B	Solids captured on Merit Assembly 1	ND	ND	ND	ND	ND	ND	ND	ND	ND

Notes:

ND = no data collected for these samples

B: compound was found in the blank and sample

E: result exceeded calibration range;

J: result is less than the RL but greater than or equal to the MDL and the concentration is an approximate value

Table C-8

Analytical Data for Merit Tile and First Flush Tests on September 6, 2018

Sample Name	Description	Volumetric Solids (mg/l)	Percent Moisture (%)	Percent Solids (%)	Total Solids	Ash Content (%)	Nitrate Nitrite (mg/kg dry)	Total Kjeldahl Nitrogen (mg/kg dry)	Total Nitrogen on Solids (mg/kg dry)	Total Phosphorus on Solids (mg/kg dry)	Nitrate Nitrite (mg/kg dry)	Total Kjeldahl Nitrogen (mg/kg dry)	Total Nitrogen on Solids (mg/kg dry)	Total Phosphorus on Solids (mg/kg dry)	Total Organic Matter (%)
HW-1B	Harvest Water Bucket #1B	ND	98.2	1.8	ND	66.1	34 J	35,000	35,000	5,200	ND	ND	ND	ND	33.9
HW-1B DUP	Harvest Water Bucket #1B (duplicate)	ND	ND	ND	ND	61.7	ND	ND	ND	ND	ND	ND	ND	ND	38.3
HW-2B	Harvest Water Bucket #2B	ND	97.4	2.6	ND	60.6	29 J	29,000	29,000	4,400	ND	ND	ND	ND	39.4
HW-3B	Harvest Water Bucket #3B	ND	97.3	2.7	ND	70.1	28 J	27,000	27,000	4,900	ND	ND	ND	ND	29.9
MERIT1 FINAL	--	ND	28.7	71.3	ND	77.5	2.5	12,000	12,000	1,200	ND	ND	ND	ND	22.5
MERIT2 FINAL	--	ND	14.9	85.1	ND	76.6	4.3	14,000	14,000	1,400	ND	ND	ND	ND	23.4
FIRST FLUSH	Composite of First Flush	2500 E	ND	ND	ND	ND	ND	ND	ND	ND	ND	ND	ND	ND	ND
FIRST FLUSH DUP	Composite of First Flush (duplicate)	2540 E	ND	ND	ND	ND	ND	ND	ND	ND	ND	ND	ND	ND	ND
AMB RIVER	Ambient Harbor Water	2500 E	ND	ND	ND	ND	ND	ND	ND	ND	ND	ND	ND	ND	ND
MERIT1-R2-EFF	Merit Assembly 1 effluent	3900 E	ND	ND	ND	ND	ND	ND	ND	ND	0.034 J	17 B	17	0.21	ND
MERIT2-R2-EFF	Merit Assembly 2 effluent	4400 E	ND	ND	ND	ND	ND	ND	ND	ND	0.063 J	14 B	14	2.1	ND

Notes:

ND = no data collected for these samples

E: result exceeded calibration range

J: result is less than the RL but greater than or equal to the MDL and the concentration is an approximate value

Table C-9
Analytical Data for Flow-Way Inflow Samples

Sample Name	Description	Total Solids (Volumetric) (mg/L)	Total Suspended Solids (mg/L)	Nitrate Nitrite as N (mg/L)	Total Kjeldahl Nitrogen (mg/L)	Total Nitrogen (mg/L)	Total Phosphorus (mg/L)
8/30-INFLOW	Inflow water sample	ND	ND	0.28	5 U	0.28 J	0.1 U
Inflow 9/20	Inflow water sample	1300 H	ND	0.66	3.4 J	4.1 J	0.1 U
Inflow 9/28	Inflow water sample	4400 E	ND	0.75	7.8	8.6	0.1 U
Inflow 10/4	Inflow water sample	2400 E	ND	ND	14	ND	0.1 U
AF18-Inflow 10/12	Inflow water sample	2800 E	ND	0.62	5 U	0.62 J	0.1 U
AF18-Inflow 10/18	Inflow water sample	5500 E	ND	0.67	5 U	0.67	0.1 U
AF18-Inflow 10/25	Inflow water sample	6900 E	5	0.65	1.7 J	2.4 J	0.1 U
AF18-Inflow 11/14	Inflow water sample	3600 E	3.1	0.78	34	35	0.1 U

Notes:

ND = no data collected for these samples

J: result is less than the RL but greater than or equal to the MDL and the concentration is an approximate value

Table C-10

Analytical Data for Perpendicular Harvest, First Flush, and Merit Tile Tests on September 13, 2018

Sample Name	Description	Volumetric Solids (mg/L)	Nitrate Nitrite (mg/L)	Total Kjeldahl Nitrogen (mg/L)	Total Nitrogen (mg/L)	Total Phosphorus (mg/L)	Percent Moisture (%)	Percent Solids (%)	Ash Content (%)	Nitrate Nitrite (mg/kg dry)	Total Kjeldahl Nitrogen (mg/kg dry)	Total Nitrogen (mg/kg dry)	Phosphorus (mg/kg dry)	Total Organic Matter (%)
HW-1C	Harvest Water Bucket #1C	ND	ND	ND	ND	ND	96.9	3.1	86.4	30 J	8,800	8,800	1,400	13.6
HW-1C DUP	Harvest Water Bucket #1C (duplicate)	ND	ND	ND	ND	ND	ND	ND	87.1	ND	ND	ND	ND	12.9
solids water harvest	Solids Water (squeegeed) from perpendicular harvest	ND	ND	ND	ND	ND	93.5	6.5	76.5	12 J	2,600	2,600	750	23.5
free water harvest	Free Water from perpendicular harvest	ND	ND	ND	ND	ND	99.3	0.7	69.4	61 J	21,000	21,000	6,100	30.6
FIRST FLUSH 2 *	Composite of First Flush	3900 E	ND	ND	ND	ND	ND	ND	ND	ND	ND	ND	ND	ND
AMB RIVER 2	Ambient Harbor Water	3700 E	ND	ND	ND	ND	ND	ND	ND	ND	ND	ND	ND	ND
AMB RIVER 2 DUP	Ambient Harbor Water (duplicate)	3740 E	ND	ND	ND	ND	ND	ND	ND	ND	ND	ND	ND	ND
Merit1-R2-SOL-FINAL	Solids captured on Merit Assembly 1	ND	ND	ND	ND	ND	87.4	12.6	74.3	11	22,000	22,000	2,000	25.7
Merit2-R2-SOL-FINAL	Solids captured on Merit Assembly 2	ND	ND	ND	ND	ND	93.3	6.7	75.5	19	7,200	7,200	780	24.5
MERIT1-R3-EFF	Merit Assembly 1 effluent	5900 E	0.19	13	13	1.2	ND	ND	ND	ND	ND	ND	ND	ND
MERIT2-R3-EFF	Merit Assembly 2 effluent	7500 E	1.6	50	52	7.6	ND	ND	ND	ND	ND	ND	ND	ND

Notes:

ND = no data collected for these samples

E: result exceeded calibration range

J: result is less than the RL but greater than or equal to the MDL and the concentration is an approximate value

Table C-11**Analytical Data for First Flush and Merit Tile Tests on September 20, 2018**

Sample Name	Volumetric Solids (mg/L)	Nitrate Nitrite as N (mg/L)	Total Kjeldahl Nitrogen (mg/L)	Total Nitrogen (mg/L)	Total Phosphorus (mg/L)	Percent Moisture (%)	Percent Solids (%)	Ash Content (%)	Nitrate Nitrite as N (mg/kg dry)	Total Kjeldahl Nitrogen (mg/kg dry)	Total Nitrogen (mg/kg dry)	Phosphorus (mg/kg dry)	Total Organic Matter (%)
HW-1D	70000 HE	0.19	62	62	7.1	ND	ND	ND	ND	ND	ND	ND	ND
HW-1E Top	4000 HE	0.26	9.5	9.8	0.18	ND	ND	ND	ND	ND	ND	ND	ND
HW-1E TOP DUP	4180 E	ND	ND	ND	ND	ND	ND	ND	ND	ND	ND	ND	ND
HW-1E Bot	110000 HE	0.25	130	130	14	ND	ND	ND	ND	ND	ND	ND	ND
FIRST FLUSH 3	3900 HE	1.0	2.2 J	3.2 J	0.1 U	ND	ND	ND	ND	ND	ND	ND	ND
Amb 3	1600 H	0.7	1.7 J	2.4 J	0.1U	ND	ND	ND	ND	ND	ND	ND	ND
Merit1-R3-SOL-FINAL	ND	ND	ND	ND	ND	79.0	21.0	78.1	11 B	15,000	15,000	2,000	21.9
Merit1-R3_SOL-FINAL DUP	ND	ND	ND	ND	ND	ND	ND	78.5	ND	ND	ND	ND	21.5
Merit2-R3-SOL-FINAL	ND	ND	ND	ND	ND	88.5	11.5	77.4	15 B	12,000	12,000	2,300	22.6
MERIT1-R4-EFF	4500 HE	ND	ND	ND	ND	ND	ND	ND	ND	ND	ND	ND	ND
MERIT2-R4-EFF	3900 HE	ND	ND	ND	ND	ND	ND	ND	ND	ND	ND	ND	ND

Notes:

ND = no data collected for these samples

B: compound was found in the blank and sample

E: result exceeded calibration range

J: result is less than the RL but greater than or equal to the MDL and the concentration is an approximate value

Table C-12**Analytical Data for First Flush, Merit Tile Effluent, Sand Filter Effluent Samples on September 27, 2018**

Sample Name	Description	Total Solids (mg/L)
HW-1F	Harvest Water Bucket #1F	23,000 E
HW-1G	Harvest Water Bucket #1G	34,000 E
FF 000	First flush at time 0	6,100 E
FF 030	First flush at 30 seconds	5,100 E
FF 100	First flush at 1 minute	5,000 E
FF 130	First flush at 1 minute 30 seconds	4,900 E
FF 200	First flush at 2 minutes	4,600 E
FF 230	First flush at 2 minute 30 seconds	5,000 E
FF 300	First flush at 3 minutes	5,000 E
FF 330	First flush at 3 minute 30 seconds	5,000 E
FF 400	First flush at 4 minutes	5,200 E
FF 430	First flush at 4 minute 30 seconds	5,200 E
FF 500	First flush at 5 minutes	5,100 E
MERIT EFF COMBINED	Merit tile effluent	5,200 E
MERIT EFF COMBINED DUP	Merit tile effluent duplicate	5,200 E
SF-EFF-1	Sand filter effluent	6,000 E
SF-EFF-1 DUP	Sand filter effluent duplicate	6,200 E

Notes:

E: result exceeded calibration range

Table C-13**Analytical Data for Harvest Water and First Flush Samples on October 4, 2018**

Sample Name	Description	Volumetric Solids (mg/L)	Total Suspended Solids (mg/L)	Nitrate Nitrite as N (mg/L)	Total Kjeldahl Nitrogen (mg/L)	Total Nitrogen (mg/L)	Total Phosphorus (mg/L)
HW-10/4 (1)	Harvest Water Bucket	28,000 E	ND	1.3	240	240	36
HW-10/4 (2)	Harvest Water Bucket	30,000 E	ND	0.53	280	280	41
HW-10/4 (3)	Harvest Water Bucket	40,000 E	ND	0.57	680	680	48
FIRST FLUSH COMP	first flush composite	ND	28	ND	ND	ND	ND

Notes:

ND = no data collected for these samples

E: result exceeded calibration range

Table C-14**Analytical Data for Merit Tile and Sand Filter Tests on October 9, 2018**

Sample Name	Description	Total Solids (mg/L)	Total Suspended Solids (mg/L)	Nitrate Nitrite as N (mg/L)	Kjeldahl Nitrogen (mg/L)	Total Nitrogen (mg/L)	Total Phosphorus (mg/L)	Percent Moisture (%)	Percent Solids (%)	Ash Content (%)	Nitrate Nitrite as N (mg/kg dry)	Total Kjeldahl Nitrogen (mg/kg dry)	Total Nitrogen (mg/kg dry)	Phosphorus (mg/kg dry)	Total Organic Matter (%)
AF18-TS-10-9	Solids from Merit 1 tile	ND	ND	ND	ND	ND	ND	83.6	16.4	76.1	13 B	16,000	16,000	2,800	23.9
AF18-TS-10-9 DUP	Solids from Merit 1 tile duplicate	ND	ND	ND	ND	ND	ND	ND	ND	77	ND	ND	ND	ND	23
AF18-TE-10-9	Merit tile effluent	2,900	350	0.1 U	64	64	2.2	ND	ND	ND	ND	ND	ND	ND	ND
AF18-TE-10-9 DUP	Merit tile effluent duplicate	2,940	ND	ND	ND	ND	ND	ND	ND	ND	ND	ND	ND	ND	ND

Notes:

ND = no data collected for these samples

Table C-15**Analytical Data for Wedge Wire Screen and Sand Filter Tests on October 12, 2018**

Sample Name	Total Solids (mg/L)	Total Suspended Solids (mg/L)	Nitrate Nitrite as N (mg/L)	Total Kjeldahl Nitrogen (mg/L)	Total Nitrogen (mg/L)	Total Phosphorus (mg/L)	Percent Moisture (%)	Percent Solids (%)	Nitrate Nitrite as N (mg/kg dry)	Total Kjeldahl Nitrogen (mg/kg dry)	Total Nitrogen (mg/kg dry)	Phosphorus (mg/kg dry)
AF18-HB1-10/12	85,000 E	ND	0.60	38	39	2.8	ND	ND	ND	ND	ND	ND
AF18-HB2-10/12	76,000 E	ND	0.83	64	65	4.5	ND	ND	ND	ND	ND	ND
AF18-WWEFF-10/12	31,000 E	ND	0.34	36	36	2.8	ND	ND	ND	ND	ND	ND
AF18-WWSOL-10/12	ND	ND	ND	ND	ND	ND	95.3	4.7	24	20,000	20,000	2,500
AF18-MT-SFEFF-10/12	2,900 HE	68 H	1.7	8.4	10	0.051 J	ND	ND	ND	ND	ND	ND
AF18-WW-SFEFF-10/12	3,200 HE	98 H	0.71	6.7	7.4	0.1 U	ND	ND	ND	ND	ND	ND

Notes:

ND = no data collected for these samples

B: compound was found in the blank and sample

E: result exceeded calibration range

J: result is less than the RL but greater than or equal to the MDL and the concentration is an approximate value

Table C-16

Analytical Data for Perpendicular Harvest, Merit Tile, Wedge Wire Screen, and Sand Filter Tests on October 18, 2018

Sample Name	Description	Total Solids (mg/L)	Suspended Solids (mg/L)	Nitrate Nitrite (mg/L)	Kjeldahl Nitrogen (mg/L)	Total Nitrogen (mg/L)	Total Phosphorus (mg/L)	Percent Moisture (%)	Percent Solids (%)	Ash Content (%)	Nitrate Nitrite (mg/kg dry)	Total Kjeldahl Nitrogen (mg/kg dry)	Total Nitrogen (mg/kg dry)	Phosphorus (mg/kg dry)	Total Organic Matter (%)
AF18-MERIT1-SOL-10/18	Dried solids remaining on Merit1 from last week	ND	ND	ND	ND	ND	ND	83.2	16.8	75.9	28	19,000	19,000	2,200	24.1
AF18-MERIT1-SOL-10/18 DUP	Dried solids remaining on Merit1 from last week	ND	ND	ND	ND	ND	ND	ND	ND	74.9	ND	ND	ND	ND	25.1
AF18-MERIT2-SOL-10/18	Dried solids remaining on Merit2 from last week	ND	ND	ND	ND	ND	ND	82.9	17.1	76.8	19	20,000	20,000	2,400	23.2
AF18-WWEFF-FW-10/18	Effluent from running the perpendicular harvest free water sample buckets over the wedge wire screen	6400 HE	450 H	0.55	8.4	9	0.35	ND	ND	ND	ND	ND	ND	ND	ND
AF18-WWEFF-PS-10/18	Effluent from running the perpendicular harvest pushed solids sample buckets over the wedge wire screen	43000 HE	ND	2.7	510	510	56	ND	ND	ND	ND	ND	ND	ND	ND
AF18-WWSOL-10/18	Separated solids generated by running the HAR-PUSHED-SOL sample buckets over the wedge wire screen	ND	ND	ND	ND	ND	ND	88.7	11.3	73.6	360	14,000	14,000	1,600	26.4
AF18-WW-SFEFF-10/12	Effluent from the sand filter after loading with WW-EFF-FW and WW-EFF-PS	3200 HE	98 H	0.71	6.7	7.4	0.1 U	ND	ND	ND	ND	ND	ND	ND	ND
AF18-MT-SFEFF-10/12		2900 HE	68 H	1.7	8.4	10	0.051 J	ND	ND	ND	ND	ND	ND	ND	ND

Notes:

ND = no data collected for these samples

B: compound was found in the blank and sample

E: result exceeded calibration range

J: result is less than the RL but greater than or equal to the MDL and the concentration is an approximate value

H: sample was prepped or analyzed beyond the specified holding time

Table C-17

Analytical Data for Perpendicular Harvest, Wedge Wire Screen, and Sand Filter Tests on October 25, 2018

Sample Name	Description	Total Solids (mg/L)	Total Suspended Solids (mg/L)	Nitrate Nitrite (mg/L)	Total Kjeldahl Nitrogen (mg/L)	Total Nitrogen (mg/L)	Total Phosphorus (mg/L)	Percent Moisture (%)	Percent Solids (%)	Ash Content (%)	Nitrate Nitrite (mg/kg dry)	Total Kjeldahl Nitrogen (mg/kg dry)	Total Nitrogen (mg/kg dry)	Phosphorus (mg/kg dry)	Total Organic Matter (%)
AF18-WWEFF-FW-10/25	Effluent from running the perpendicular harvest free water sample buckets over the wedge wire screen	8,300 E	860	0.27	7.3	7.6	0.13	ND	ND	ND	ND	ND	ND	ND	ND
AF18-WWEFF-PS-10/25	Effluent from running the perpendicular harvest pushed solids sample buckets over the wedge wire screen	39,000 E	ND	0.5	20	21	5.6	ND	ND	ND	ND	ND	ND	ND	ND
AF18-WWSOL-10/25	Separated solids generated by running the HAR-PUSHED-SOL sample buckets over the wedge wire screen	ND	ND	ND	ND	ND	ND	89.6	10.4	72.8	7.7 J	11,000	11,000	15,000	27.2

Notes:

ND = no data collected for these samples

E: result exceeded calibration range

J: result is less than the RL but greater than or equal to the MDL and the concentration is an approximate value

Table C-18**Analytical Data for Sand Filter Tests on November 1, 2018**

Sample Name	Total Solids (mg/L)	Total Suspended Solids (mg/L)	Nitrate Nitrite (mg/L)	Total Kjeldahl Nitrogen (mg/L)	Total Nitrogen (mg/L)	Total Phosphorus (mg/L)	Percent Moisture (%)	Percent Solids (%)	Ash Content (%)	Nitrate Nitrite (mg/kg dry)	Total Kjeldahl Nitrogen (mg/kg dry)	Total Nitrogen (mg/kg dry)	Phosphorus (mg/kg dry)	Total Organic Matter (%)
SAND FILTER CRUST	ND	ND	ND	ND	ND	ND	54.7	45.3	89.7	6.5	9,100	9,100	980	10.3
AF18-SWFF-10/25	7,100 E	90	3.7	6.7	10	0.19	ND	ND	ND	ND	ND	ND	ND	ND

ND = no data collected for these samples

E: result exceeded calibration range

Table C-19

Analytical Data for Perpendicular Harvest, Wedge Wire Screen, Sand Filter, and Drying Subplot Tests on November 14, 2018

Sample Name	Description	Total Solids (mg/L)	Total Suspended Solids (mg/L)	Nitrate Nitrite (mg/L)	Total Kjeldahl Nitrogen (mg/L)	Total Nitrogen (mg/L)	Total Phosphorus (mg/L)	Percent Moisture (%)	Percent Solids (%)	Ash Content (%)	Nitrate Nitrite (mg/kg dry)	Total Kjeldahl Nitrogen (mg/kg dry)	Total Nitrogen (mg/kg dry)	Phosphorus (mg/kg dry)	Total Organic Matter (%)
AF-18-FFCOMP-11/14	Composite of First Flush Water	3600 E	110	1.1	6.2	7.3	0.44	ND	ND	ND	ND	ND	ND	ND	ND
AF18-WWEFF-FW-11/14	Effluent from running the perpendicular harvest free water sample buckets over the wedge wire screen	4500 E	790	0.22	20	20	3.1	ND	ND	ND	ND	ND	ND	ND	ND
AF18-WWEFF-PS-11/14	Effluent from running the perpendicular harvest pushed solids sample buckets over the wedge wire screen	21000 E	10,000	0.3	43	43	15	ND	ND	ND	ND	ND	ND	ND	ND
AF18-WWSOL-11/14	Separated solids generated by running the AF18-WWEFF-PS-11/14 sample buckets over the wedge wire screen	ND	ND	ND	ND	ND	ND	92	8	ND	75.2	370	21,000	3,900	24.8
SF-EFF-11/14	Effluent from the sand filter after loading with AF18-WWEFF-FW-11/14 and AF18-WWEFF-PS-11/14	4800 E	26	ND	ND	ND	ND	ND	ND	ND	ND	ND	ND	ND	ND
CENTRAL CHANNEL SUBPLOT	Central Channel Subplot, set up on 10/25/2018, entire dried volume collected and bagged up on about 11/1/18	ND	ND	ND	ND	ND	ND	79.9	20.1	ND	74	9.6	21,000	1,600	26
CENTRAL CHANNEL SUBPLOT DUP	Central Channel Subplot, set up on 10/25/2018, entire dried volume collected and bagged up on about 11/1/18	ND	ND	ND	ND	ND	ND	ND	ND	ND	75.3	ND	ND	ND	24.7
WWSOL 1 WEEK	Screened Solids Subplot, set up on 10/25/2018, entire dried volume collected and bagged up on about 11/1/18	ND	ND	ND	ND	ND	ND	90.8	9.2	ND	71.1	380	20,000	2,900	28.9

ND = no data collected for these samples

E: result exceeded calibration range

Table C-20

Analytical Data for Wedge Wire Screen, Sand Filter, and Desktop Settling Tests on November 29, 2018

Sample Name	Description	Total Solids (mg/L)	Suspended Solids (mg/L)	Nitrate Nitrite (mg/L)	Kjeldahl Nitrogen (mg/L)	Total Nitrogen (mg/L)	Total Phosphorus (mg/L)	Percent Moisture (%)	Percent Solids (%)	Ash Content (%)	Nitrate Nitrite (mg/kg dry)	Total Kjeldahl Nitrogen (mg/kg dry)	Total Nitrogen (mg/kg dry)	Phosphorus (mg/kg dry)	Total Organic Matter (%)
AF18-HAR29-SET TEST-11/29	Harvest material sample from the portion set aside for the desktop settling test	ND	ND	ND	ND	ND	ND	97.2	2.8	78.4	150	30,000	30,000	2,000	21.6
AF18-SAND FILTER CRUST-11/29	Solids crust on top of sand filter	ND	ND	ND	ND	ND	ND	33.1	66.9	90.5	3.1	3,500	3,500	760	9.5
SF-EFF-11/29	Sand filter effluent after loading with HAR buckets	2500 E	12	16 B	5	21	0.1 U	ND	ND	ND	ND	ND	ND	ND	ND
AF18-WWEFF-SET TEST-11/29	Effluent for the desktop settling test, created by running the harvest sample over the wedge wire screen	16000 E	6,200	0.07 J	13	13	1.1	ND	ND	ND	ND	ND	ND	ND	ND
AF18-WWSOL-11/29	Separated solids generated by running the harvest sample over the wedge wire screen	ND	ND	ND	ND	ND	ND	92.0	8.0	75.6	350	13,000	13,000	2,700	24.4
CENTRAL CHANNEL SUBPLOT-DRY-11/29	Central Channel Subplot material, set up on 11/14/2018	ND	ND	ND	ND	ND	ND	76.4	23.6	78	6.5	15,000	15,000	1,900	22
WWSOL-SUBPLOT-DRY-11/29	Screened Solids Subplot material, set up on 11/14/2018	ND	ND	ND	ND	ND	ND	55.1	44.9	76.1	3.9	13,000	13,000	1,400	23.9

ND = no data collected for these samples

E: result exceeded calibration range

J: result is less than the RL but greater than or equal to the MDL and the concentration is an approximate value

Attachment A
Algal Digester Report
University of Maryland

1 Algal Digestion

In addition to sequestering nutrients through the algal turf scrubber (ATS) operation, an additional project goal was to design, build, and determine the effectiveness of an anaerobic digestion (AD) system capable of producing renewable energy from the algae harvested from the ATS system. Batch-scale experiments in Phase I concluded that anaerobic digestion of the ATS-harvested algae could successfully produce biogas, and enabled us to design an appropriately sized system for collecting the expected biogas production from the algal biomass. In Phase II, the process was scaled up to pilot-scale unit, which was installed at the Dundalk Terminal at the Port of Baltimore in 2017. The pilot-scale system consisted of three digesters in series. Digesters 1 and 2 (D1 and D2) each had an effective digestion capacity of 1700 L, while Digester 3 (D3) had a 500 L capacity. During Phase II, the three digesters were plumbed in series and operated as a single continuous unit. This design resulted in a high overall hydraulic retention time (HRT) for the algae digestion system, and limited replicability due to the use of a single digestion system connected in series. For the second season of pilot-scale testing in Phase III, modifications were implemented to the system to improve upon the system design from Phase II.

A timeline of the Phase III ATS digestion proof-of-concept is provided in Appendix A-1.

1.1 Phase I: Batch-Scale Studies

Phase I was completed in December 2016, and consisted of a 60-day biomethane potential (BMP) test performed at batch-scale at the University of Maryland. The purpose of this experiment was to determine if algae was suitable as a feedstock for digestion, as well as the impact of algal moisture content on CH₄ production. It was determined that CH₄ production could occur using fresh algae (93% moisture content) supplied directly to the digester without drying. While slightly higher production was observed using 'dry' and 'medium-wet' algae (22% and 62% moisture content, respectively), it was determined that pre-processing in the field would add energy, time, and management complications when the system was scaled up to the pilot-scale.

1.2 Phase II: First Season of Pilot-Scale Digester Operation

Construction of pilot-scale AD units at the Port of Baltimore was completed in 2017. Two digesters with 1700 L capacity (D1 and D2) each and a third digester with a 500 L capacity (D3) were plumbed in series and started on August 17, 2017. The three-unit system proceeded to operate successfully for 18 weeks. The first eight weeks consisted of digester startup, after which digester operations stabilized and biogas production increased. After achieving stability, the system produced 1430 L/week of biogas. The CH₄ concentration in the biogas in all three digesters was higher than expected based on the results of Phase I, with 60-80% CH₄ in the pilot-scale operation compared to 60-65% CH₄ in the biogas in the lab-scale systems.

There were several flaws observed in the system design during Phase II. One of the most immediate problems observed was malfunction of the digester heating systems. Given that the pilot-scale AD system was located outdoors, the temperature within the digesters was subject to fluctuation based on ambient atmospheric temperatures. Bacteria used in anaerobic digestion process require elevated (100 °F), consistent temperature for optimal growth. A basic heating system was included with the delivered digesters. This heating system proved ineffective in Phase II, as the lack of insulation around the digestion units led to release of heat into the atmosphere more rapidly than the heaters could heat the systems. This heat loss occurred even after installation of a greenhouse cover and fiberglass around the digester units, leading to unstable digester temperatures and a gradual decline in biogas production in Phase II as seasonal temperature declined. It was also discovered at the end of Phase II that the heaters had physically damaged the digesters, as the heat supplied melted and burned the digester bags and fiberglass insulation. As a result, the conductive heating systems were discarded at the end of Phase II in favor of a new system designed to extract the digester contents and externally heat the AD content through an external heater unit.

Secondly, the pilot-scale digestion systems lacked replicability as designed. As each digester was connected in series and shared a single flow of digestate, and could not be considered replicates. For Phase III, D1 was disconnected from D2 and operated in parallel rather than in series. While D2 and D3 operated in series with a longer HRT compared to D1.

1.3 Phase III: Experimental Design and System Modification

The goal of Phase III was to improve the anaerobic digestion process and increase CH₄ output from the Phase II design by reconfiguring the system based on knowledge gained from the pilot-scale AD testing in Fall 2017. For Phase III, D1 was disconnected from the other digesters and operated in parallel to D2 and D3, which remained connected and operated in series. This allowed D1 to act as a replicate of D2, while also testing the effect of two HRTs on the production of CH₄-enriched biogas. Construction to re-plumb the digestion system was performed between June and July 2019, after which the digesters were operated according to the experimental design provided in Table 1.

Table 1: Experimental design for Phase III pilot-scale algal digestion system, which operated from 7/25/2018 to 11/21/2018.

Phase III Digester Operation
- Algal harvest was pumped into the AD decant tank every Thursday
- Digesters were fed according to schedule in Table 2
- Digesters were sampled M-W-F until 09/07/2018, and then W-F until digester shutdown on 11/21/2018
- Laboratory analysis of biogas, and algal influent and AD effluent samples

A new heating system was installed in D1 and D2 to provide external heat to the systems regardless of atmospheric temperature. Construction on the new heating system was performed concurrently with D1 and D2 replumbing efforts, which were completed in July 2019. A delay in delivery of a custom-ordered electronic board to operate the new system led to a delay in deployment of the heating system until October 2018. While the start-up tests were successful and suggested the system was capable of effectively maintaining a stable digester temperature of 80-100 °F, the pumps used to recirculate the digestate were too strong for the volume of fluid being recirculated. The pumping force resulted in excessive draw-down of the digester fluid, which in turn created a vacuum within D1 and D2 that nearly led to digester rupture via inflation. An emergency shut-down and evacuation of digester headspace gas was conducted, but the resulting loss of an anaerobic environment destabilized the two digesters for the remainder of the study. The initial success of the system indicates that recirculation heating is effective for the system as designed but a smaller pump is needed to prevent draw-down of digester fluid. A re-design of the heating system will be conducted in the future to maintain a stable digestion temperature throughout the study period.

1.4 Phase III: Digester Start-Up and Operations

The Phase III operation time-period of the algal digestion was 18 weeks from July 23, 2018 through November 21, 2018. Manure inoculum was loaded into the system on July 23, 2018, followed by the first algal addition on July 25, 2018. With a volume of 1700 L and an estimated feeding rate of 68 L of algae per day, the D1 system was designed with an expected HRT of 25 days. With a combined volume of 2200 L and the same feeding rate, the D2-D3 system had an expected HRT of 32 days. Feeding was scheduled to be performed on a M-W-F schedule for the duration of the study. This feeding schedule was designed based on the volume of algae produced from the ATS system during Phase II.

During Phase III operation, however, the volume of algae harvested from the ATS in Phase III was lower than was observed in Phase II, and therefore, the supply of feeding material for the digestion system was much less than expected. The Baltimore region received more rainfall in Summer 2018 than any prior year on record, which in turn reduced salinity in the Patapsco River and negatively impacted algal growth on the ATS. The planned feeding volume of 68 L/day could not be met with the algal biomass available, so an adjusted feeding plan was adopted to feed all of the algae available to the digesters to maintain methane production. The volume of the weekly algal harvest to be feed each Monday, Wednesday and Friday was calculated using Equation 1.

Equation #1

$$\text{Feed} = \text{Harvest}/14 * x$$

where:

Feed = Volume of algae to feed to digester (gal)

Harvest = Volume of algae harvested from the ATS (gal)

x = Number of days before next feeding (for example, x=2 if feeding on Mon and then Wed and x=3 if feeding Tues and then Friday)

No feeding was performed on Wednesday of Week 6 (August 29, 2019) due to complete depletion of algae available. An adjusted feeding schedule was also used in Week 7, with algae addition on Tuesday and Friday, due to the Labor Day holiday that Monday. The Monday, Wednesday, Friday feeding schedule resumed in Week 8 (September 10, 2018) and was maintained until Week 13 (October 19, 2018). Supply was again depleted in Week 14, and therefore, feeding of the digesters did not occur until after MES harvested additional substrate on October 25, 2018. In November 2018, MES staff reduced the harvest schedule from weekly to biweekly collections due to declining growth of the algal turf. To account for this, the feeding formula was adjusted in Week 16 to conserve supply using Equation 2.

Equation #2

$$\text{Feed} = \text{Harvest}/28 * x$$

where:

Feed = Volume of algae to feed to digester (gal)

Harvest = Volume of algae harvested from the ATS (gal)

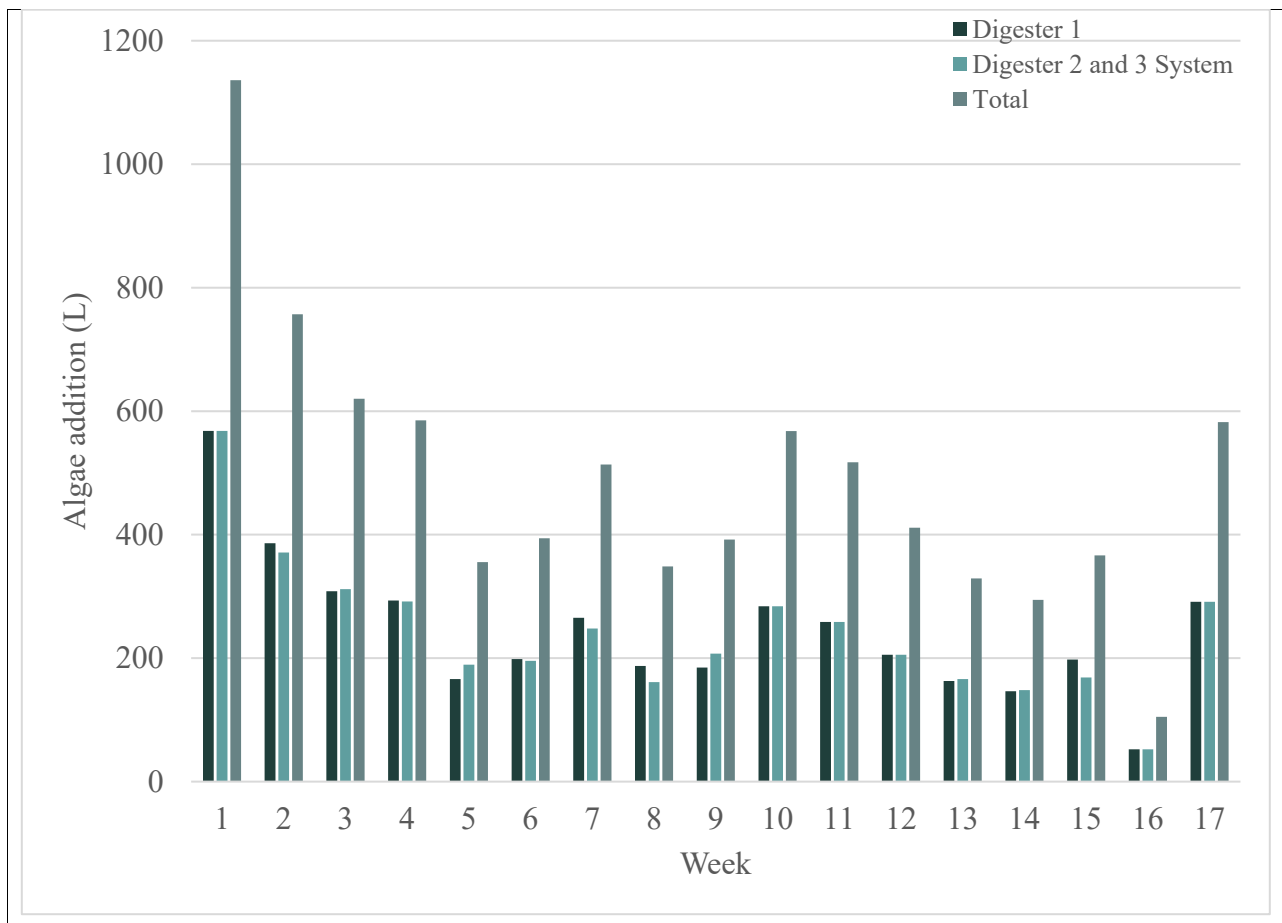
x = Number of days before next feeding (for example, x=2 if feeding on Mon and then Wed and x=3 if feeding Tues and then Friday)

The final feeding was performed in Week 17 (November 16, 2018), with only one feeding that week, and then the digesters were shut down in Week 18 (November 21, 2018). Over the 18-week study, a total of 4,156 L of algal biomass was fed to D1 and 4,119 L of algal biomass was fed to the D2-D3 system. Due to the feeding schedule adjustments, there was an average feeding of 35 ± 4 L/day for each of the two digestion systems. The HRT of each system averaged 63 ± 11 days in D1 and 82 ± 14 days in the D2-D3 system (Table 2, Figure 1).

Table 2: The quantity of algae fed each week to the Digesters and the resulting changes in the overall HRT of digestion units for Phase III.

Week	Feeding Schedule	Digester 1 Fed (L)	Digester 2 + 3 Fed (L)	Total Fed (L)	HRT of D1 (days)	HRT of D2 + D3 (days)
1	W-F	568	568	1136	21.0	27.1
2	M-W-F	386	371	757	30.8	41.5
3	M-W-F	308	312	620	38.6	49.4
4	M-W-F	293	292	585	40.6	52.8
5	M-W-F	166	189	355	71.7	81.3
6	M-F	198	196	394	60.0	78.7
7	Tu-F	265	248	513	44.8	62.1
8	M-W-F	187	161	349	63.5	95.5
9	M-W-F	185	207	392	64.4	74.3
10	M-W-F	284	284	568	41.9	54.2
11	M-W-F	259	259	517	46.0	59.6
12	M-W-F	206	206	411	57.9	74.9
13	M-W-F	163	166	329	73.0	92.8
14	M-F	146	148	294	81.3	104.0
15	M-W-F	198	169	366	60.2	91.3
16	M-F	52	52	105	227.0	293.8
17	F	291	291	582	40.9	52.9
18	N/A	N/A	N/A	N/A	N/A	N/A
Total		4156	4119	8275	1060	1390
Average		244	242	487	62.6	81.5
SE		28	27	55	11.0	14.2

Figure 1: Volume of algae fed to the digestion systems during Phase III.



1.5 Phase III: Biogas Production

Stable digester operations were maintained for 13 weeks, from July 25 through October 19, 2018. During this period, D1 and the D2-D3 system produced 1840 and 2461 L of biogas consisting of 1290 L and 1620 L of CH₄, respectively. Overall, there was an average CH₄ production of 107 ± 20 L CH₄/week for D1 and 135 ± 19 L CH₄/week for the D2-D3 system.

Chemical composition of biogas in digester headspace was measured during each day of feeding using a Landtec Biogas 5000+ gas meter. This was performed via a sampling port connected to the top of each digester bag's gas removal system. Measurements were averaged on a weekly basis to determine the mean percent composition of four primary gas components, methane (CH₄), carbon dioxide (CO₂), oxygen (O₂), and balance gas (N₂), in each digester during each week of study (Table 3).

Table 3: Total biogas production and average composition of the biogas during algal digestion from Weeks 1-13. (Data from Weeks 14-18 omitted due to instability in D1 and D2 starting in Week 14).

Source	Total Biogas (L)	CH ₄ (%)	CO ₂ (%)	O ₂ (%)	N ₂ (%)
D1	1840	73.0 ± 1.57	16.7 ± 0.45	0.25 ± 0.05	10.2 ± 1.69
D2	1781	68.9 ± 3.42	16.7 ± 0.45	0.34 ± 0.15	14.1 ± 3.6
D3	680	69.2 ± 2.81	13.5 ± 0.48	0.20 ± 0.01	17.2 ± 3.11

The percentage of CH₄ in the digester headspace gas rose steadily in all three digesters during the startup period from Weeks 1-3. Production remained steady between, with 70-80% CH₄ in the biogas of Digesters 1 and 2 until Week 14. At Week 14, there was a malfunction during start-up testing of the heating and recirculation system that had been installed for Phase III, as the pump was too strong and led to atmospheric air intrusion into the two digesters through the recirculation pumps. The problem was detected during gas composition analysis, with a sudden drop in CH₄ percentage and corresponding rise in N₂ and O₂ in the biogas composition. The heating and recirculation systems were shut down indefinitely during Week 15, and the composition of the headspace gas began returning to expected levels. Digester 3 was unaffected by the malfunction, as it was not connected directly to the heating and recirculation systems. With the exception of a small decrease in percent CH₄ in Week 8 due to a leak, Digester 3 maintained biogas production with 70-80% methane content for the duration of the study. As in Phase II, the concentration of CH₄ present during optimal digester operations was higher than that predicted in Phase I (Figures 2-4).

Figure 2: Digester 1 headspace biogas composition.

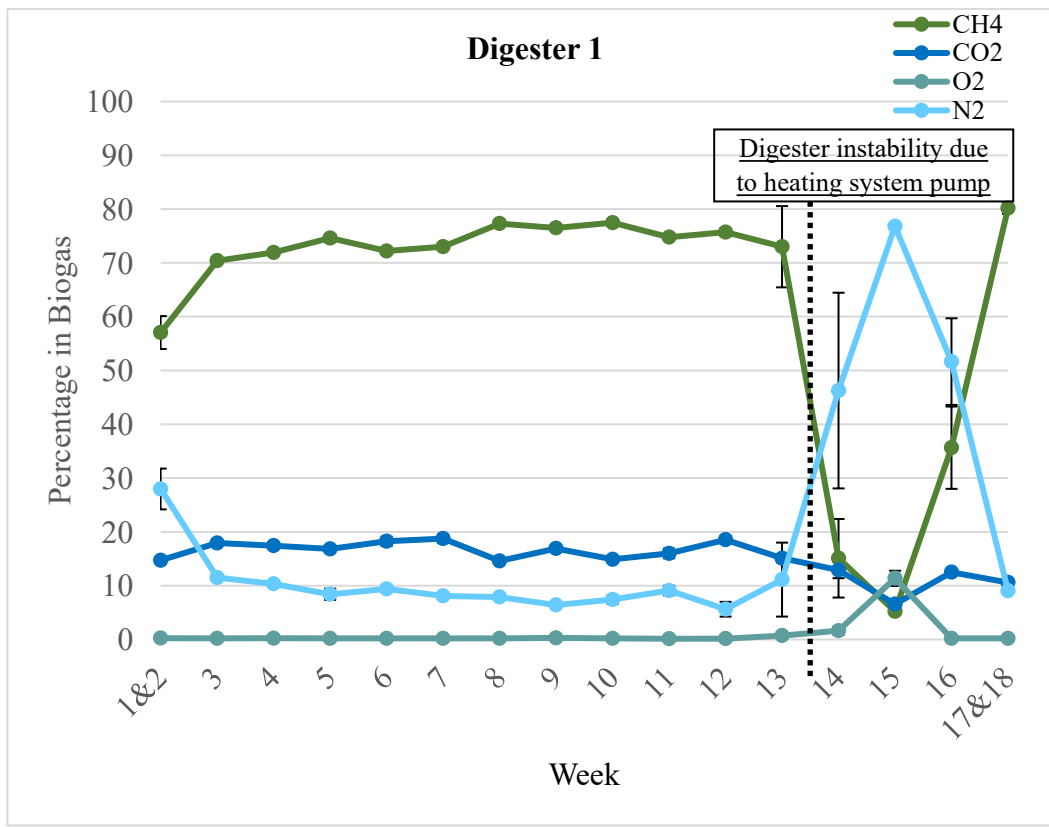


Figure 3: Digester 2 headspace biogas composition.

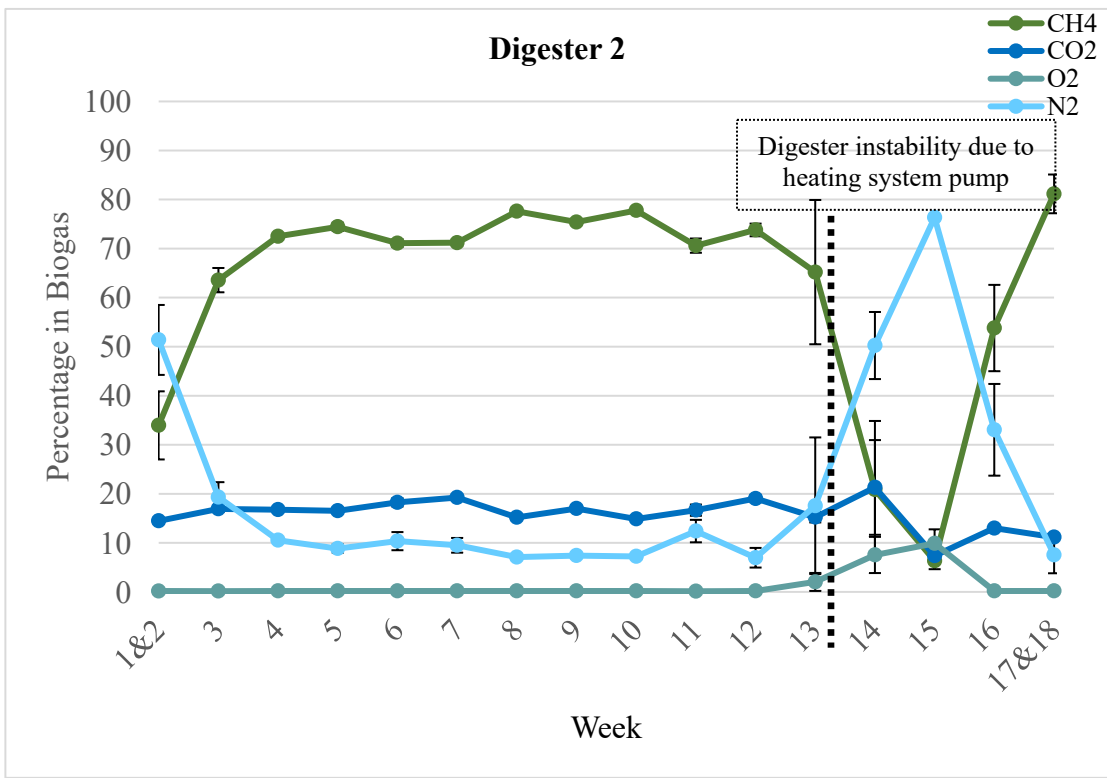
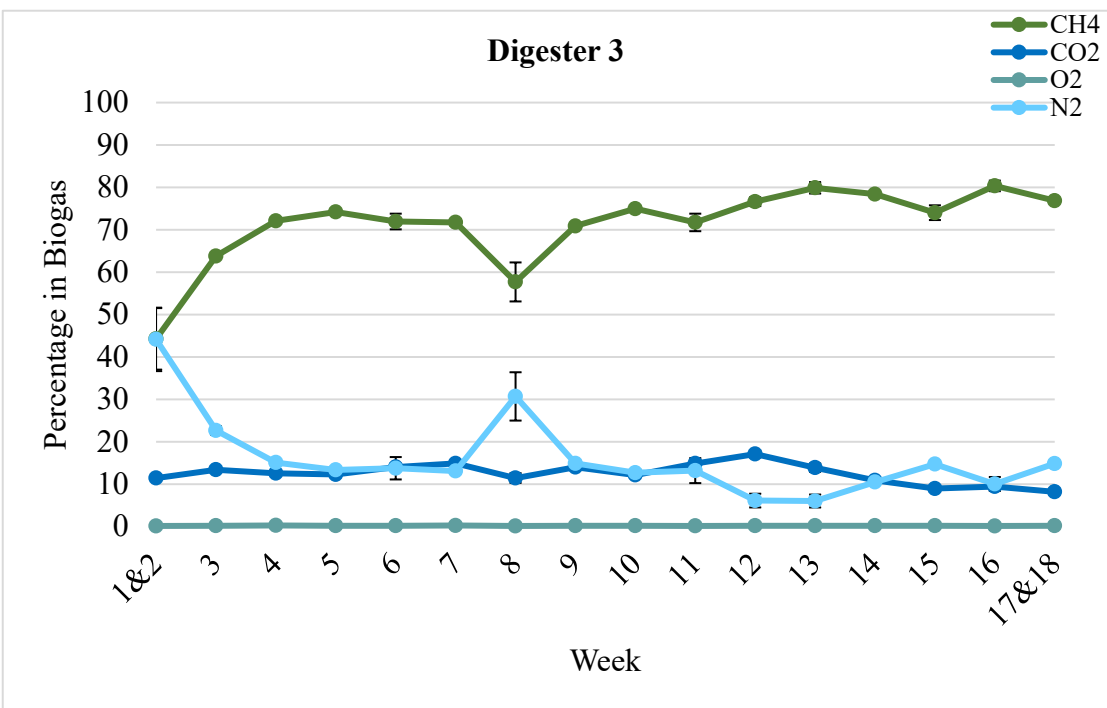


Figure 4: Digester 3 headspace biogas composition.

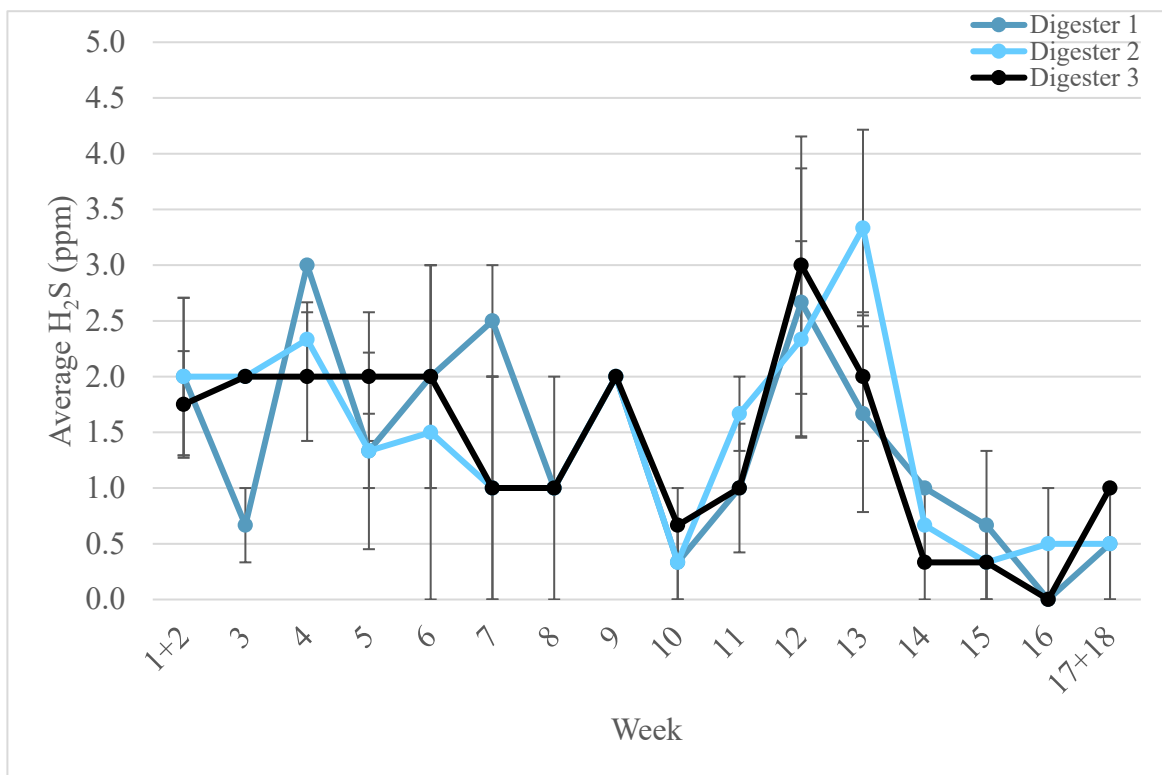


Hydrogen sulfide (H₂S) content of the headspace gas was also measured via Landtec. The H₂S concentration varied from 0 - 4.5 ppm (0 to 0.00045%) over the course of the study in all three digesters. Production of H₂S was extremely low. For context, dairy manure digesters often have H₂S production up to 10,000 ppm (1% of total biogas content). Previous experiments from Phase I also yielded lower than expected H₂S, with 17-56% less H₂S production in the digesters co-digesting algae compared to those utilizing manure inoculum alone. It was hypothesized that this may be due to the high iron content of the algae reducing the H₂S through FeS formation (Figure 5). Samples of algal influent from Weeks 2, 9, 12, and 15 were analyzed for mineral analysis to determine iron content of the influent. The results indicated an iron content of 1138 ± 161 ppm Fe (Table 4).

Table 4: Iron (Fe) content in the algal substrate. Analyses performed by AgroLab.

Sample Name	Date of Collection	Iron (ppm Fe)
I-W1-pIII-2	07/25/2018	1143
I-W9-M-pIII	09/17/2018	1568
I-W12-F-pIII-3	10/12/2018	1050
I-W15-F-pIII-1	11/02/2018	792.6
Average	-	1138
SE	-	161

Figure 5: Hydrogen sulfide (H₂S) content of digester headspace biogas.



Following the initial startup period, biogas production was maintained in all three digesters until Week 9, when leaks were discovered in the digester gas collection system. Subsequent repairs required the headspace to be purged, and the digester systems be reset. Repairs on Digester 2 and 3 were completed in Week 10, allowing data to be collected once again. Repairs on Digester 1 continued until the end of Week 10, resulting in a loss of another week of biogas volume data. Biogas accumulation resumed in all three digesters starting in Week 11 and began to rise steadily, peaking in Week 13 before the aforementioned malfunction of the heating and pumping systems in Week 14. Repairs once again resulted in a loss of biogas quantity data in Week 14. Biogas levels temporarily rose again in Week 15, but declining ambient temperatures and a lack of heat from the disabled recirculation system resulted in a steady drop in production until the end of the study in Week 18 (Figures 6-9).

Figure 6: Total biogas production from algal digestion.

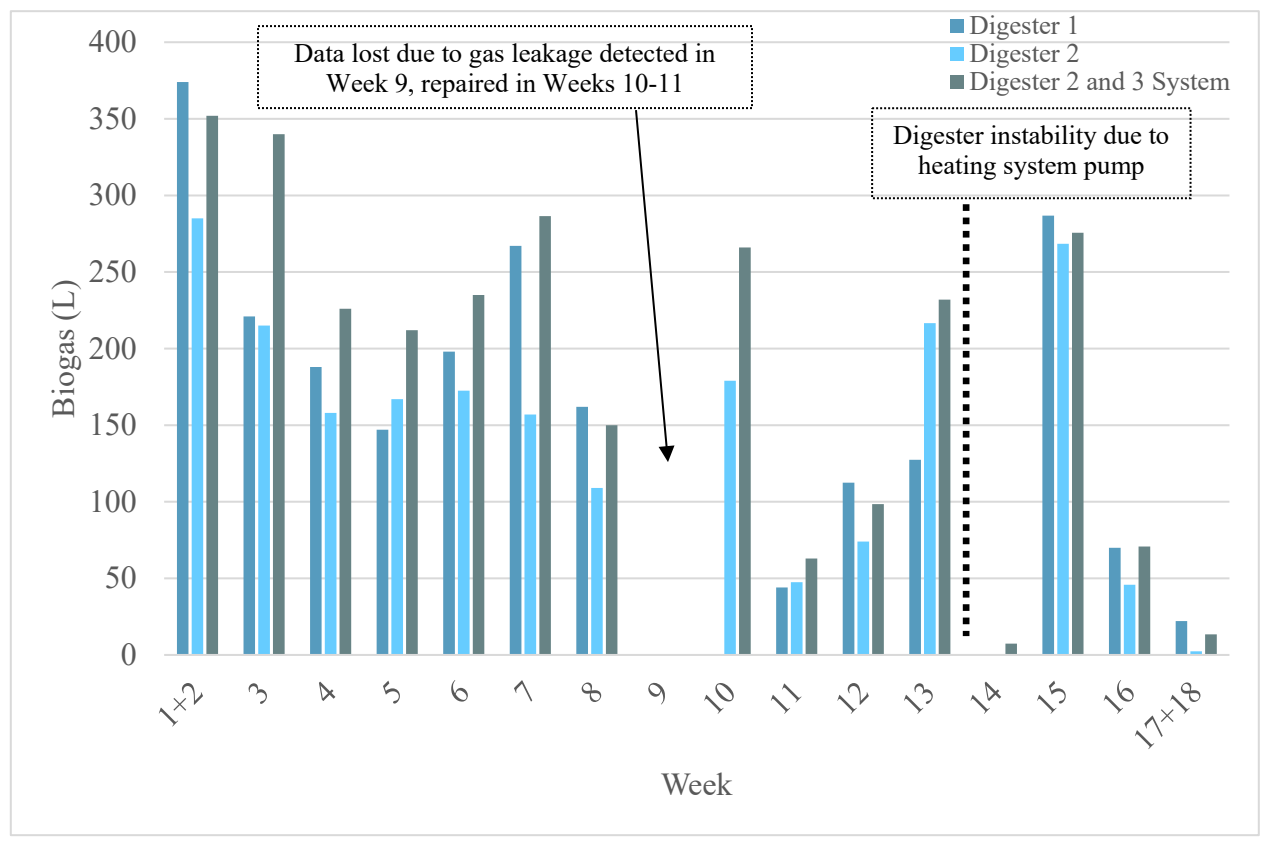


Figure 7: Total methane production from algal digestion.

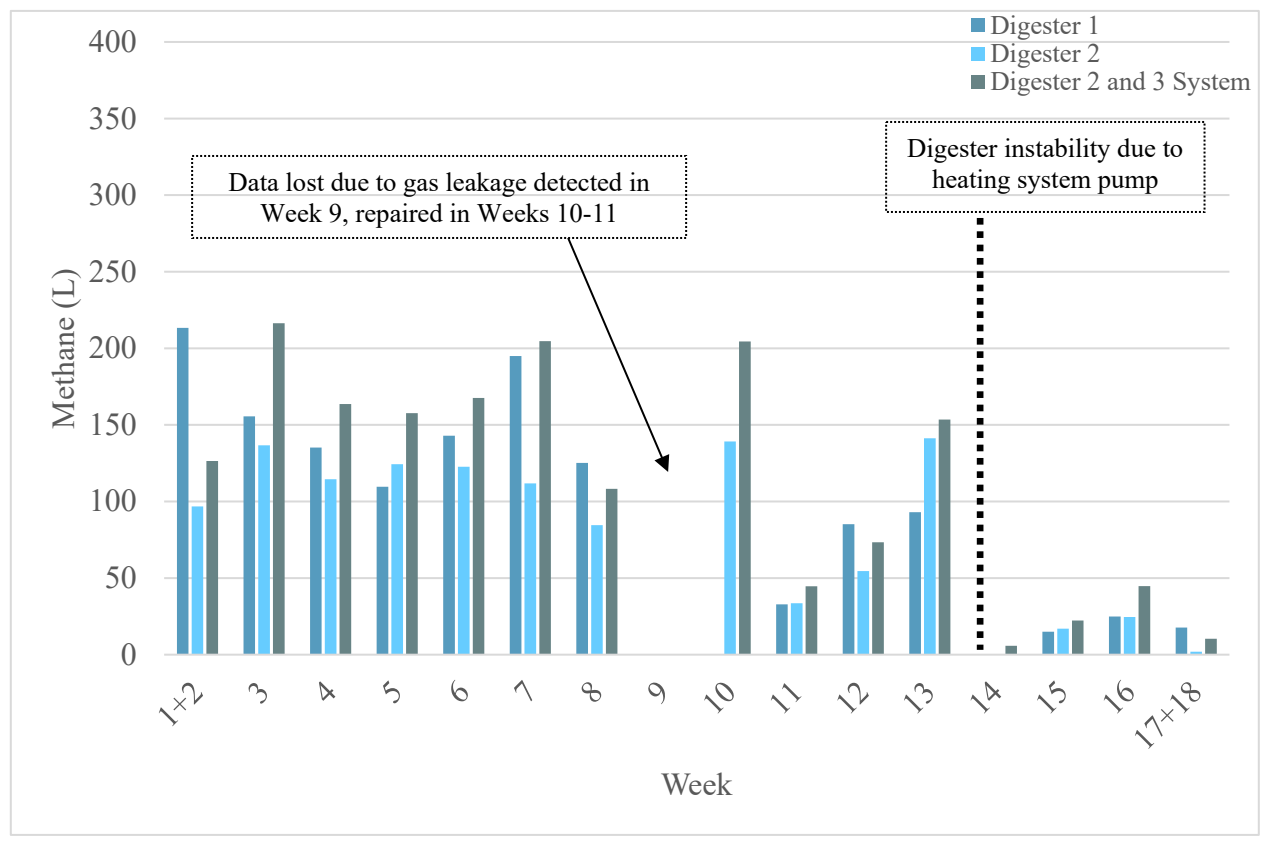


Figure 8: Methane production normalized by L of algae fed.

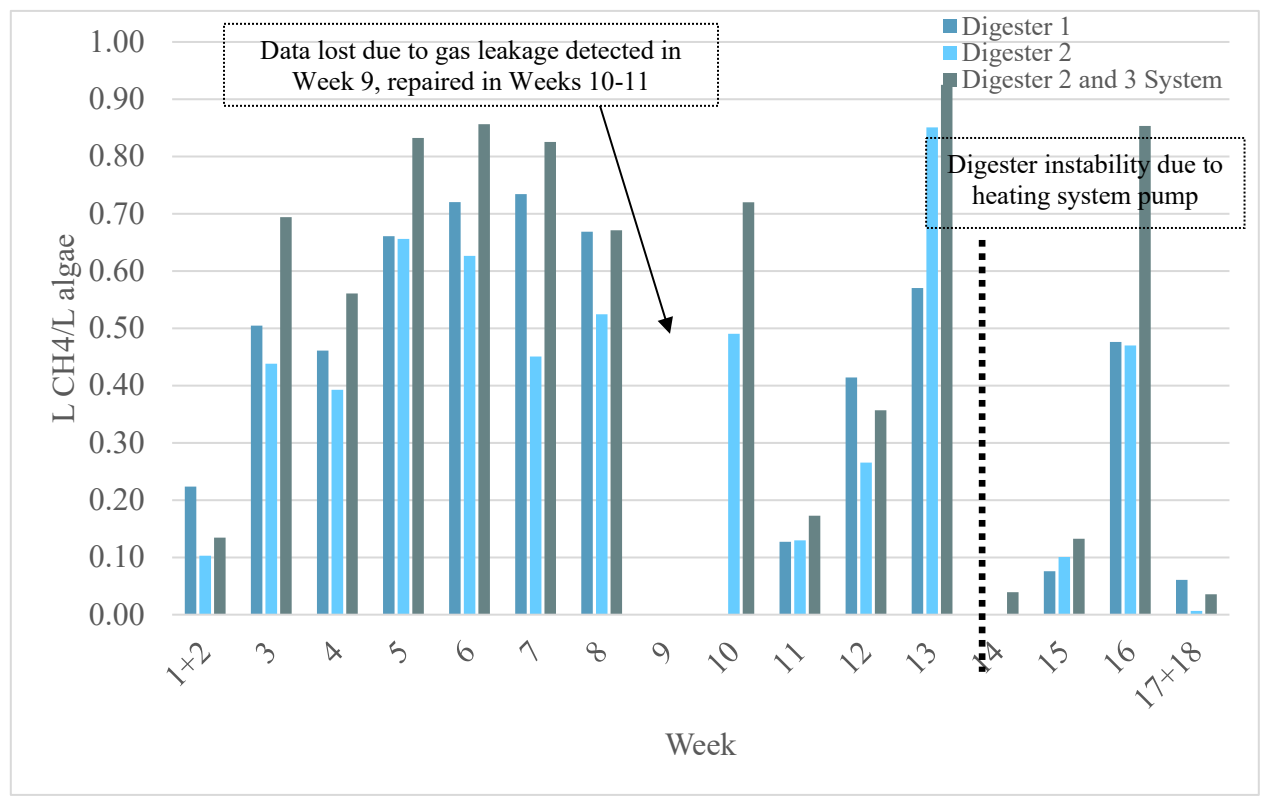
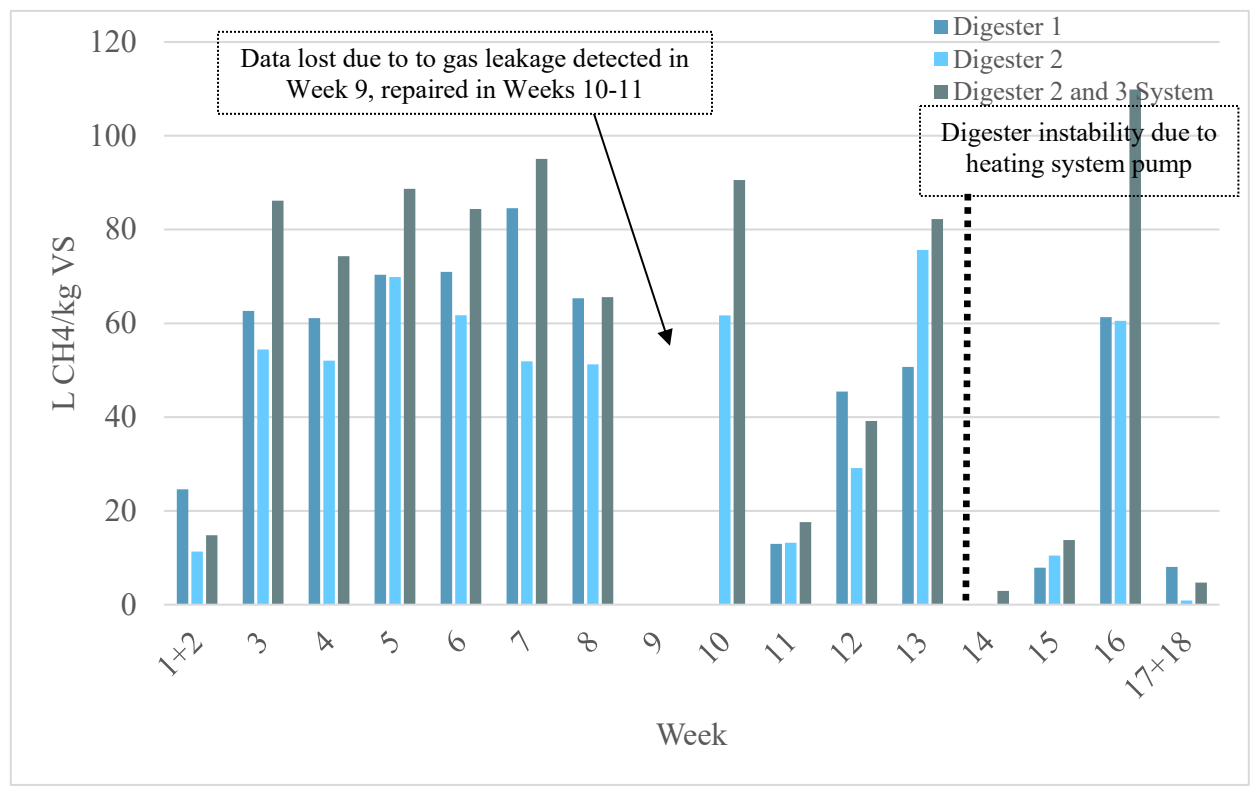


Figure 9: Methane production normalized by kg VS in algal feedstock.



A detailed analysis of volatile solids (VS), chemical oxygen demand (COD), and volatile fatty acids (VFAs) is presented in Appendix A-2 for the influent and effluent of each digester. The results of the mass balance and biogas measurements suggest an overall 20-26% greater digestion of the algal feedstock in the D2-D3 system, with the corresponding increase in CH₄ production due to the increased HRT of the D2-D3 system compared to D1.

1.6 Phase III: Nutrient Loading

The uptake of dissolved inorganic nutrients from the Patapsco River was a primary goal of the ATS operation. Ammonia, TKN, and TP concentrations in the algal feedstock averaged 139 ± 13 mg NH₄/L, 762 ± 78 mg N/L, and 169 ± 39 mg P/L, respectively. During digestion, organic matter is decreases, which increases the dissolved NH₄ concentrations in the digestate. As expected, there was an increase in NH₄ during digestion of 100% in D1 and 129% in the D2-D3 system. There was an average decrease in the total nitrogen (TKN) of 35% and 31% in D1 and the D2-D3 systems, respectively, and an average decrease in TP of 41% and 57% observed in D1 and the D2-D3 systems, respectively. While no change in TKN or TP is expected during digestion processes, settling of solids inside the digesters can result in accumulation of TKN and TP in settled solids and less N and P in the digester effluent, which was observed in this case. There was no mixing of the digester contents,

which should have occurred with the installation of the new heating recirculation system. The operation of the heating and recirculation of digestate will be a priority for future work to obtain a better mass balance of nutrient flow through the system.

The ATS data collected by MES and analyzed at TestAmerica was compared to the digester influent samples tested by UMD. MES collected ATS data from May 31, 2018 through November 29, 2018, consisting of 15 TKN samples and 11 TP samples. Within the digester operational period (July 26, 2018 through November 1, 2018), there were 13 TKN samples and 9 TP samples collected by MES and analyzed. To compare between TestAmerica’s data, reported in kg TKN/kg dry weight and kg TP/kg dry weight, the data from UMD for TKN and TP data was converted to kg/kg TS using corresponding influent TS data (Table 5).

Table 5: Comparison of algae TKN and TP data from TestAmerica and UMD.

Data Source	Date	TKN (mg/kg TS)	TP (mg/kg TS)
Test America	05/31/2018-11/29/2018	15,200 ± 1,710	1,550 ± 152
	07/26/2018-11/1/2018	12,800 ± 1,310	1,380 ± 166
UMD	07/23/2018-11/21/2018	19,200 ± 1,850	4,560 ± 1,280

The data comparison does show differences in analyses, especially in terms of the TP data. A detailed report of nutrient concentrations collected and analyzed by UMD is provided in Appendix A-2.

1.7 Phase IV: Proposal and Future System Operations

While the digestion systems successfully utilized ATS algae as a feedstock for CH₄-enriched biogas production, operation was performed under sub-optimal conditions due to the shorten time frame of study (late July to late November), the lack of heating, and the low quantity of ATS-derived algae harvested. Record rainfall and a malfunction of the heating systems resulted in disruptions to operation plans. Due to the lower algal biomass production, lower CH₄ production was observed than Phase II. Whereas the single 3-unit digester used in Phase II produced 588 ± 68 L/CH₄/week, the combined production of the three digester units in Phase III was only 107 ± 20 L CH₄/week for D1 and 135 ± 19 for the D2-D3 system. Combined, the digestion units in Phase III produced an average of 242 ± 34 L CH₄/week over the thirteen weeks of stable production, representing a decline in production of 59% compared to that of Phase II. There was low H₂S observed in Phase III, which suggested that the biogas could be used in a fuel cell with only minimal post-processing prior to use. In order to further explore the potential for production of high-quality biogas produced from

anaerobic digestion of algae, it is recommended that a third season of digester operation be performed under more normal ATS operation conditions with heated digesters over an entire ATS growing season (June – December).

The proposed Phase IV would utilize operational lessons learned in Phases II and III to operate the system under more optimal ATS operation conditions. The results of the nutrient analysis indicate that more complete mixing of digestate will result in more accurate measurements of nutrient flow through the digestion system. Thus, the recirculation system could remain in place for D1 and D2 in Phase IV, but a smaller pump size will be installed to prevent the malfunctions observed in Phase III. Additionally, to minimize the impact of ambient temperature changes on digester operations, Phase IV of operations will commence in late May 2019. It should be noted that D1 will also need to be reconstructed for Phase IV due to wind damage to the structure during overwintering in February 2019. While the existing structure will be removed, the loss of D1 presents an opportunity to test a new type of digester to compare production with D2. If a new digester is installed, it is expected that it will be run in the same parallel configuration used in Phase III.

Appendix A

Laboratory Report

Appendix A-1: Timeline of Phase III

Event	Completion Date
Contracts	
Contract extension with new funds sent to UMD	5/2/2018
Contract extension with new funds signed and returned to MES	5/8/2018
Contract adjustment to include Peter May in UMD portion sent to UMD	5/27/2018
Contract adjustment to include Peter May in UMD signed and returned to MES	7/6/2018
Heating Design and Procurement	
Detailed heating design sent to CVL Tech	5/8/2018
Detailed heating design sent to WATTCO	5/11/2018
Heating Vendor/Design Recommendation sent to MES in report	6/15/2018
MES initially preferred the less expensive option (WATTCO), so specifications with WATTCO's control panel were altered to match requirements being filled by CVL Tech	6/21/2018
WATTCO could not meet the delivery needs, so CVL Tech heating package was the final decision, CVL Purchase made	6/28/2018
Installed heaters	7/13/2018
Received control panel	9/19/2018
Electrical panel installation completed	10/01/2018
Operational training for new heating and circulation systems	10/17/2018
Activation of heating and circulation systems	10/17/2018
Testing heating and circulation systems	10/17/2018
Commence overnight operation of heating and circulation systems	10/20/2018
Shutdown of heating and circulation systems	10/26/2018
Winterization of heating and circulation systems	11/21/2018
Replumbing	
Deconstructed existing piping	7/13/2018
Purchase and install piping	7/13/2018
Hooked up electric	8/1/2018
Hooked up a grill to burn off vented biogas	7/16/2018
Repaired leaks discovered in Digester 2 gas lines	10/01/2018
Replaced cracked water trap on Digester 3 gas output line	10/01/2018
Re-sealed weathered influent pipe sealant on Digesters 2 and 3 with silicone	10/17/2018
Inoculum Loading	
Used Port's vacuum truck to collect and transport 4 m ³ of dairy manure digester inoculum	7/18/2018
Digester Loading and Operation	
Pumped algae from algal harvest into decant tank for digester feed	7/19/2018
Fed digesters 100 L of algae for startup (Week 1)	7/25/2018
Fed digesters continuously according to schedule in Table 3 & Figure 2 for 18 weeks, with continuous monitoring and sample collection.	Table 2 and Figure 1
Used Port's vacuum truck to drain digesters for winterization, leaving ~5" of digestate in system for next startup cycle	11/21/2018

Appendix A-2: Chemical Analysis of Algal Influent and Digester Effluent

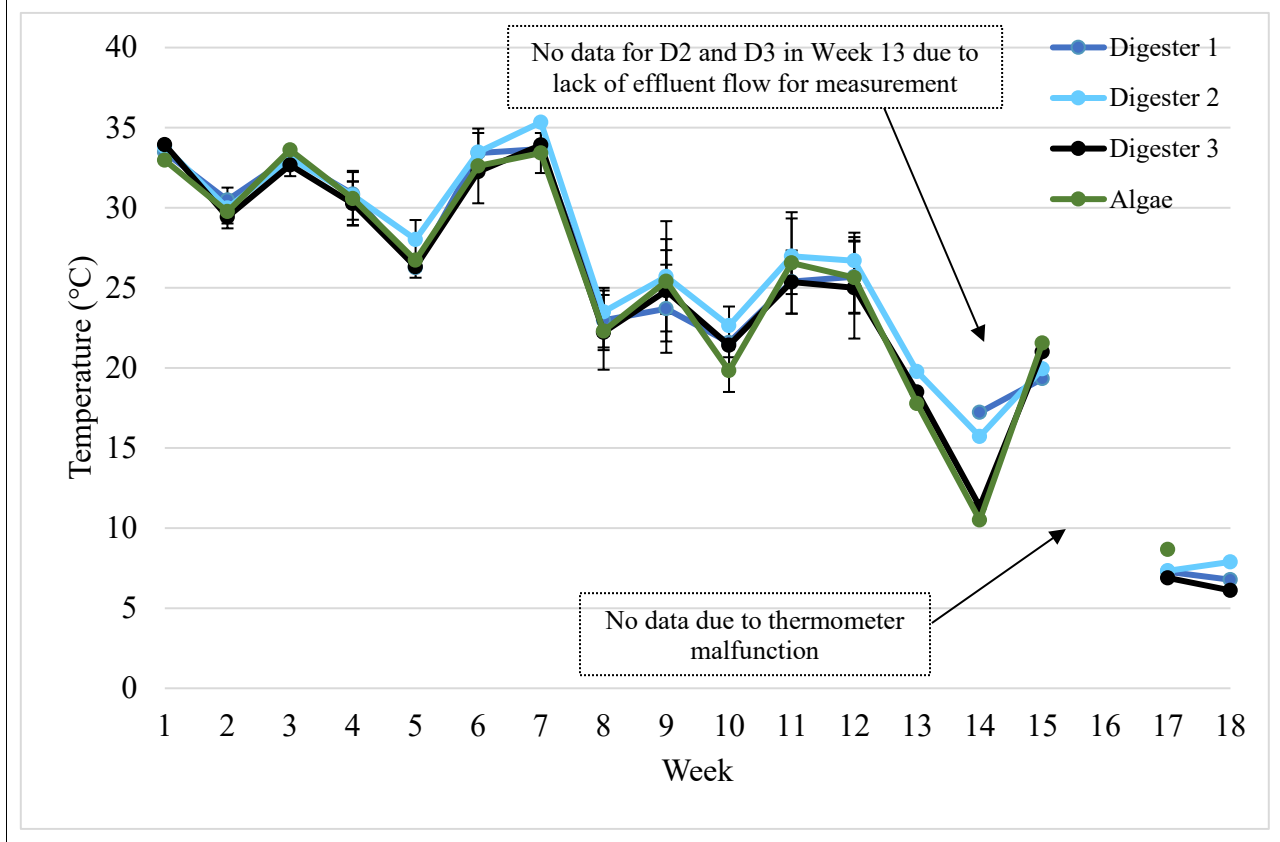
Algal influent samples to D1 and D2 were collected from the feeding pipe between the decant tank and D1 and D2 (one sample). Effluent samples were collected from the outflow of D1, D2, and D3. No effluent samples were collected on Friday, October 19 2018 from D2 and D3 in Week 13 due to a digestate leak in D2, which dropped the fluid level inside D2 such that effluent flow could not be induced via feeding until digestate levels were restored to regular levels in Week 14. No influent sample was collected during Week 18, as the last feeding of algae was performed at the end of Week 17.

pH and Temperature

The pH data was collected for the algal influent and digester effluents at the lab using a pH meter, prior to preservation for chemical testing. pH remained consistent throughout the study in all samples, with the pH of the algal feedstock averaging 7.18 ± 0.09 , and the pH of Digesters 1, 2, and 3 averaging 7.24 ± 0.16 , 7.26 ± 0.20 , and 7.31 ± 0.06 , respectively.

The temperature of the algal feedstock and digester effluents were measured in the field using a thermometer probe attachment for a Landtec Biogas 5000+. Maintaining a constant temperature in the digester systems was a high priority due to the negative impact of seasonal ambient temperature fluctuations on biogas production in Phase II, but due to the malfunction of the heating and recirculation system, heating could not be consistently supplied to the system as planned. Without active heating, the temperature of the influent and digesters was strongly affected by the ambient temperature. As a result, a gradual decline in temperature was observed over the 18 weeks as seasonal temperature changes impacted the digesters. This will be a priority for repairs in subsequent experiments.

Figure 10: Temperature data for algal influent and digester effluent.



Total and Volatile Solids Analysis

The total solids (TS) content of algae and digester effluent were analyzed by drying samples overnight at 100 °C. The percent of total solids in the algal feedstock averaged $3.92 \pm 0.20\%$ (39.5 ± 1.7 g/L) over the 18-week study period. The percent of total solids in effluent from D1 and the D2-D3 system over the same period averaged $1.56 \pm 0.52\%$ (16.0 ± 1.4 g/L) and $0.80 \pm 0.29\%$ (8.04 ± 0.70 g/L), respectively, representing a reduction of 60 and 80%, respectively, during digestion.

The volatile solids (VS) content of the samples was determined by incinerating the dried samples at 550 °C for two hours. The VS content is a proxy for the organic matter that is available for degradation by microbes in the digester. The VS content of the algal feedstock averaged $0.94\% \pm 0.16$, while that of the Digester 1 and Digester 2+ 3 system was $0.36\% \pm 0.12$ and $0.19\% \pm 0.08$, respectively. This indicates a removal efficiency of 62% and 80% in D1 and the D2-D3 systems, respectively. The increased reduction in solids in the Digester 2+ 3 system effluent reflects the increased digestion time due to a higher HRT (Tables 7-9)

Table 7: Total solid (TS) content of algal feedstock and digester effluent (%).

Week	Influent (%)	Digester 1 Effluent (%)	Digester 2 Effluent (%)	Digester 3 Effluent (%)
1	4.36 ± 0.63	0.88 ± 0.20	1.58 ± 0.49	1.27 ± 0.17
2	3.60 ± 0.10	1.14 ± 0.05	0.88 ± 0.08	0.58 ± 0.02
3	3.40 ± 0.10	1.13 ± 0.15	2.11 ± 0.35	0.71 ± 0.05
4	3.16 ± 0.14	1.41 ± 0.15	2.20 ± 0.47	0.51 ± 0.03
5	3.99 ± 0.13	1.00 ± 0.22	1.56 ± 0.04	0.57 ± 0.01
6	4.32 ± 0.20	1.97 ± 0.35	2.67 ± 0.14	0.74 ± 0.09
7	3.72 ± 0.05	1.64 ± 0.02	2.02 ± 0.10	0.88 ± 0.06
8	3.95 ± 0.22	1.87 ± 0.34	2.56 ± 0.24	0.65 ± 0.05
9	4.51 ± 0.10	2.66 ± 0.32	2.85 ± 0.41	0.85 ± 0.09
10	3.68 ± 0.77	1.75 ± 0.33	2.19 ± 0.52	0.91 ± 0.02
11	3.78 ± 0.08	1.61 ± 0.16	2.61 ± 0.13	1.03 ± 0.14
12	3.95 ± 0.18	2.35 ± 0.17	2.38 ± 0.21	1.36 ± 0.26
13	4.45 ± 0.19	1.49 ± 0.32	0.70 ± 0.02	1.28 ± 0.03
14	5.58 ± 0.01	1.41 ± 0.17	0.42 ± 0.03	0.44 ± 0.00
15	4.15 ± 0.39	1.59 ± 0.00	3.42 ± 0.01	0.48 ± 0.01
16	2.99 ± 0.01	1.72 ± 0.03	1.26 ± 0.07	0.75 ± 0.10
17	3.15 ± 0.04	1.99 ± 0.03	1.67 ± 0.04	1.02 ± 0.01
18	ND	0.56 ± 0.12	0.89 ± 0.02	0.43 ± 0.01
Average	3.92	1.56	1.89	0.80
SE	0.15	0.12	0.19	0.07

Table 8: Total solid (TS) content of algal feedstock and digester effluent (g/kg)

Week	Influent (g/kg)	Digester 1 Effluent (g/kg)	Digester 2 Effluent (g/kg)	Digester 3 Effluent (g/kg)
1	43.6 ± 6.3	8.8 ± 2	15.8 ± 4.9	12.7 ± 1.7
2	36 ± 1	11.4 ± 0.5	8.8 ± 0.8	5.8 ± 0.2
3	34 ± 1	11.3 ± 1.5	21.1 ± 3.5	7.1 ± 0.5
4	31.6 ± 1.4	14.1 ± 1.5	22 ± 4.7	5.1 ± 0.3
5	39.9 ± 1.3	10 ± 2.2	15.6 ± 0.4	5.7 ± 0.1
6	43.2 ± 2	19.7 ± 3.5	26.7 ± 1.4	7.4 ± 0.9
7	37.2 ± 0.5	16.4 ± 0.2	20.2 ± 1	8.8 ± 0.6
8	39.5 ± 2.2	18.7 ± 3.4	25.6 ± 2.4	6.5 ± 0.5
9	45.1 ± 1	26.6 ± 3.2	28.5 ± 4.1	8.5 ± 0.9
10	36.8 ± 7.7	17.5 ± 3.3	21.9 ± 5.2	9.1 ± 0.2
11	37.8 ± 0.8	16.1 ± 1.6	26.1 ± 1.3	10.3 ± 1.4
12	39.5 ± 1.8	23.5 ± 1.7	23.8 ± 2.1	13.6 ± 2.6
13	44.5 ± 1.9	14.9 ± 3.2	7 ± 0.2	12.8 ± 0.3
14	55.8 ± 0.1	14.1 ± 1.7	4.2 ± 0.3	4.4 ± 0
15	41.5 ± 3.9	15.9 ± 0	34.2 ± 0.1	4.8 ± 0.1
16	29.9 ± 0.1	17.2 ± 0.3	12.6 ± 0.7	7.5 ± 1
17	31.5 ± 0.4	19.9 ± 0.3	16.7 ± 0.4	10.2 ± 0.1
18	ND	5.6 ± 1.2	8.9 ± 0.2	4.3 ± 0.1
Average	39.1	15.7	18.9	8.03
SE	1.5	1.2	2.0	0.69

Table 9: Volatile solid (VS) content of algal feedstock and digester effluent (% dry weight)

Week	Influent (%)	Digester 1 Effluent (%)	Digester 2 Effluent (%)	Digester 3 Effluent (%)
1	23.5 ± 0.48	31.7 ± 2.34	27.3 ± 2.26	30.3 ± 1.67
2	22.7 ± 0.68	24.3 ± 0.61	26.3 ± 0.89	31.2 ± 1.05
3	23.5 ± 0.11	22.1 ± 0.67	22.4 ± 0.53	24.6 ± 0.95
4	23.7 ± 0.29	22.6 ± 0.47	17.0 ± 3.12	25.7 ± 1.74
5	23.7 ± 0.35	23.6 ± 0.44	22.9 ± 0.31	24.8 ± 0.46
6	23.7 ± 0.26	21.7 ± 0.65	21.3 ± 0.34	22.4 ± 1.38
7	23.6 ± 0.87	23.3 ± 0.67	21.6 ± 0.27	20.1 ± 0.63
8	24.7 ± 0.35	23.0 ± 0.47	21.5 ± 0.98	21.4 ± 0.88
9	23.3 ± 0.33	21.7 ± 0.29	21.9 ± 0.26	21.5 ± 1.09
10	22.3 ± 0.59	26.0 ± 3.11	23.6 ± 1.95	20.2 ± 3.78
11	24.7 ± 0.39	22.5 ± 1.72	21.7 ± 0.75	19.9 ± 2.90
12	23.6 ± 0.44	20.4 ± 0.67	21.6 ± 0.46	16.0 ± 2.26
13	24.1 ± 0.53	19.9 ± 1.21	26.1 ± 3.90	22.6 ± 0.52
14	25.9 ± 0.37	22.8 ± 3.71	25.0 ± 4.94	46.0 ± 6.92
15	23.8 ± 1.92	23.8 ± 0.18	22.5 ± 0.21	16.1 ± 0.72
16	27.3 ± 0.82	25.9 ± 1.84	25.6 ± 0.88	29.0 ± 4.00
17	25.2 ± 0.09	23.7 ± 0.33	23.9 ± 0.34	21.6 ± 0.53
18	-	13.7 ± 1.58	17.1 ± 1.59	6.2 ± 2.02
Average	24.1	22.9	22.8	23.3
SE	0.3	0.8	0.7	1.9

Organic Content Analysis

The chemical oxygen demand (COD) of acidified samples was measured using HACH COD test vials. The average COD of the algal influent over the course of the study was 10,500 ± 1170 mg COD/L. The average COD of D1 and the D2-D3 system was 3990 ± 590 mg COD/L and 1,450 ± 200 mg COD/L, respectively. This represents an average reduction in COD of 62% in Digester 1 and 87% in the Digester 2+3 system, suggesting that the increased HRT of the Digester 2 and 3 system allowed for greater reduction of COD. As COD represents the total amount of organic material potentially available for microbes to utilize for growth, a higher reduction in COD reflects more complete digestion of the algal feedstock (Table 10).

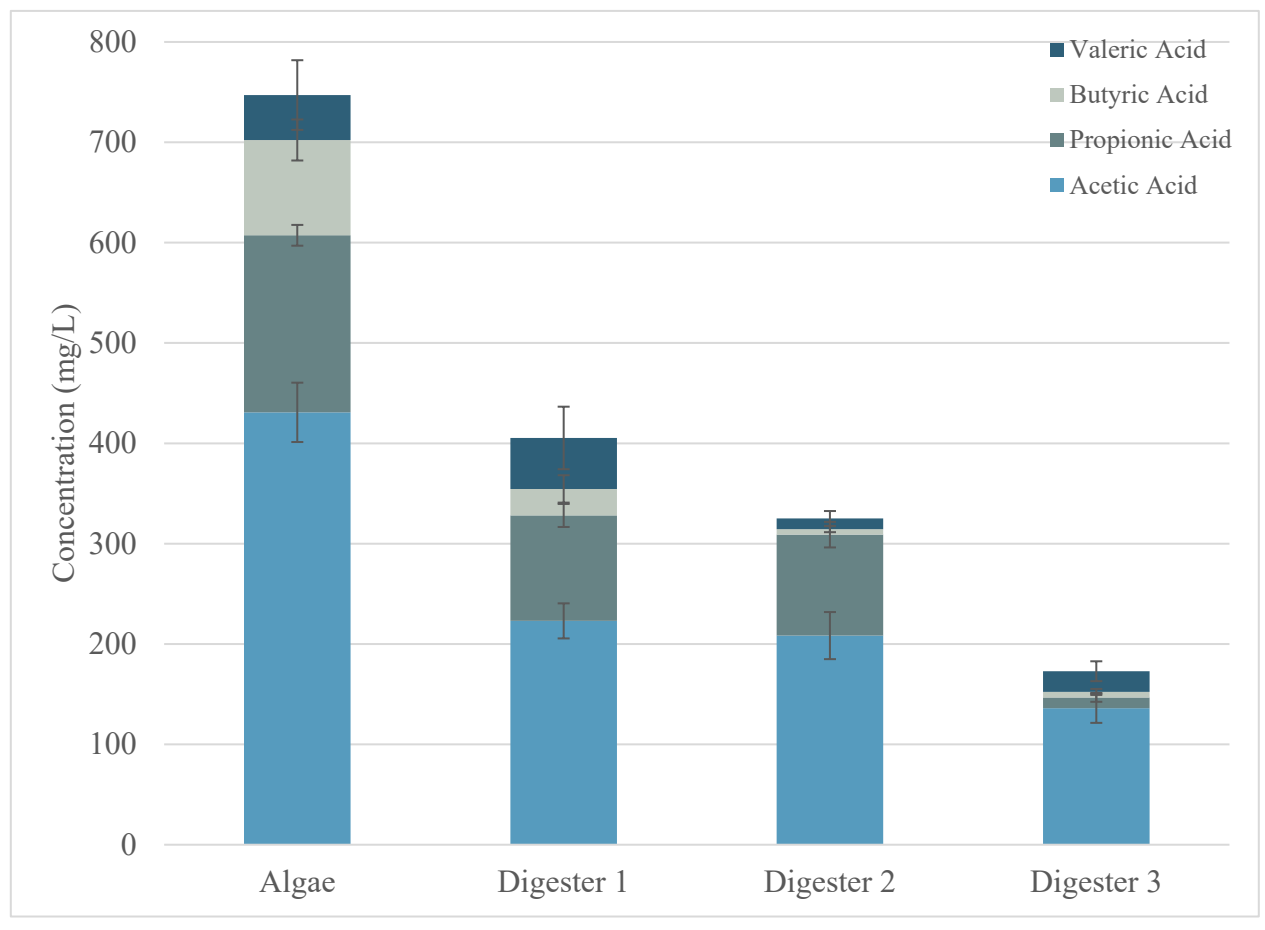
Table 10: Chemical oxygen demand (COD) analysis results.

Week	Algae (mg COD/L)	Digester 1 Effluent (mg COD/L)	Digester 2 Effluent (mg COD/L)	Digester 3 Effluent (mg COD/L)
1	13,000 ± 500	5,070 ± 670	4,230 ± 1020	2,400 ± 270
2	11,900 ± 300	3,720 ± 210	2,960 ± 130	1,760 ± 60
3	11,200 ± 900	2,640 ± 420	4,760 ± 880	1,660 ± 210
4	2,440 ± 120	1,130 ± 140	902 ± 231	388 ± 29
5	5,000 ± 260	2,220 ± 170	810 ± 232	503 ± 28
6	1,840 ± 300	1,720 ± 680	1,940 ± 416	410 ± 146
7	12,500 ± 800	5,980 ± 980	8,750 ± 1480	1,830 ± 90
8	7,750 ± 3,750	1,850 ± 50	4,100 ± 1750	825 ± 275
9	11,800 ± 30	9,850 ± 50	12,300 ± 50	3,280 ± 80
10	5,460 ± 210	1,580 ± 100	1,790 ± 140	1,460 ± 110
11	12,700 ± 30	3,830 ± 80	7,200 ± 50	2,730 ± 130
12	14,900 ± 700	7,350 ± 50	6,880 ± 2,230	1,880 ± 2780
13	16,700 ± 1,300	7,900 ± 350	-	-
14	19,200 ± 800	3,030 ± 30	775 ± 175	700 ± 50
15	13,900 ± 700	5,280 ± 430	10,400 ± 600	550 ± 0
16	9,030 ± 930	3,780 ± 630	1,700 ± 0	1,330 ± 180
17	8,900 ± 700	3,980 ± 380	4,430 ± 180	1,600 ± 850
18	-	1,000 ± 80	3,150 ± 400	1,380 ± 130
Average	10,500	3,990	4,530	1,450
SE	1,170	590	842	203

The percent reduction in COD in the D1 and D2-D3 systems (60 and 80%, respectively) were similar to the observed reductions in VS. This reduction was also reflected in the quantity of biogas produced by the two systems, as the D2-D3 system produced approximately 26% more biogas than D1 in Phase III. This indicates that the increased HRT of the D2-D3 system allowed for 20-26% greater processing of the algal influent biomass than D1 was able to process alone.

To determine the specific organic materials available to the microbes in the digestate, volatile fatty acid (VFA) content of samples was analyzed from filtered acidified samples using gas chromatography. As VFAs are the precursors to methanogenesis, more complete assimilation of VFAs by digester bacteria indicates more complete processing of available organic material. The concentration of four organic acids was analyzed: acetic, propionic, butyric, and valeric acids. The primary VFA present in the algal feedstock was acetic acid, with an average concentration of 431 ± 30 mg/L over the 18-week study. Propionic acid was present in the second-highest quantity, with an average observed concentration of 176 ± 10 mg/L. Butyric acid was the third highest with 95 ± 20 mg/L, and valeric acid was present in the feedstock in the smallest quantity, with a concentration of 44.8 ± 20.6 mg/L observed over the same period. The relatively high standard error of the valeric acid concentration is due to inconsistent detection throughout most of the study, as valeric acid was only detected in Weeks 1, 2, and 10 of analysis. (Figure 11; Table 11).

Figure 11: Volatile fatty acid (VFA) gas chromatography results, Week 1-18 average.



The organic acid that was most completely metabolized was butyric acid, with 72.2% reduction in concentration observed in D1 and a 94.2% reduction in the D2-D3 system. Effluent from D3 also yielded a high percent reduction of propionic acid, with a 93.9% reduction. This suggests that the increased HRT of the D2-D3 system allowed for nearly 100% assimilation of these two VFAs.

Acetic acid was in the highest concentration in the influent and thus, most utilized by methanogenic bacteria for CH₄ production. There was a 48.2% reduction in acetic acid concentration observed in D1, while 68.4% reduction was observed in D2-D3. This represents an increase in uptake of acetic acid, and thus increase in CH₄ production of 20.2% associated with the D2-D3 system. As this value is within the 20-26% range of increased digestion in the D2-D3 system from the results of the VS and COD analyses, the results of the VFA analysis support the conclusion that the D2-D3 system was approximately 20-26% more effective at digesting algae for CH₄ production.

Table 11: Average percent reduction in VFA concentration, Phase 3 Weeks 1-18

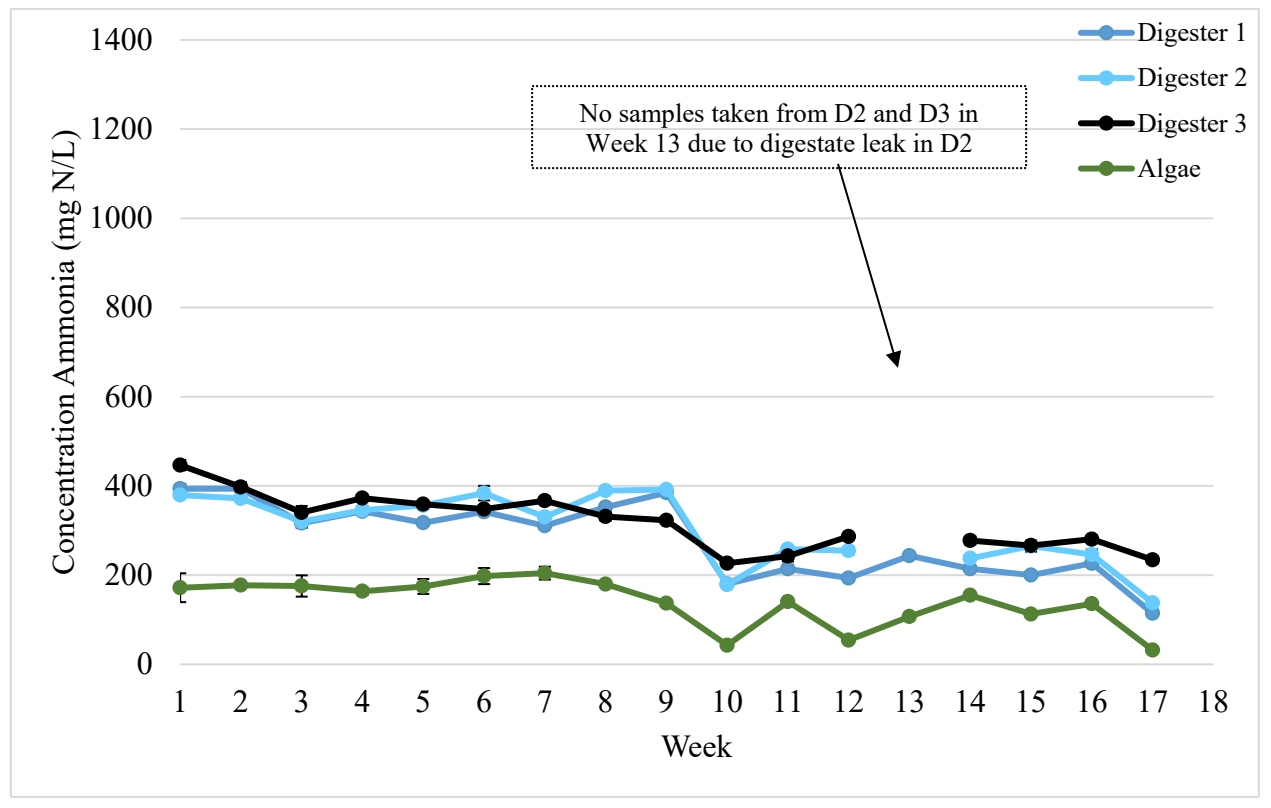
Organic Acid	Digester 1 (%)	Digester 2 (%)	Digester 3 (%)
Acetic Acid	48.2	51.6	68.4
Propionic Acid	40.5	43.0	93.9
Butyric Acid	72.2	94.2	94.2
Valeric Acid	-13.5	76.3	54.0

Nutrient Analysis

Digester influent and effluent samples were analyzed for ammonia, total Kjeldahl nitrogen (TKN) and total phosphorous (TP) content (Figures 12-14). TKN and TP data were not collected for Weeks 4-6.

Ammonia gradually declined in all sources measured over the course of the study, and was consistently lowest in the algal feedstock and highest in Digester 3, which was expected. Ammonia is a byproduct of the digestion process, so the digester with the highest retention time was expected to have the highest ammonia. During Weeks 8 and 9, NH₄ production declined in the algae feed and all of the digesters. This was likely due to reduced ambient temperatures impacting algal uptake of nitrogen as well as the microbial metabolism inside the digester, as a sharp decline in temperature was also observed in Week 8 (Figure 12).

Figure 12: Ammonia analysis results.



The TKN content of the algal feedstock was more variable than ammonia, with fluctuations between 223-1,240 mg/L observed, with an average of 762 ± 78 mg N/L over 18 weeks. The TKN of the digesters was not expected to be different from that of the influent, but the TKN content of D1, D2, and D3 averaged 497 ± 46 , 528 ± 52 , and 363 ± 30 mg N/L, respectively. The TP of the algae was lower, as expected than nitrogen, with an average of 169 ± 39 mg P/L observed over the same period of study. TP concentration in the digestate of D1, D2, and D3 averaged 99 ± 25 , 115 ± 34 , and 50 ± 15 mg P/L (Figures 13 and 14)

Figure 13: Total Kjeldal nitrogen (TKN) analysis.

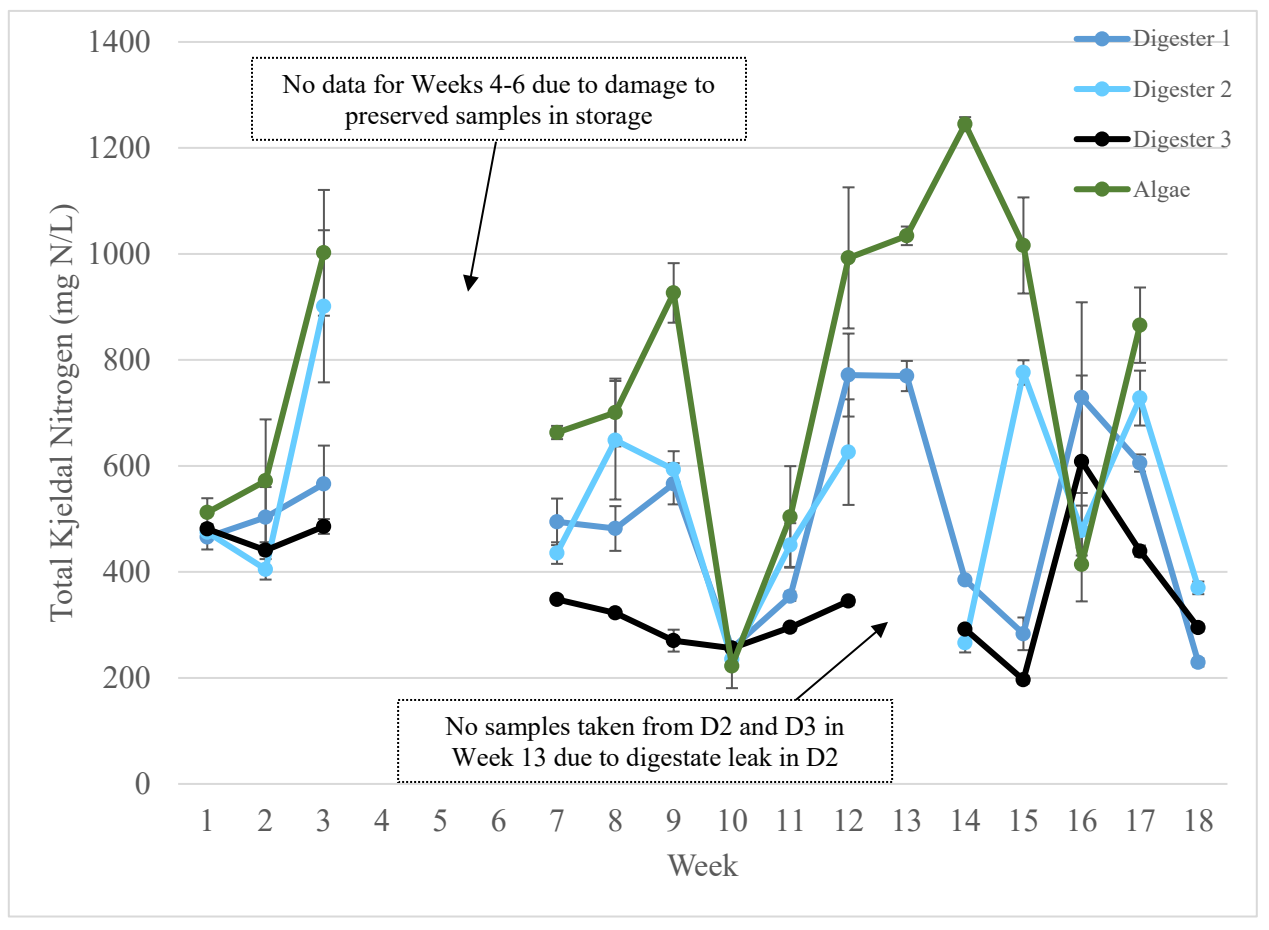
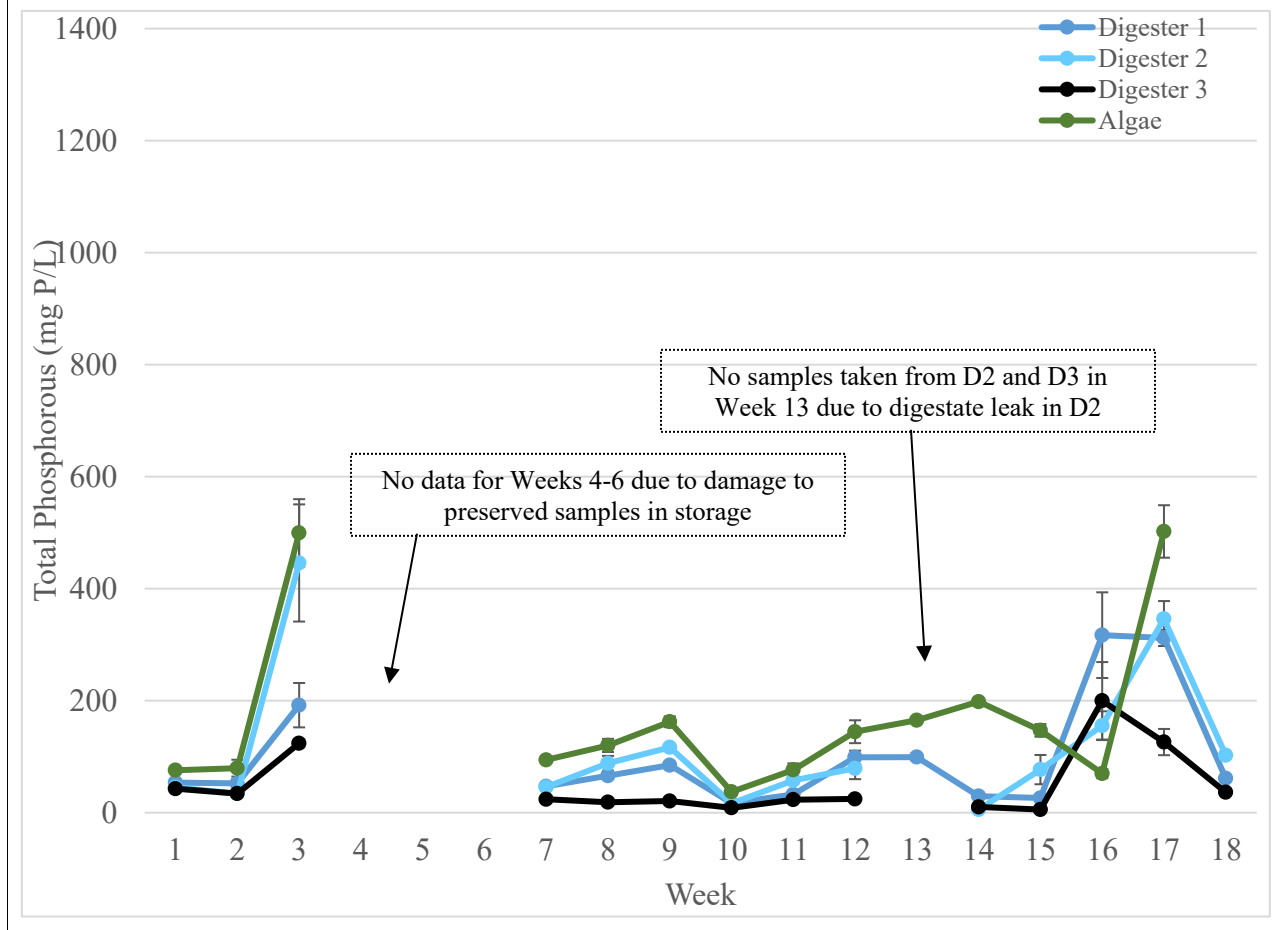


Figure 14: Total Phosphorous (TP) analysis results.



The TKN and TP values reflected an average reduction in TKN of 35% from D1 and 53% from the D2-D3 system, despite no reduction expected. A reduction of TP was also observed in D1 and the D2-D3 system of 41% and 71%, respectively. Similar trends were observed in Phase II, with the reduction likely due to solids settling within the digesters rather than an actual decline due to metabolism of nutrients. This was confirmed in Week 18, when during digester pump-down an additional sample of digestate was taken from near the middle of each digester (~2 ft. depth) using a bailer to determine if stratification had occurred due to a lack of mixing. Comparison between Sample 1 (a normal effluent sample) and Sample 2 (from the middle of the digester) indicated increased TKN and TP concentration in the digester compared to the digester effluent (Table 11). This indicates a need for better recirculation systems to be utilized in future work to allow for more complete mixing and more representative samples of nutrients in digester effluent.

Table 11: TKN and TP analysis of digestate samples from digester layers collected during digester shutdown on November 21, 2018. Sample 1 consists of a normal effluent sample collected using method from Weeks 1-1., Sample 2 collected from depth of ~2 ft. using bailer during pump-down.

Sample	Digester Effluent TKN (mg N/L)	Inside Digester TKN (mg N/L)	Digester Effluent TP (mg P/L)	Inside Digester TP (mg P/L)
Digester 1	229 ± 7	2220 ± 39	61 ± 1	1480 ± 20
Digester 2	370 ± 12	2110 ± 51	103 ± 2	15,10 ± 30
Digester 3	294 ± 7	636 ± 91	36 ± 4	306 ± 30

Attachment B

Feasibility of Fuel Cell Use at Ports

Environmental Defense Fund Report

Feasibility of Stationary Fuel Cells for Distributed Power Generation in a Port Environment

Environmental Defense Fund
Port of Baltimore
EDF Climate Corps 2018
August 2018

Written by
Justin Krupa
Appalachian State University MS Technology Candidate, Class of 2019



EDF Climate Corps embeds trained graduate students in organizations to help meet their energy goals by accelerating clean energy projects in their facilities.

The following report is the result of a 10-week Climate Corps fellowship at Port of Baltimore.

Table of Contents

EXECUTIVE SUMMARY	5
1. INTRODUCTION	5
1.1 BACKGROUND	9
1.2 OBJECTIVES AND GOALS	10
1.3 CAVEATS	11
1.4 REPORT ORGANIZATION	11
2. DESCRIPTION OF FUEL CELL TECHNOLOGIES	11
2.1 PROTON-EXCHANGE MEMBRANE FUEL CELL (PEMFC)	12
2.2 SOLID OXIDE FUEL CELL (SOFC)	13
2.3 APPLICATIONS AT PORTS	16
3. APPLICATION CONSIDERATIONS FOR MDOT MPA PUBLIC TERMINAL	17
3.1 OPERATION MODE CONSIDERATIONS	17
3.2 ENERGY LOAD CONSIDERATIONS	19
3.3 INFRASTRUCTURE REQUIREMENTS	20
3.4 PROJECT OPTION A – 0.5 kW	21
3.5 PROJECT OPTION B – 1.5 kW	22
3.6 PROJECT OPTION C – 5 kW	22
3.7 PROJECT OPTION D – 200 kW	22
4. EMISSIONS ANALYSIS	22
5. ECONOMIC ASSESSMENT	23
5.1 PROJECT OPTION A – 0.5 kW	25
5.2 PROJECT OPTION B – 1.5 kW	26
5.3 PROJECT OPTION C – 5.5 kW	27
5.4 PROJECT OPTION D – 200 kW	28
5.5 ADDITIONAL DEPLOYMENT CONSIDERATIONS	29
6. REGULATORY CONSIDERATIONS	33
7. CONCLUSION AND NEXT STEPS	33
REFERENCES	35
APPENDIX	38

Acronyms

AES	annual energy savings
BAU	business as usual
BGE	Baltimore Gas & Electric
BOS	balance of system
CAPX	capital expense
CCFAT	Climate Corps Financial Analysis Tool
CCS	carbon capture and storage
CHP	combined heat and power
COE	cost of energy
CO ₂	carbon dioxide
CPACE	Commercial Property-Assessed Clean Energy
DER	distributed energy resources
DG	distributed generation
DMFC	direct methanol fuel cell
DMT	Dundalk Marine Terminal
EA/REDA	Audit and Renewable Energy Development Assistance
EAA	equivalent annual annuity
EMS	energy management system
FC	fuel cell
GDP	global domestic product
GHG	greenhouse gas
IMO	International Maritime Organization
IRR	internal rate of return
kW	kilowatt
kWh	kilowatt hour
LCCA	levelized cost of carbon avoided
LCOE	levelized cost of energy
MARAD	United States Maritime Administration
MCFC	molten carbonate fuel cell
MDOT	Maryland Department of Transportation
MPA	Maryland Port Administration
MT	metric ton
MW	megawatt
NEM	net energy metering
NG	natural gas
NGDG	natural gas distributed generation
NREL	National Renewable Energy Laboratory

OPX	operational expense
O&M	operation and maintenance
PBK PD	payback period
PEMFC	proton exchange membrane fuel cell
PI	profitability index
PNG	pipeline natural gas
POB	Port of Baltimore
POH	Port of Houston
POLB	Port of Long Beach
RE	renewable energy
R&D	research and development
SERM	Safety, Environmental, and Risk Management Division
SOFC	solid oxide fuel cell
T&D	transmission and distribution
W	watt

List of Figures

Figure 1: Distributed energy resources nationwide.....	7
Figure 2: RE Market Trends	8
Figure 3: PEMFC Functional Schematic	12
Figure 4: SOFC Functional Schematic.....	14
Figure 5: Map of DMT and Target Buildings.....	19
Figure 6: Energy Load Models for Target Buildings	20
Figure 7: Utility financial savings created by DG.	24
Figure 8: 0.5 kW System Lifetime Value & Performance	25
Figure 9: 1.5 kW System Lifetime Value & Performance.....	27
Figure 10: 5.5 kW System Lifetime Value & Performance.....	28
Figure 11: 200 kW System Lifetime Value & Performance.....	29
Figure 12: Performance Regression Model for Various Extrapolated FC System Sizes.....	30
Figure 13: System Performance Augmentations with Existing 0.5 kW FC System.....	31

List of Tables

Table 1: GHG Emissions Reductions for Deployment Options.....	22
Table 2: 0.5 kW Key Assumptions, Savings, and Installation Charges	26
Table 3: 1.5 kW Key Assumptions, Savings, and Installation Charges.....	27
Table 4: 5.5 kW Key Assumptions, Savings, and Installation Charges	28
Table 5: 200 kW Key Assumptions, Savings, and Installation Charges.....	29
Table 6: Financial Analysis Output Table.....	32

EXECUTIVE SUMMARY

The Maryland Department of Transportation Maryland Port Administration's (MPA) Safety, Environmental & Risk Management Department (SERM) at Port of Baltimore (POB) is investigating opportunities and feasibility for on-site fuel cell (FC) implementation as a part of the Greenport strategy to reduce its dependency on the electrical grid and receive benefits of a cleaner fuel. This recently commercialized technology can facilitate a shift away from fossil fuel-based power production that is necessary for sustainable development within the maritime industry by generating electricity through electrochemical reactions fundamentally different from thermomechanical combustion currently in use across the shipping sector.

A product of SERM's partnership with Environmental Defense Fund Climate Corps, this report evaluates options for and feasibility of stationary FC deployments to power buildings composing land-side emissions at MPA's Dundalk Marine Terminal. After performing an internal energy audit on four buildings and consulting fuel cell vendors and Baltimore Gas & Electric (BGE, the regional utility,) four FC deployment options were evaluated for power co-generation with the existing electrical grid. These options included solid oxide fuel cells (SOFCs) from two different manufacturers capable of producing 0.5 kW, 1.5 kW, 5.5 kW, and 200 kW. Emissions and economic analyses were performed for each deployment option and are herein presented followed by a regulations assessment.

The cost-benefit analysis indicates that a 0.5 kW FC system capable of interconnecting to the electrical grid and operating nonstop off pipeline natural gas (PNG) to offset a portion of the baseload of a single building is the best option for fuel cell implementation at POB. MPA currently has 0.5 kW FC on site at DMT which can be installed by itself or in combination with larger FCs. The second-ranked option is a 5.5 kW FC, which has a suboptimal payback period of twenty-five years. However, it is projected to offer financial incentive of a \$2700 equivalent annual annuity while reducing regional emissions and lessening electrical grid loads via its higher distributed generation capacity. Other financially feasible options presented herein include the 200 kW system with levelized costs of energy (LCOE) of 4 to 6 cents/kWh.

This analysis demonstrates the flexibility and scalability of fuel cell technologies and explains how they allow for grid modernization to occur smoothly, without an immediate leap from fossil fuel infrastructure.

1. INTRODUCTION

Considering scientific indications of anthropogenic links to intensified global weather conditions, the eventual depletion in fossil fuel supply and increasing regulations on pollutant emissions, pursuing more efficient and environmentally friendly means of power production is imperative. Shipping ports around the world contribute to and have a stake in these conditions.

Maritime industries were responsible for 2.2% of global emissions in 2012, while facilitating 90% of world trade by volume (International Maritime Organization, 2015). Domestically, seaport cargo activity accounts for 26% of the economy, generating nearly \$4.6 trillion in total economic activity (American Association of Port Authorities, n.d.).

With a normalized annual global GDP expansion rate of just over 2%, these figures are expected to increase. For POB, port activity has grown even faster as a result of a recent expansion of the Panama Canal. Allen Clifford, executive vice president of Mediterranean Shipping Co., explains:

The expansion of the Panama Canal hails a significant change in the world of maritime... Inevitably the move will see East Coast ports, such as the Port of Baltimore, benefit as carriers optimize services through the expanded canal. (Ahead of the curve, 2016)

Due to additional growth in east coast shipping traffic, POB has been North America's fourth fastest-growing port for the past two years (Dinsmore, 2017). With this growth, the POB is committed to reducing emissions related to port activities. Reducing emissions protects the health of citizens and the environment.

Maritime power generation is moving away from fossil fuel combustion. Electricity use at the Port of Long Beach provides an example of the reactive measures taken thus far. It is projected to quadruple its electric consumption by 2030 due to industry growth paired with other factors including terminal automation and the increasing policy-driven electrification of port technologies such as shore power and battery-run cargo handling equipment (Curtin & Gangi, 2015). Electrification does reduce local emissions but results in increased electrical demand that places stress on power-producing facilities and transmission and distribution (T&D) system, or the electrical grid. This raises concerns regarding reliability, resiliency, and quality given the age of its infrastructure and its other electrical inefficiencies (MacKinnon & Samuelsen, 2016).

This evidence calls for the widespread advancement of appropriate distributed generation (DG) technologies to address both components of an axiomatic, economy-wide approach to emissions reduction. Few renewable energy technologies provide power independent of intermittent environmental conditions, and so they have not been able to effectively offset traditional methods without added battery and sophisticated energy management systems (EMS). The best solution comes from technology that can power broad load profiles without any additional controls, reliably, in a renewable fashion, and with resilience, defined as being "the ability to resist, absorb, recover from, or successfully adapt to adversity or a change in conditions" (MacKinnon & Samuelsen, 2016). FCs fulfill these specifications for appropriate DG, and with an established market presence they can facilitate a great shift towards a stronger and smarter power grid.

Overall, the DG utilization of distributed energy resources (DER) has a net value determined by the sum of the theoretical benefits listed above and occasionally apparent downsides such as capital and operational costs. Arguably, the main issue with FC technology is that it is too typically cost-prohibitive, and its lack of operational resiliency also introduces complications to be discussed in Section 3. Figure 1 displays the nationwide imbalance in domestic DERs, a large component in determining the cost-competitiveness of corresponding power generation technologies. In its Interconnection Seams Study, the National Renewable Energy Laboratory (NREL) conveys the importance of location-sourced DG until a “macrogrid” is constructed to carry RE from areas of high concentration to the white and gray shaded areas representing oil and natural gas (NG) in the Figure 1. Presently, electrical infrastructure is not “smart” enough for such allocation, and 100% of the new power generation proposed by the state of Maryland is NG-fired. This properly utilizes DER in terms of efficient resource management promoted by NREL (State of Maryland, 2016), and unlike wind/water turbines or photovoltaic modules, FCs are an advanced technology that can facilitate grid modernization despite these fossil fuel conditions.

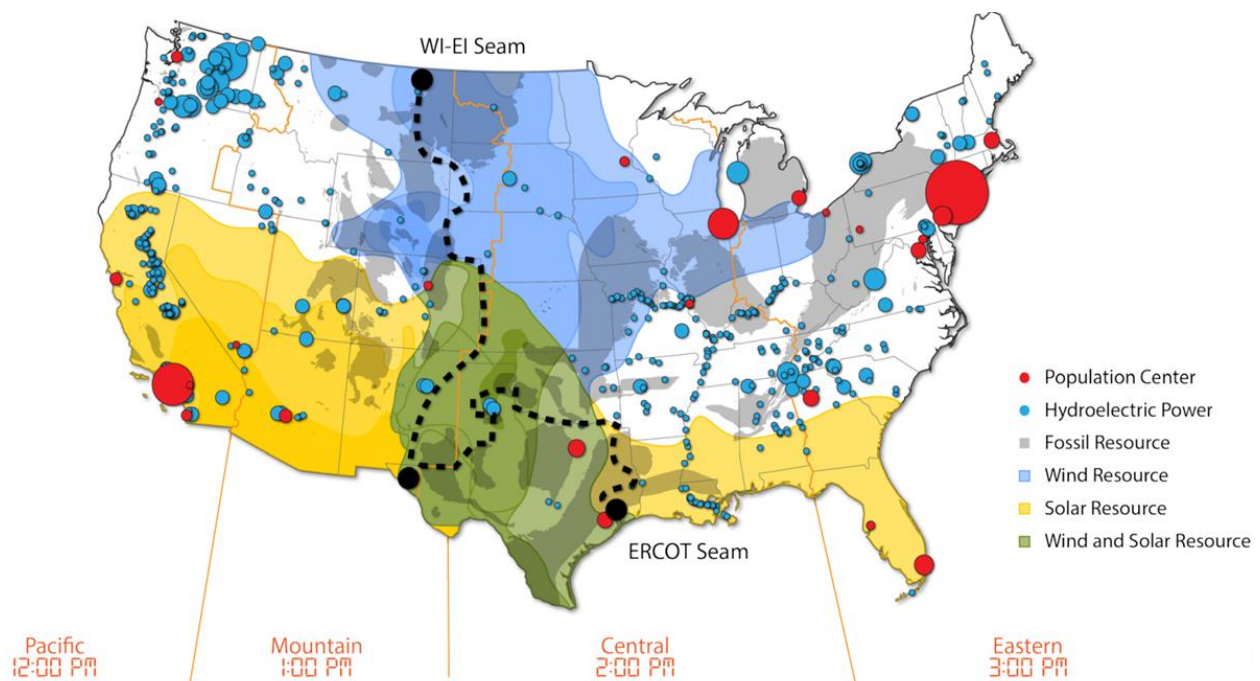


Figure 1: Distributed energy resources nationwide.¹

Many non-maritime entities along with POB have recognized FC technology’s present-day potential for application. The Fuel Cell & Hydrogen Energy Association estimates that hundreds of thousands of FCs have been installed around the world in the past few decades for primary or backup power as well as portable and emergency backup power scenarios ranging from heat and electricity for homes, material handling, passenger vehicles, buses and consumer electronics. Furthermore, the fifth annual Deloitte Resources Study of more than 600 U.S. companies found that 55% of businesses generate at least some portion of their electricity supply on-site, of which

¹ (Bloom, 2018)

9% are with FCs. Most notably, the FC percentage increases to 23% within the Fortune 100. Global markets report sales of FCs above \$2 billion annually (Curtin & Gangi, 2015). U.S. port and private sector partners are projected to spend \$154.8 billion on port-related infrastructure with an additional \$24.8 billion of investment by the federal government in U.S. ports through 2020, and it is important that some of that is allocated to FCs in the least as a reflection of current energy market conditions (American Association of Port Authorities, 2016).

As displayed in Figure 2, the annual production of electricity by fuel cell technologies appears to be growing at a similar rate to solar and wind technologies, which developed a few decades earlier. The growth reflects a 30% year-over-year increase. FC markets have tripled over the past three years, and they in total are projected to increase another 50% in 2018. This is consistent with solar and wind markets at similar points in their commercialization. Last year’s 670 megawatts (MW) compares well with solar’s 454 MW in 2002 and wind’s 500 MW in 1994 (Klippenstein, 2017).

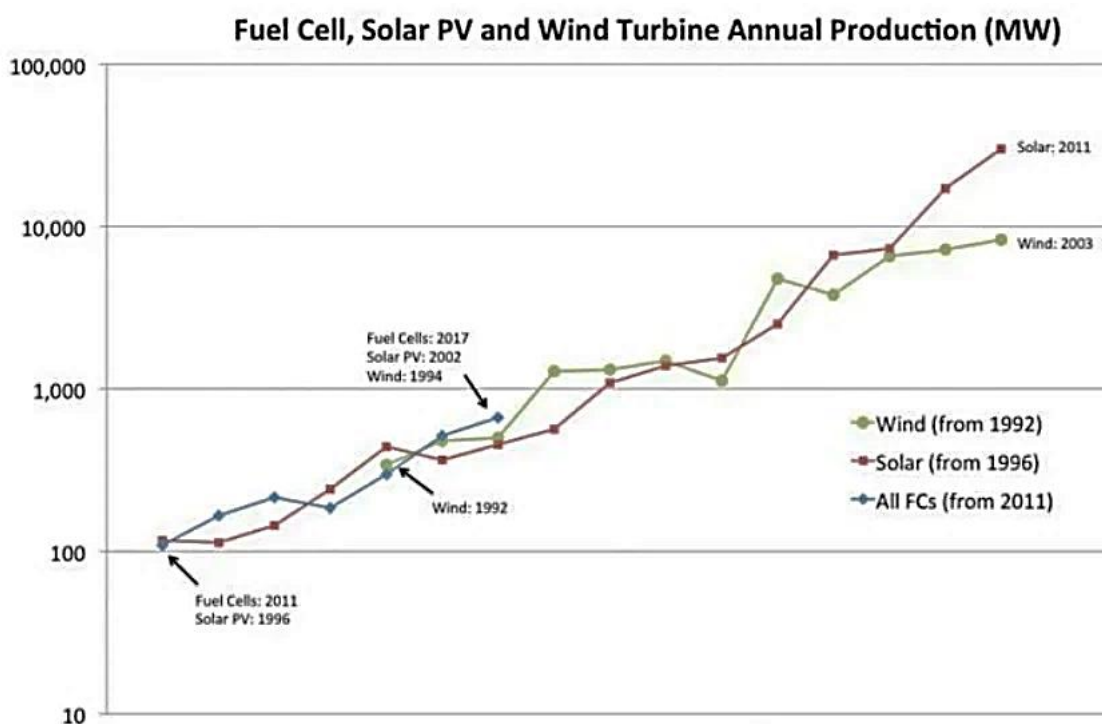


Figure 2: RE Market Trends²

Most companies in the FC market are between third to fifth generation product releases. Though FC products have matured, they are still mostly backed by government subsidies and/or high-value specialty markets. Popular demand has yet to materialize, so free market competition can only do so much to further progress (E4tech, 2017). Emergent technologies have in the past been nurtured by government spending, and FCs are no different.

² (Klippenstein, 2017)

In this way, MDOT MPA can continue to be a leader in sustainable port development by bringing high exposure and attention to cutting edge power systems.

1.1 BACKGROUND

FCs have their origins in the 1830s when chemists thought of reversing the reaction known as hydrolysis, in which energy is put into a water molecule to split it into hydrogen and oxygen, to in effect combine the two gases and produce water and electrical energy. This was a laboratory novelty at the time, as there were no practical systems to which the technology could be applied. In the 1950s, however, NASA scientists were looking for low-temperature, combustion-less and non-toxic methods to power satellites and space modules. Because no other options existed besides solar power, a large portion of government funding went into developing hydrogen powered FC technology.

Resulting from its origins in space exploration, the industry has developed slightly off-center as described by Eric Wachsman of Redox Energy:

Unfortunately, government policy, the popular press, and many scientific publications have focused on fuel cells as part of a broader hydrogen economy, thereby relegating fuel cells to a "future energy" solution due to the need for a required overhaul of our current hydrocarbon fueling infrastructure. (Wachsman & Lee, 2011)

Just as combining the steam engine with ingenious machinery drove the industrial revolution, or how the combination of computers and distributed networks led to the digital revolution in the late eighties, appropriate power generation technologies need to be developed in tandem with conjoining grid transmission technologies.

An overhaul of current fueling infrastructure need not be the case for large-scale FC implementation; as will be demonstrated herein, they are a proven *present-day* solution. This work is within the context of developments in new types of FC technologies that can run on a broad variety of fuels (as discussed in Section 2). It also comes on the cusp of a substantial influx of NG supply found in vast domestic reserves of shale that have renewed global interest in NG for power generation as displayed in Figure 1. This resource has a significantly reduced carbon footprint compared to liquid and solid carbonaceous substances like oil and coal, so it is rapidly becoming the preferred fuel for thermomechanical power generation (Gur, 2016). However, the utilization of NG by *electrochemical* power generation offers even greater benefits. FCs are the most efficient means to directly convert stored chemical energy to electrical energy (an electrochemical reaction) at levels double to that of thermodynamic combustion (Wachsman & Lee, 2011). So, as NG floods the market and combines with deep decarbonization policies projected to cause a 59-77 GW of grid capacity loss from coal plant closures, FCs could be well positioned to catalyze a grid-modernization project of massive proportions (Chick, Weimar, Whyatt, & Powell, 2014).

MDOT MPA has already led an innovative project using a FC. In 2016 and 2017, the on-site environmental team designed, built, and operated an integrated algal flow-way, anaerobic algal digester, biogas collection and conditioning, and fuel cell system during a demonstration project funded by the US Maritime Administration (MARAD) to convert algae to energy (Anchor QEA, 2018). With a FC capable of using biogas generated from the digestion of algae as supplemental fuel to natural gas, power output was achieved at a steady 300 watts. This project sought to close the energy loop by producing on-site electricity from growing algae along a flow-way, digesting the algae to create biogas, and using the biogas as feed to a fuel cell to power lights and a circulation pump. Further benefits come with the algae's metabolic consumption of atmospheric carbon and excessive nitrogen and phosphorus from Chesapeake Bay-water.

The successful design, installation, and operation of the fuel cell during the demonstration project provided MDOT MPA and MARAD the confidence that a fuel cell is a reliable alternative energy source that can replace existing energy sources if fuel is available for the fuel cell. Hence, this paper has been commissioned to continue the port's exploration of options for FC power generation.

1.2 OBJECTIVES AND GOALS

This study was commissioned by MDOT MPA to continue its MARAD-supported investigation of the technological feasibility for FCs to aid port electrification while simultaneously reducing sector-based emissions. Initiative for maritime FC use is here reinforced by an analysis of current grid-modernization trends backing new and upcoming decarbonization policies and the developmental state of FC technologies in kind. The intended outcome of this work is to describe what differentiates this type of clean power system from other RE sources powering maritime applications within the broader scope of facilitating grid-modernization and emissions reduction across all sectors.

This report is designed with a business case for FCs at the POB composed of implementation options and their financial outcomes. This involved conducting research onsite to assemble the most desirable functional outline for FC system performance and to put together a picture of what the most environmentally and economically sustainable deployment would look like. The initial aim was to perform an in-depth energy audit on candidate buildings to evaluate model energy loads available for offsetting with distributed power generation. To match these loads, FC operation modes required understanding enough to evaluate the technology's ability to match dynamic demand curves present in the most common deployment scenarios. In line with this, FC market maturity had to be gauged and a corresponding timeline for port implementation devised. The regional utility required consultation for their support of NGDG and grid interconnection. Additionally, the national FC market needed canvassing to select the best vendors and products for implementation. Furthermore, this report aimed to encourage repurposing the fuel cell already owned by MDOT MPA, which was accounted in the financial analysis.

1.3 CAVEATS

This report does not consider emissions from methane leaks that may result from the FC system itself and/or an increased port reliance on NG infrastructure. To characterize this and to get a system commissioned, extensive engineering work is required beyond the scope of this report. Additional technical work will be required to design the interconnection circuitry, the method for connecting the FC to the load, and the exact fees, rules, and regulations for doing so as specified by the FC provider, BGE, PJM, and standard electric code. Emissions and financial analyses are based on content provided in FC specification sheets provided by the manufacturer. Due to large gaps in the nominal power ratings of currently available FCs, and given the technology's modularity and capability for conjoining, manufacturer-specified values were linearly extrapolated to provide cost-scenario estimates for systems in the 10-100 kW range. Capital cost for such systems are likely overestimates, as economies of scale are likely to factor into production and commissioning of multi-module FC arrays. Current energy market trends are also extrapolated to provide metrics across the deployment duration. During contract negotiations, the quoted prices used for the 5 kW and 200 kW deployment options may be subject to change as well.

1.4 REPORT ORGANIZATION

A description of the history and science behind contemporary FCs on the market is presented first, tracing the thought process behind choosing the solid oxide type of technology to focus the analysis on. Then, prior maritime FC deployments are summarized before detailing the most appropriate implementation plan for POB given available energy loads, resources, and products. Four deployment options are covered in detail, with emissions and economic analyses performed for each and other hypothetical systems predicted to be released within the next decade. In conclusion, this report describes the rationale for each option is discussed and short and longer-term action plans are presented.

2. DESCRIPTION OF FUEL CELL TECHNOLOGIES

FCs are essentially electrochemical engines that convert the chemical energy of fuels directly into electrical energy. They have the unique capability of overcoming the Carnot efficiency and other thermodynamic limitations in combustion cycles. By means of two oppositely charged electrodes, ions are passed through an electrolyte wherein they react to produce electricity and heat at proven efficiencies of up to 90%.

Various types of FCs have been developed as scientists attempt to achieve reliable, high-efficiency reactions in a reproduceable and modular unit compatible with the widest possible range of potential implementations. They are separated based on the electrolyte they employ, on which the other vital components of a FC system, such as the fuel required, operational temperature, and necessary catalysts³, rely. Depending on the specific application scenario (stationary vs portable, backup vs baseload power, urban vs rural), some are better than others and, as is the case for POB, there may be one clear choice of type. There are six prominent FC

³ Catalysts are the material composing FC electrodes, which increase the rate of chemical reactions without themselves being consumed.

technologies: alkaline, direct methanol (DM), phosphoric acid, molten carbonate (MC), proton exchange membrane (PEM), and solid oxide (SO). Although all configurations are hypothetically employable, PEMFCs and SOFCs were the only types considered due to their commercial availability to MDOT MPA, their broad range in power rating, and their specific fuels of hydrogen and methane respectively which are to be compared and contrasted.

In most all cases besides DMFCs which consume liquid methanol, methane or NG is likely the starting fuel stock, but methane-derived hydrogen has been the desired and most extensively employed fuel for FC deployments, namely with alkaline and PEMFC technologies. This is despite the fact that hydrogen gas is not a primary, natural energy source but rather an energy carrier. The main reason for this is due to its pure water-based emissions, and hydrogen's oxidative proclivity makes for an elegant technology while methane activation is more challenging (Gur, 2016).

2.1 PROTON-EXCHANGE MEMBRANE FUEL CELL (PEMFC)

PEMFCs are the simplest form of the technology as they are adapted to be fueled solely by pure hydrogen, the fundamental electrochemical energy carrier. In this project's beginning, it was considered as a potential candidate for port deployment for its local environmental benefit. Furthermore, its low operating temperature allows for fast start/stop cycling, which bodes well for their use in transport. They have the largest share of sales in the FC market representing almost three-quarters of the 670 MW shipped in 2017 primarily due to the subsidized hydrogen car industry (Klippenstein, 2017).

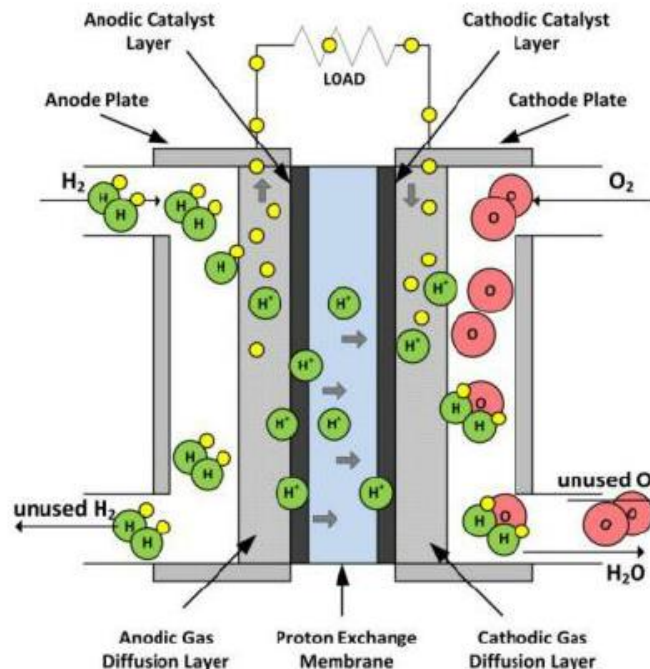


Figure 3: PEMFC Functional Schematic⁴

⁴ (Abbaspour, Parsa, & Sadeghi, 2014)

However, this technology exhibits a major problem based around Wachman's postulated "hydrogen economy." Apart from specific regions within California, Texas, and Louisiana where large reforming plants are located, sourcing hydrogen presents a major bottleneck for hydrogen-based technological development. Although PEMFCs exhaust no carbon emissions, the reformation process does, given 95% of pure hydrogen comes from NG, currently the cheapest source, and other fossil fuels (*Fuel Cell Technologies Office, 2018*). Other sustainable methods to produce hydrogen, such as electrolysis, are the ultimate solution to this problem in hydrogen production, but the economics for this process have yet to be realized.

As competition in power generation sector increases, other more recently developed technologies have emerged that can intake energy *sources* as fuels more so than just energy *carriers*. Despite their internal elegance, hydrogen FCs are being outcompeted by more systematic approaches in FC technology.

2.2 SOLID OXIDE FUEL CELL (SOFC)

SOFCs require high temperatures and highly active catalytic electrodes to accommodate the larger molecules composing energy sources. They promise clean, efficient and environmentally friendly power production, and offer a wide range of fuel flexibility including not only gaseous fuels but also liquids, and even solids including carbon, untreated coal and biomass. This technology, consisting of 76 out of the 670 MW in 2017's market total, is second most popular behind PEMFC and gaining ground (Klippenstein, 2017).

Apart from commercial availability, to be discussed in Sections 2 & 3, fuel flexibility is SOFC's main differentiator from competing FC technologies; they even can switch sequentially from one hydrocarbon fuel to another in real time. This property is due to the solid oxide inter-electrode layer composed of a ceramic material. At high temperatures, oxide ions can diffuse from the cathode to the fuel-immersed anode. These ions are very powerful oxidizing agents, so the reaction can occur with a great number of substances; if it reacts with oxygen, it can potentially be used as fuel for the cell. On the contrary, in PEMFCs the electrolyte transports a hydrogen ion (a proton), which can only bind with electrons and not atoms.

With SOFCs, internal reforming overcomes the need for external fuel processing, which adds cost and complexity and reduces overall system efficiency. Mechanistic details and technical challenges that come with internal reformation are the main challenges in optimizing the technology and understanding NG utilization for electricity generation. The image below portrays this electrocatalytic oxidation of methane, the primary constituent of NG, at levels typically around 90%. The exceptional stability of methane's intramolecular bonds is why high temperatures and effective catalysts are required to activate it (Gur, 2016). In the presence of the anode, a reaction between electrochemically produced and recycled steam and methane is induced to produce a combination of carbon monoxide and hydrogen gas typically referred to as syngas. These two constituents then combine with oxygen ions at the catalytic boundary where current is generated as syngas becomes oxidized (van Beurden, 2004). The consequent full

oxidation of methane is referred to as catalytic combustion, as opposed to the traditional thermodynamic combustion.

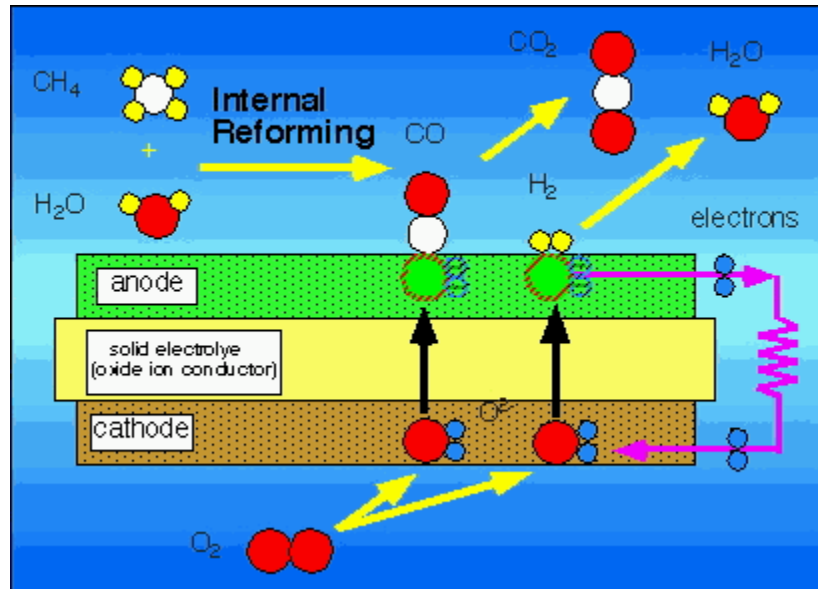
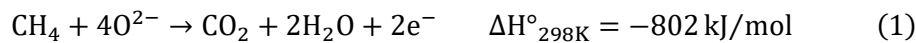


Figure 4: SOFC Functional Schematic⁵

An SOFC consists of three major components: two porous electrodes (cathode and anode) separated by a solid oxygen ion conducting electrolyte. At the cathode, O₂ from air is reduced and the resulting ions are transported through the electrolyte lattice to the anode where they react with gaseous fuel, yielding heat, water, and carbon dioxide, and releasing electrons to an external circuit.

Many different reactions between syngas species occur in the anodic environment within SOFCs and produce variation in operational efficiencies:

Full oxidation



Partial oxidation



Steam reforming



Dry reforming



Water-gas shift

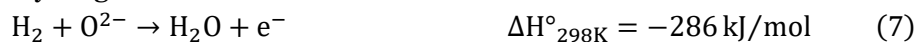


⁵ (Schmitt, 2001)

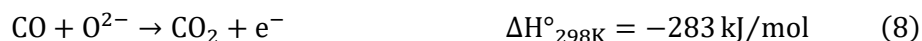
Boudouard reaction



Hydrogen oxidation



Carbon monoxide oxidation



The associated enthalpy changes indicate a thermodynamic property of each reaction—negative values indicate exothermic processes and positive endothermic. So, as the total enthalpy is positive, the net temperature change at the anode is positive enabling the SOFC operating temperature to be self-sustaining even at 60% conversion efficiency (where the enthalpy change is nearly balanced) (Gur, 2016). In addition to providing oxygen for oxidation reactions [(1), (2), (7), (8)], the cathode inlet gas also provides cooling of the cells to maintain an acceptable temperature distribution. Cell cooling is further aided by the endothermic reactions above dealing with methane reformation and syngas production [(3), (4), (6)] (Newby & Keairns, 2013).

The key parameters determining system efficiency are stack thermal operating conditions in combination with cell voltage between the electrodes (J. Thijssen, LLC, 2009). It can be argued these electrodes are the most critical and demanding SOFC components that dominate cell performance, because they have to be able to catalyze oxygen reduction and fuel oxidation at high turnover frequencies. This is also why they are a major focus in SOFC R&D, particularly regarding improving the full electro-oxidation efficiency of unreformed methane. Voltages within FCs are surprisingly low, being typically around a few volts. This is primarily due to finite rates of electrode processes (i.e., Activation losses) and finite electrical resistance in cell components (i.e., Ohmic losses). Both losses also reduce efficiency and performance (Gur, 2016).

Another limitation of the voltage is catalyst deactivation due to carbon deposition or coking on the anode. Although SOFC electrodes are designed to handle carbonaceous species, they have not yet developed a resistance to the effect of longer chains found in fractional amounts in PNG—they simply wear out. Commercial FC stacks, as they are referred to being commonly found as many electrode pairs in series, typically last only 4-6 years, or 40,000 hours (Atrex Energy).

Additionally, sulfurous content if present within the fuel will cause rather rapid degradation in electrode performance. PNG typically contains mercaptan, a sulfur-bearing odorant, for leak detection, and dihydrogen sulfide, mercaptan's scientific name, is present at trace levels no greater than 10 ppm or up to 1% composition depending on the source of gas (Gur, 2016). To prevent catalytic deactivation caused by sulfur, sinks/filters are added upstream from the FCs, and they are typically replaced every three years.

With higher reaction yields and increased rates in the full oxidation of methane, high quality waste heat can be produced in SOFC exhaust, which creates opportunities for combined heat and power (CHP) generation. This capability results in even higher FC efficiencies unprecedented in electric heating equipment due to the simple fact that less NG is consumed per unit of energy output. FCs represent the lowest emitting self-generation technology that can capture the benefits of CHP (MacKinnon & Samuelsen, 2016). SOFCs with CHP technology reach levels of 75-90% efficiency while SOFCs alone currently have a maximum of 60%.

2.3 APPLICATIONS AT PORTS

FC implementation at ports has been limited to PEMFC technology with the exception of the one used in POB's recently integrated flow-way system. The most publicized case studies have been conducted by the Port of Honolulu and the Port of Long Beach (POLB). Sandia's Maritime Fuel Cell Generator Report published in May 2017 claims to have initiated the first test of FCs specifically deployed at a port, but the general applicability of the study is limited by its use of hydrogen fuel, which is cost-intensive to source in large quantities (consequently dominating the logistical sections of the report), and the nature of its implementation, to power non-grid-tied onboard refrigeration units for perishable goods transported by the shipping company Young Brothers (Pratt & Chan, 2017). Nonetheless, it was a successful demonstration of FCs' ability to fit custom power needs and vastly improve local emissions, and the empirical detail in its 200+ pages serves to reduce investment risk for future FC systems.

POLB has their own microgrid-promoting Energy Island Initiative and in 2016 published a study assessing the potential of FCs to directly support it along with green power, DG & grid-support, and emissions reduction initiatives (MacKinnon & Samuelsen, 2016). In late 2017, they along with Port of Los Angeles announced that contract negotiations were underway with Fuel Cell Energy, provider of the MCFCs on the MW scale, for an onsite plant and Toyota for a new fleet of PEMFC powered Mirai's along with their new Class 8⁶ PEMFC semi-truck, the focus of their Project Portal. The entire system is planned to go online in 2020. The most significant part of this project involves Shell, which has been working with Toyota and Honda to expand local hydrogen fueling infrastructure, entering as a fourth party to design the world's first hydrogen production plant using a 2.35 MW reversible MCFC to condition locally-sourced biogas into pure hydrogen while generating electricity (Chen, 2018). This is accomplished by new catalyst technology consummating reversible FCs that can take in electricity to produce different gases similar to electrolysis. Although their 2016 study predicted reasonable LCOEs for power production, this complex project is likely more about proving a concept than presenting an immediate business case, despite its large industry players.

In 2010, Port of New York & New Jersey struck a similar partnership with Toyota, General Motors and Shell for a four-year deployment of a fleet of 12 PEMFC Highlander SUVs (Incantalupo, 2011). A hydrogen fueling station was built at JFK International Airport to join

⁶ Class 8 trucks have a gross vehicle weight rating exceeding 33,000 lbs; the typical class of 18-wheeler semi-trucks.

four others in three spread-out locations within New Jersey. To date, the Port has not released any information on continuing this work (Reinish, 2014).

Port Houston has also incorporated FCs to power cargo-handling equipment with hydrogen. They partnered with Environmental Defense Fund, the U.S. Department of Energy, the Houston-Galveston Area Council, the Gas Technology Institute, U.S. Hybrid, Richardson Trucking, and the University of Texas Center for Electromechanics in a three-year demonstration project for the technology that started in 2015 (Wolfe, 2015).

Although FC-related activity has not yet been announced, Port of San Diego this year received a \$4.9 million grant from the California Energy Commission that they plan to match with \$4.4 of their own funds for the construction of their own microgrid. It will have a 700 MW capacity and be supported by solar and battery systems. The RE in combination with increased EMS capabilities and retrofitting is expected to cut the Port's grid-energy usage by 60%, equivalent to 300 million tons of CO₂ per year (Cohn, 2018).

3. APPLICATION CONSIDERATIONS FOR MDOT MPA PUBLIC TERMINAL

To further MDOT MPA's work on FC integration, DG with SOFCs firmly presents itself as the best option. Benefits to the user include an assured, reliable electricity supply with better energy management control than other clean power methods along with a significantly reduced cost of energy (COE). The technology is also modular, which means it is available in a broad range of sizes and can be added upon and reduced in incremental amounts according to the desires/needs of the project. The limitations of FC technology are apparent in their needs for precise control of internal conditions necessary to achieve maximum efficiency and for a regulated fuel supply infrastructure. Balancing these pros and cons regarding fuel cell performance is discussed in the proceeding subsections.

3.1 OPERATION MODE CONSIDERATIONS

The flexibility, modularity and scalability of stationary FC systems allow for different deployment options. FC technology can be used for primary, backup, or off-grid power generation and can be scaled to fit electrical needs ranging from watts to MW. These different deployments result in a range of business cases that can be made for SOFCs in relation to the operating costs and associated capital required to commission the system.

Four options for FC operation modes were considered at POB:

1. Baseload power generation provides a constant, steady supply of clean power at some value below the minimum energy usage, if the system circuitry lacks an energy sink like a grid interconnection or air-cooled resistor bank, or at some higher offset value throughout the day. It would be carried out in direct comparison to central grid generation.

2. Variable power supply consisting of a top-hat⁷ daily production profile with seasonal adjustment is aimed at covering most of energy use during the day and idling or shutting off at night. This strategy would compete with central grid generation as well as with peaking plants designed to feed the grid in times of high demand. This strategy makes sense if the system is isolated and/or if the cost of producing power during minimum demand hours is significantly higher than grid-sourced electricity.
3. Constant FC operation and variable power output can be achieved simultaneously with the addition of a battery pack, which discharges for extra demand during the day while being backed up and recharged by FCs at night.
4. The more recently developed CHP-enabled SOFC, in which remaining waste heat in the cathode exhaust is typically cycled through the module to warm incoming gas, is cooled providing hot water or sensible heat for indoor air instead. This requires an add-on heat exchange mechanism but results in significantly higher FC efficiency.

Premium power systems generally supply baseload demand for their emissions and efficiency to thereby take a more significant role in the encompassing energy portfolio. For SOFCs specifically, supplying a baseload demand is also more advantageous as their high operational temperatures discourage a start/stop cycle. Stack⁸ damage from thermal stress can occur under circumstances of variable operation, which is why idling/standby features are normally included for top-hat operation. Idling is recommended because relatively large amount of energy is required to raise the core to the desired temperature before the FC can sustain itself in normal active mode.

If the grid is available for interconnection, as will be discussed in detail herein, supplying a fraction of the load becomes a possibility. The FC would be able to operate steadily with the grid, providing any additional load and absorbing any excess onsite power generation. If the grid is not available, excess electricity must be dissipated via hardware such as an air-cooled resistor bank at times when electricity generated by the FC is not needed.

Ideally, the stack should be sized at a slightly higher value than the upper quartile of the energy load, given that stack efficiency increases at lower power levels relative to its rated capacity. This effect allows for systems with excellent load-following characteristics. However, SOFCs normally take 30-45 minutes to adjust to a 25% change in load, so load-following operational modes are not realistic without backup by the grid or a battery system. In the latter case, the batteries must provide at least enough stored energy to accommodate a single 25% load step up, and preferably two 25% step ups in succession, which can be a significant addition to the lifetime cost of the system (Battelle, 2017).

With interconnection to the grid, the FC is maintained at a power level chosen by the system operator and is subject to any agreements in place with the utility for power buy-back if the FC power exceeds facility usage. Grid interconnection would enable the FC to run in a baseload,

⁷ Referring to the shape of a time-of-use electricity demand curve as it peaks during maximum daytime activity and levels at a minimum during nighttime periods of inactivity.

⁸ The series circuit of planar electrode pairs arranged in the FC core to sum their produced voltages.

steady operating mode; this mode is ideal since top-hat, load-following modes reduce total efficiency and require extra equipment, which raises the already high capital cost required to commission the system. CHP technology is just starting to enter the market, and the only commercialized products currently available are in the MW range. For these reasons, using a FC for baseload power generation while connected to the electrical grid was the operation mode selected for the emissions analyses and economic assessments below.

3.2 ENERGY LOAD CONSIDERATIONS

In order to commission the most effective system, buildings compatible with a baseload operation mode were identified. Before that, however, the largest factor to consider was locations of preexisting NG pipeline infrastructure. Four buildings were targeted based on drawings of NG pipeline termination points obtained from the port engineering division: buildings 1702 (bottom right corner), 91A, 91B, and 91C (upper corner).

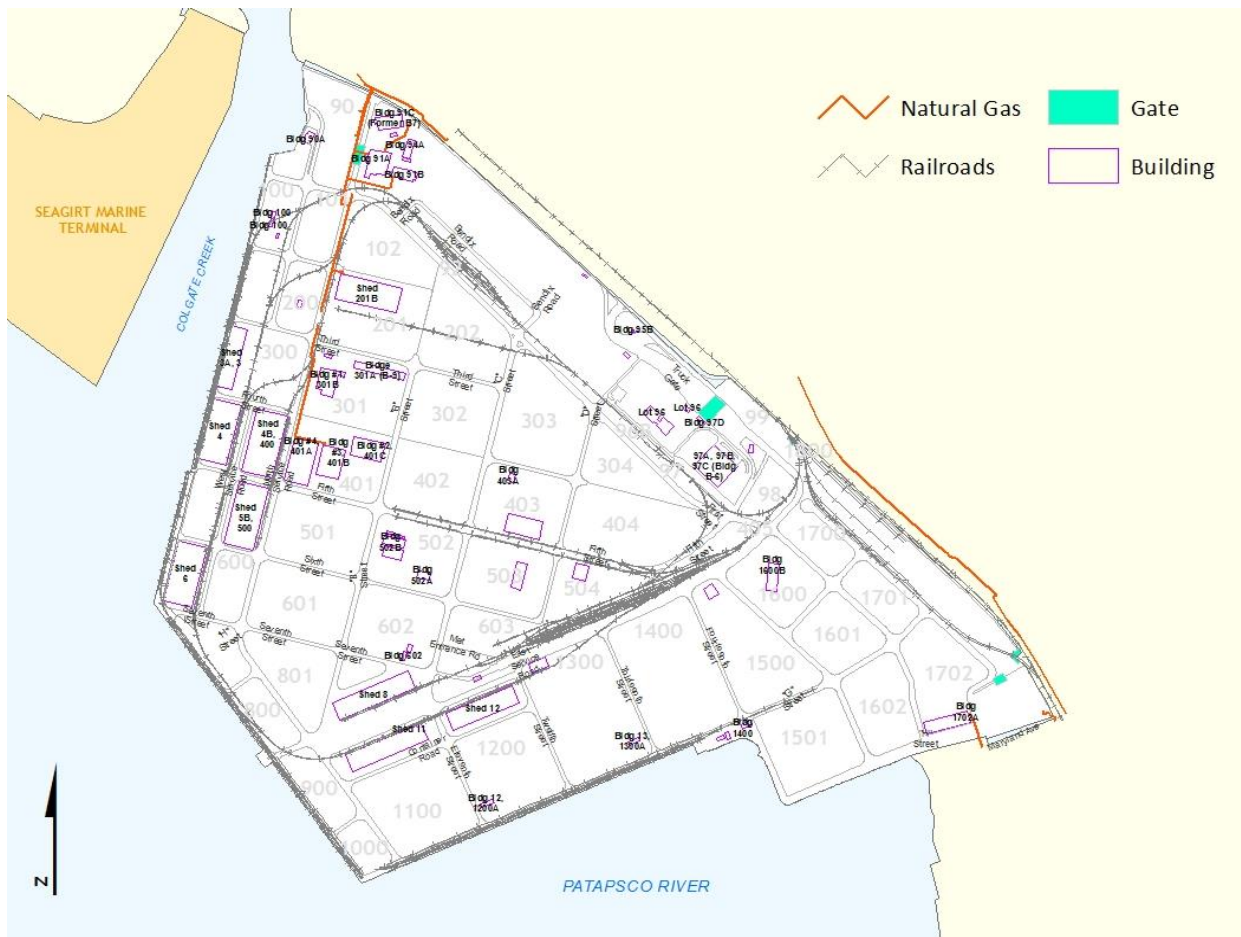


Figure 5: Map of DMT and Target Buildings

These buildings are compatible with baseload operation because they host two work shifts a day as opposed to one, which means that they function under operating conditions for 16 hours out of every day. This directly maximizes the onsite benefits of a FC system, as it will be operating constantly to maximize net operation efficiency and produce clean power for the terminal.

The energy usage data for these buildings were obtained from monthly utility bills for 2017. Figure 6 show the average daily electrical usage for each building, as calculated from available utility bills. Buildings 91A&B share the same billing meter. MDOT MPA only has access to half of the meters running 1702 because the other half is leased by private companies. For baseload supply systems, monthly utility bill information is sufficient for this project.

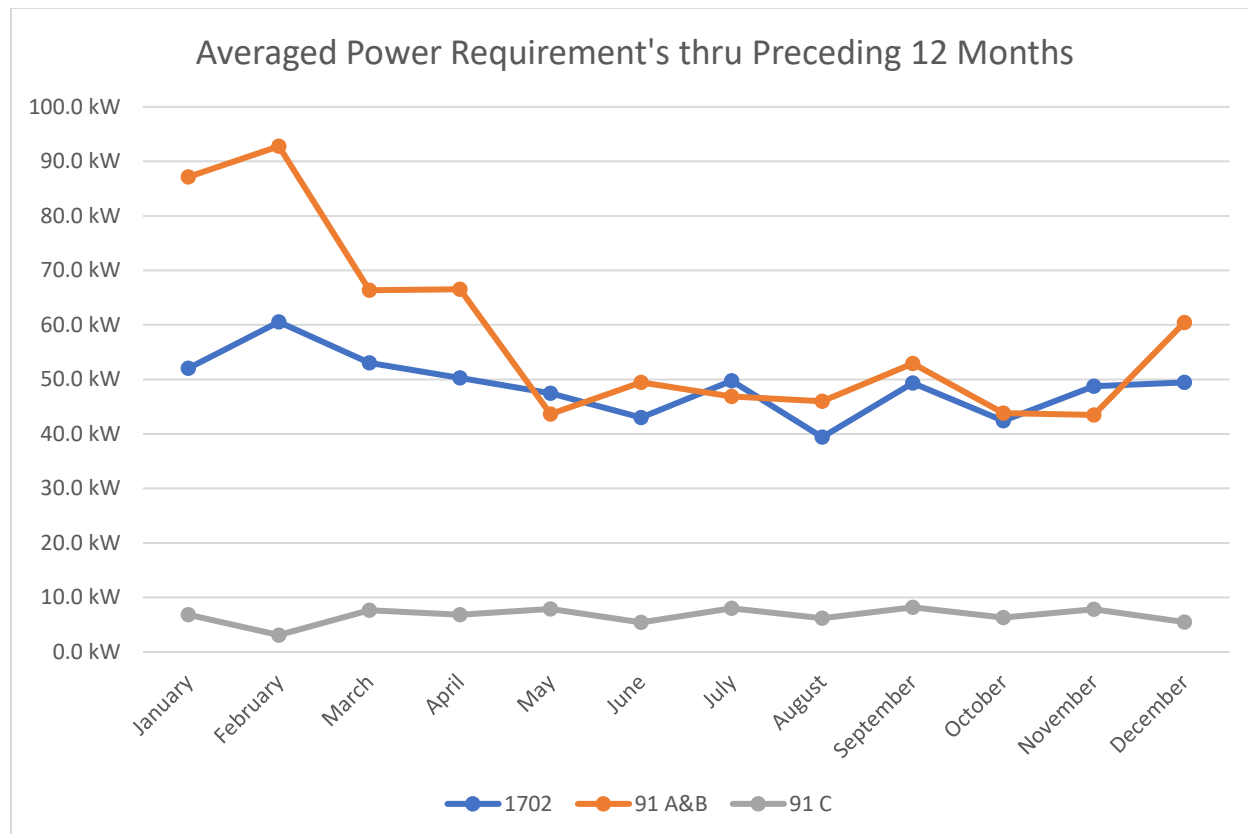


Figure 6: Energy Load Models for Target Buildings

Equipment of varying power ratings cumulate to the amount signified in the figures. The largest electrical devices were identified to be air conditioning units used to condition office-space air. Starting these systems can produce sudden power draws up to 10 kW—an important factor should they be fitted into an isolated microgrid. However, since the grid would be available and on the downstream side of the inverter, a FC would be isolated from such transient surges.

Because Buildings 91 A, B, and C are clustered together, and their daily energy usage can sum to a near 100 kW through most of the year, building 1702 was ruled out. Powering Buildings 91A, B, and C with one FC was initially considered, but since no commercially available 100 kW SOFC modules were found, it was decided to either power a portion of one of the buildings with a smaller system or power all the buildings plus a few others nearby with a larger one.

3.3 INFRASTRUCTURE REQUIREMENTS

Site considerations will require a well-drained area with level ground. In addition to the FC stack, commercially available FCs are typically packaged with two other integrated subsystems: a fuel processor and a power conditioner. This allows for elegant system designs in which the FC

module can connect directly to a NG tap on one side and the alternating current (AC) power circuit on the other via an inverter, which is necessary to convert the direct current produced electrochemically to end-use-compatible AC. Although a microgrid structure is an appealing strategy for achieving energy management goals, it is simply not compatible with a FC in baseload operation mode lacking a dynamic, automated battery system.

For this reason, the utility BGE was contacted about the possibility of interconnecting the NG distributed generation FC system to their grid (Mirabile, 2018). This is necessary mainly because the addition of a NGDG system will alter the POB electrical load and the one-way flow of power to the Port. PJM Interconnection, LLC's website was also consulted for their own specific regulations regarding large-scale projects. Canvassing the regional utility and grid operator provided key insights into necessary project specifications. It was found that BGE requires a net energy metered (NEM) system be under 30 kW without producing more than the load it is offsetting to be fed into the grid for monetary payback. Any potential systems exceeding these metrics would incur major increases in capital cost, as BGE & PJM would likely retrofit the surrounding grid with utility substations or new T&D equipment to make it "smart" enough to handle two-way flow and accommodate the additional power transmitted. This process involves a \$10,000 down-payment before the investigation can begin. Regardless of whether or not capital improvements would be needed, specific steps required during the interconnection process would be established by BGE once a system is selected, as they will be losing income with net-metered DG.

SOFC systems require a supply of NG, and so interconnection with BGE pipeline infrastructure is also necessary. This resource generally has much higher reliability than utility electric power, is less subject to damage-related outages, and can therefore provide continued power in the event of a grid outage. Two key issues requiring consideration are quantity (pressure and flowrate) needed and available quality of the gas. In contrast to all combustion-type engines, FCs can operate at pressures typical for NG supply lines, and such is the case in three of the four implementation options presented below. The fourth option consists of a large-scale system by SOFC industry leader Bloom Energy. Because these SOFC systems are entirely air-cooled, no regular water supply is required. Apart from Bloom Energy, only Atrex Energy offers products at a reasonable scale for the baseload power generation being considered.

Four FCs with ratings of 0.5 kW, 1.5 kW, 5 kW, and 200 kW were selected. Their specifications can be found in Appendix A.

3.4 PROJECT OPTION A – 0.5 kW

The first implementation option consists of repurposing Atrex Energy's 500W ARP500 FC that was purchased by POB for a 2016-2017 flow-way demonstration project. This system will be easy to NEM and maintain, as Atrex Energy offers routine oversight and operation and maintenance (O&M) service when needed.

3.5 PROJECT OPTION B – 1.5 kW

Atrex Energy's 1.5 kW ARP1500 FC was next considered as a similar deployment to offset a fraction of the energy load while feeding into the grid at night for operational income.

3.6 PROJECT OPTION C – 5 kW

Atrex Energy indicated that a fuel cell model will enter the market by the end of 2018; it is a good candidate for potential deployment at POB (Atrex Energy personal communication, 2018). It will have a 5-kW nominal power rating composed of dual 2.5 kW modules and offer updated monitoring infrastructure and battery system capability. Since this project evaluated simple baseload offsetting, batteries were not necessary and would only add to capital expenses, so the FC on its own was considered.

3.7 PROJECT OPTION D – 200 kW

Bloom Energy is the leading provider of SOFC systems ranging from 200 kW to 2 MW. To contrast with the smaller system options, their Bloom ES2 FC was included as a final option for the port to consider for the potential of large scale NGDG.

4. EMISSIONS ANALYSIS

SOFCs produce energy with about 75% less emissions than the traditional grid mix at typical values around 340 gCO₂/kWh (Gur, 2016). Taking full advantage of emerging CHP FC technologies could reduce that to 260 gCO₂/kWh (J. Thijssen, LLC, 2009). Both situations are without carbon capture and storage (CCS) capabilities that are very compatible with the SOFC exhaust stream highly concentrated in CO₂ and lacking nitrogen or sulfur which are filtered out through the system (Battelle, 2017). Although CCS is capital intensive, it could theoretically reduce emissions to zero. Even without CCS, FC implementation will reduce POB's scope 2 emissions.⁹

Both market- and location-based emission reductions in metric tons (MT) of CO₂-equivalent units, which stand for total emissions that also include sulfurous and nitrogenic gases along with carbonaceous gases, produced as byproducts in energy production. Location-based metrics are calculated with an empirically obtained average of emissions intensity of the utility grid sourcing the energy, whereas market-based figures are obtained from agreed-upon terms within contractual instruments between power providers and their customers. Relevant data are contained within the proprietary 2018 Climate Corps Financial Analysis Tool (CCFAT), so with a sum total of annual energy saved by the onsite NGDG, totals were calculated as the difference between energy use offset from the grid and the amount of onsite GHG emitted by the FC itself. Due to the technology's high efficiency (almost triple that of coal power plants), the differences were all positive and clearly forecast local environmental benefits coming out of FC implementation.

Table 1: GHG Emissions Reductions for Deployment Options

⁹ Scope 2 refers to GHG emissions from the generation of purchased electricity consumed by a company.

Project Option	Annual GHG Emission Reduction (MT CO_{2eq})	GHG Emission Reduction Over System Lifetime of 35 Years (MT CO_{2eq})
A – 0.5 kW SOFC	2.16	75.6
B – 1.5 kW SOFC	6.47	226.45
C – 5.5 kW SOFC	23.71	829.85
D – 200 kW SOFC	862.04	30,171.4

5. ECONOMIC ASSESSMENT

The existing grid has reserve capacity built-in to meet unusually high demands with excess capacity added to power generation as well as T&D systems. Beyond moderate/low gas prices, the main way a NGDG system can be economically feasible is if it offers reduced costs in areas of production and distribution relative to grid power. The most obvious interaction of these factors is found in a reduced utility demand charge, of which the cost of fixed reserve T&D capacity represents more than 50% (and more than its 25% of the energy charge) (J. Thijssen, LLC, 2009). The system options in question utilize this cost benefit by offsetting at least a portion of total energy usage for the daily times of use during which demand charges apply. A sizeable additional factor is the operating income allowed for by net-metering the system. That is, even when no load is present within the buildings, the FCs will still have a positive impact by selling clean power back to the utility.

Unlike most forms of RE, the COE for any NGDG has a nonzero value due to the commodified value of NG. The COE for the range of systems considered is less than two cents/kWh without considering capital and O&M costs. This is only four times as much as that from the grid, which is notable considering the deployments are minute fractions of the utility scale of production.

FC O&M requirements are relatively low and predictable with their lack of moving parts. The FC stack has an operational lifespan of over 40,000 hours, or close to five years, and will require replacement accordingly. About just as frequently, the sulfur trap preventing catalyst poisoning needs replacing as well. The balance of system (BOS) electronic components last at least 20 years, so the financial analysis here presented assume a lifetime of 35 years under these conditions. Considering O&M, the average FC COE of options considered is ten cents. This amount is heightened primarily due to the large stack costs, which are expected to decrease as this component is a focus in FC R&D.

Although Maryland’s state energy policies characterize a price-support market for RE development and integration, MDOT MPA is limited in terms of financing options due to its tax exemption. However, Maryland currently lacks DER compensation policies recently brought forth in a report by the National Association of Regulatory Utility Commissioners (NARUC). The report tabulates utility financial savings from avoided transmission capacity, administration costs, and other factors displayed in Figure 7 with the addition of DG (Orrell, Homer, & Tang, 2018). This incentivization may very well become applicable to the port FC within its 35-year

lifespan, given the electric utility industry needs to spend as much as \$2 trillion by 2030 to maintain reliable service (O'Connor, 2018).

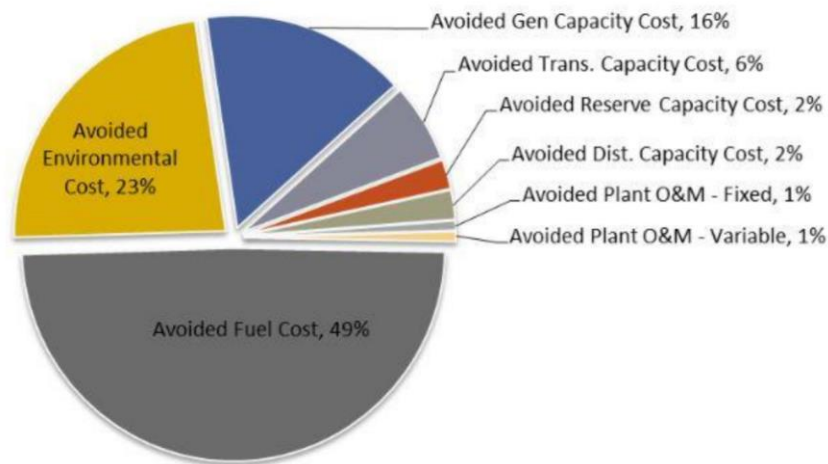


Figure 7: Utility financial savings created by DG.¹⁰

Nonetheless, additional incentives exist to help bridge the gap between the FC LCOE and BGE’s electricity rate. Financing options were investigated for offsetting a portion of the capital cost of FC deployment. Likely candidates are the federal Audit and Renewable Energy Development Assistance (EA/REDA) Grant Program, with an overall budget of \$2 million and the Maryland Smart Energy Communities grant, with a budget of \$3 million, both of which are available for state governments to apply. Maryland’s Commercial Property-Assessed Clean Energy (CPACE) Financing Program is also a potential option for funding, although as the funding would be a favorable loan with a payback period sustainable by the operational income of three of the four project options presented. These options were not included in the proceeding analyses. Interconnection and NEM standards are also in place in Maryland, which contribute greatly to the operational income of these systems. These capabilities were included in the financial analyses below.

The CCFAT, a collection of discounted cash flow analysis templates for energy projects, was used to create Figures 8 to 11 and Tables 2 through 5. It was customized to account for costs and expenses specific to FCs over their system lifespan. An Excel workbook, the CCFAT has been made modular so that any key assumptions, including the lifetime of the equipment, could be altered manually to produce automatic updates in corresponding financial projections.

Various assumptions were made to produce Figures 8 to 11. Namely, interconnection and NEM were assumed to be free for each system besides Bloom Energy’s, which was given an estimated price of \$250,000. Power fed back into the grid was assumed to be sold for 10 cents/kW. Stack replacements, which are needed every 5 years, typically cost 15% of the total system, so each stack replacement reflects that relative amount of the capital expense. O&M costs were

¹⁰ (Orrell, Homer, & Tang, 2018)

estimated to be 15% of the capital costs. The pressure of NG was assumed to be adequate to meet the inlet fuel pressure requirements of the SOFCs. Capital expenses were obtained from Atrex Energy and Bloom Energy; MDOT MPA already owns the 0.5 kW FC.

5.1 PROJECT OPTION A – 0.5 kW

Figure 8 portrays the time value of money required to finance the Atrex 0.5 kW FC if it were redeployed to provide a small baseload offset for one of the three 91-group buildings. As with the proceeding systems, money is saved by reducing power draws from the grid at a relatively low onsite COE while also selling excess power production back to the grid at BGE’s retail rate.

Figure 8: 0.5 kW System Lifetime Value & Performance

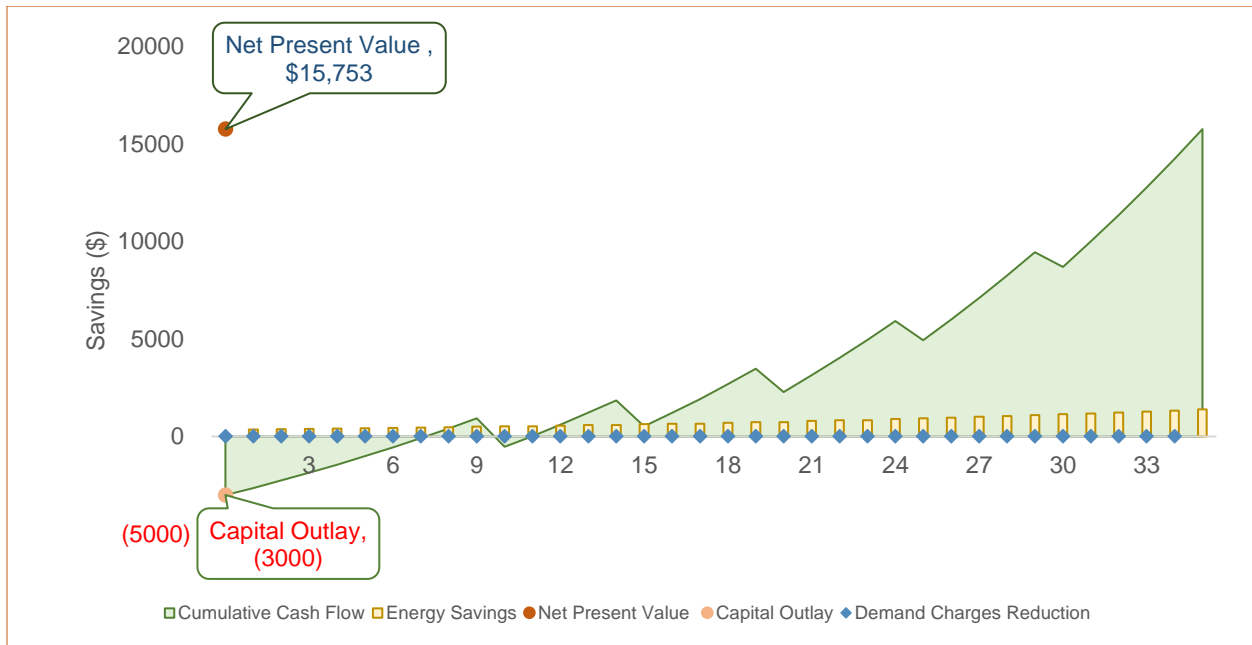


Table 2: 0.5 kW Key Assumptions, Savings, and Installation Charges

Baseyear Electricity Rate (\$/kWh)	\$0.08
Baseyear Demand Rate (\$ /kW/month)	\$4.00
Electricity Growth Rate	4%
Baseyear Natural Gas Rate (\$/therm)	\$0.39
Natural Gas Growth Rate	-0.5%
Baseyear Sellback Rate (\$/kWh)	\$0.10
Natural Gas Consumption Rate	185 ft ³ /day
Tax Rate	20%
Discount Rate (WACC)	0%
Demand Charge (\$/KW/Month)	100%
eGrid subregion	RFCE: RFC East
Annual Energy Savings (kWh)	4,380
Total Equipment Cost (\$)	\$ -
Total Labor Cost (\$)	\$3,000.00
Total Applicable Rebates (\$)	\$0.00
Demand Reduction (kW/Month)	0.5
Annual kWh Energy Savings (\$)	\$ 350.40

This system has the distinct advantage of no capital expense given that it is already owned by MDOT MPA. As a result, the payback period is significantly shorter than the other project options.

5.2 PROJECT OPTION B – 1.5 kW

Figure 9 portrays the time value of money required to finance the Atrex 1.5 kW system if it were purchased and commissioned to provide a small baseload offset for one of the three 91-group buildings. As with the other project options, dips in the time valuation curve represent O&M

charges involved in the periodic replacement of the FC stack.

Figure 9: 1.5 kW System Lifetime Value & Performance

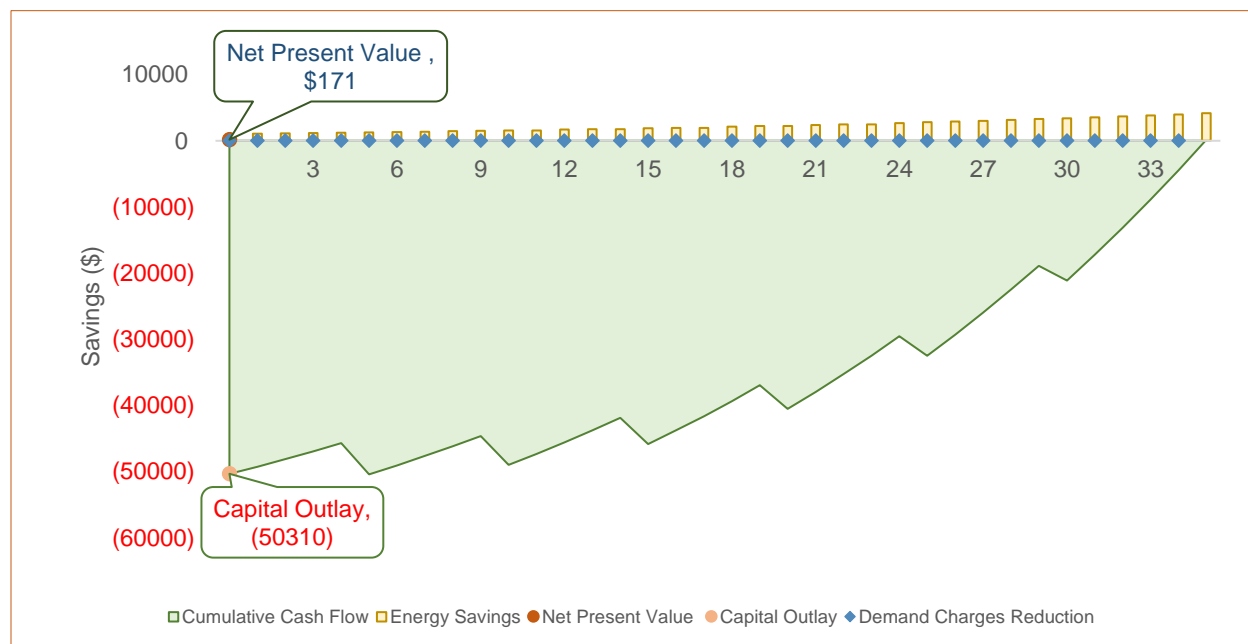


Table 3: 1.5 kW Key Assumptions, Savings, and Installation Charges

Baseyear Electricity Rate (\$/kWh)	\$0.08
Baseyear Demand Rate (\$ /kW/month)	\$4.00
Electricity Growth Rate	4%
Baseyear Natural Gas Rate (\$/therm)	\$0.39
Natural Gas Growth Rate	-0.5%
Natural Gas Consumption Rate	398 ft ³ /day
Baseyear Sellback Rate (\$/kWh)	\$0.10
Tax Rate	20%
Discount Rate (WACC)	0%
Demand Charge (\$/KW/Month)	100%
eGrid subregion	RFCE: RFC East
Annual Energy Savings (kWh)	13,140
Total Equipment Cost (\$)	\$ 47,810.00
Total Labor Cost (\$)	\$2,500.00
Total Applicable Rebates (\$)	\$0.00
Demand Reduction (kW/Month)	1.5
Annual kWh Energy Savings (\$)	\$ 1,051.20

Due to its high capital cost and low energy offset factor of 1.5 kW, this system provides the smallest financial incentive of the four options.

5.3 PROJECT OPTION C – 5.5 kW

Figure 9 portrays the time value of money required to finance the Atrex 5.5 kW system if it were purchased and commissioned to provide a small baseload offset for one of the three 91-group buildings. It may be advisable to connect this system with Building 91C since it nearly matches

the power rating (see Figure 6).

Figure 10: 5.5 kW System Lifetime Value & Performance

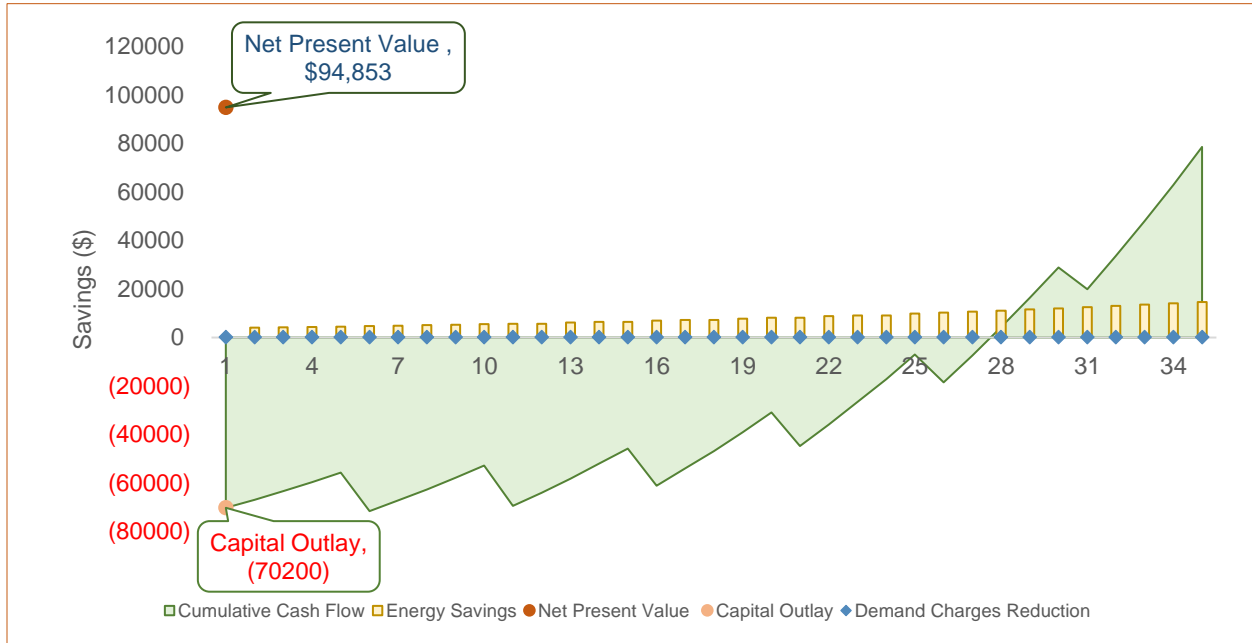


Table 4: 5.5 kW Key Assumptions, Savings, and Installation Charges

Baseyear Electricity Rate (\$/kWh)	\$0.08
Baseyear Demand Rate (\$ /kW/month)	\$4.00
Electricity Growth Rate	4%
Baseyear Natural Gas Rate (\$/therm)	\$0.39
Natural Gas Growth Rate	-0.5%
Natural Gas Consumption Rate	1460 ft ³ /day
Baseyear Sellback Rate (\$/kWh)	\$0.10
Tax Rate	20%
Discount Rate (WACC)	0%
Demand Charge (\$/KW/Month)	100%
eGrid subregion	RFCE: RFC East
Annual Energy Savings (kWh)	48,180
Total Equipment Cost (\$)	\$ 65,000.00
Total Labor Cost (\$)	\$5,200.00
Total Applicable Rebates (\$)	\$0.00
Demand Reduction (kW/Month)	5.5
Annual kWh Energy Savings (\$)	\$ 3,854.40

This system can also be combined with the 0.5 kW FC that MDOT MPA owns; doing so would increase energy production by 10% without contributing to capital cost.

5.4 PROJECT OPTION D – 200 kW

Figure 9 portrays the time value of money required to finance the Bloom 200 kW system if it were purchased and commissioned to provide a small baseload offset for one of the three 91-group buildings. This system could power the entire 91-group buildings and more, which opens

up the possibility of a microgrid establishment with a battery bank to handle variable loads.

Figure 11: 200 kW System Lifetime Value & Performance

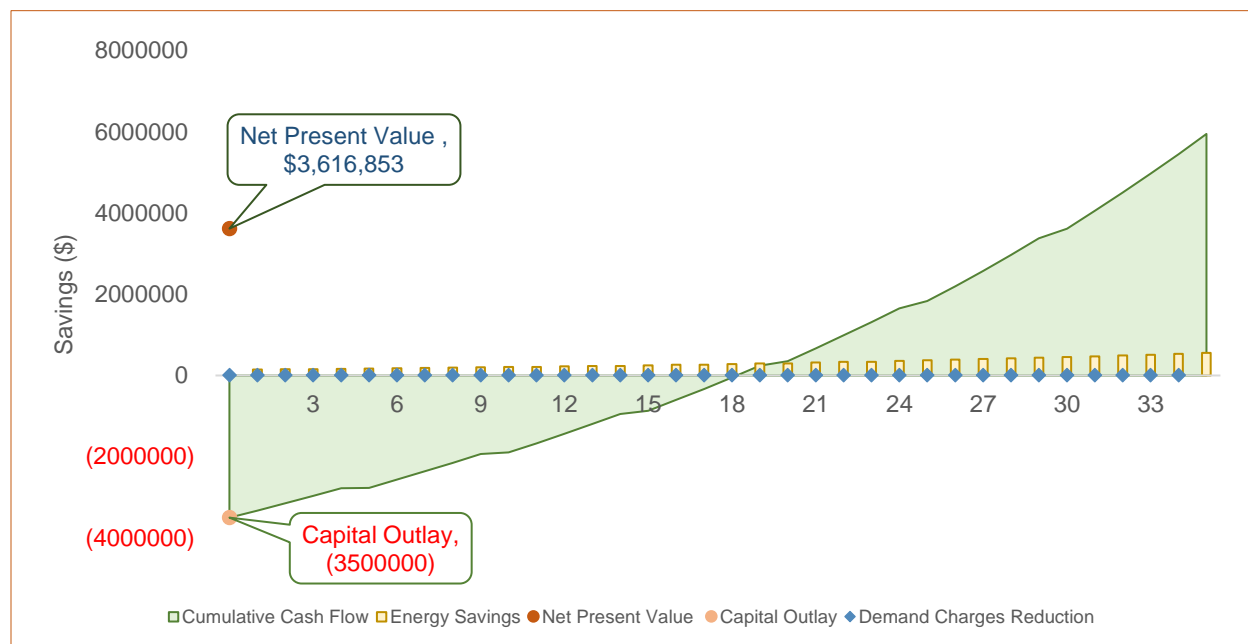


Table 5: 200 kW Key Assumptions, Savings, and Installation Charges

Baseyear Electricity Rate (\$/kWh)	\$0.08
Baseyear Demand Rate (\$ /kW/month)	\$4.00
Electricity Growth Rate	4%
Baseyear Natural Gas Rate (\$/therm)	\$0.39
Natural Gas Growth Rate	-0.5%
Natural Gas Consumption Rate	45000 ft ³ /day
Baseyear Sellback Rate (\$/kWh)	\$0.10
Tax Rate	20%
Discount Rate (WACC)	0%
Demand Charge (\$/KW/Month)	100%
eGrid subregion	RFCE: RFC East
Annual Energy Savings (kWh)	1,752,000
Total Equipment Cost (\$)	\$ 1,500,000.00
Total Labor Cost (\$)	\$2,000,000.00
Total Applicable Rebates (\$)	\$0.00
Demand Reduction (kW/Month)	200.0
Annual kWh Energy Savings (\$)	\$ 140,160.00

A significant cost increase reflected in Table 5’s “Total Labor Cost” is required to coordinate cogeneration with BGE or the construction of a microgrid at the port. Depending on the amount of T&D modification required of the utility, a microgrid may be cheaper, even with batteries.

5.5 ADDITIONAL DEPLOYMENT CONSIDERATIONS

Research on commercially available FCs revealed a sizeable gap, ranging from 5.5 to 200 kW, in the electricity produced by available products for residential/small scale up to large scale NGDG.

However, given that the modular nature of the technology permits systems to be combined in series/parallel circuits, energy solutions within that range are achievable with the implementation of a more sophisticated EMS. To simulate the modularity, the detailed specifications and breakdown of expenses obtained for Atrex Energy’s ARP1500 were extrapolated within CCFAT and the extrapolated systems were run through the same financial and emissions analyses as the four project options. To show the benefit of doing so, two key financial metrics indicating feasibilities of these extrapolated systems were calculated and are displayed in Figure 12: 1) profitability index (PI) and 2) net present value (NPV). The PI, typically calculated to gauge investment attractiveness for any type of investment, is defined to be the present value of future cash flows (not the net present value) divided by the initial investment, or:

$$PI = \frac{\text{total operating savings and income}}{\text{capital expense}}$$

A PI above 1.0 is favorable because it indicates that the total operating savings and income exceed the capital expense.

Figure 12: Performance Regression Model for Various Extrapolated FC System Sizes

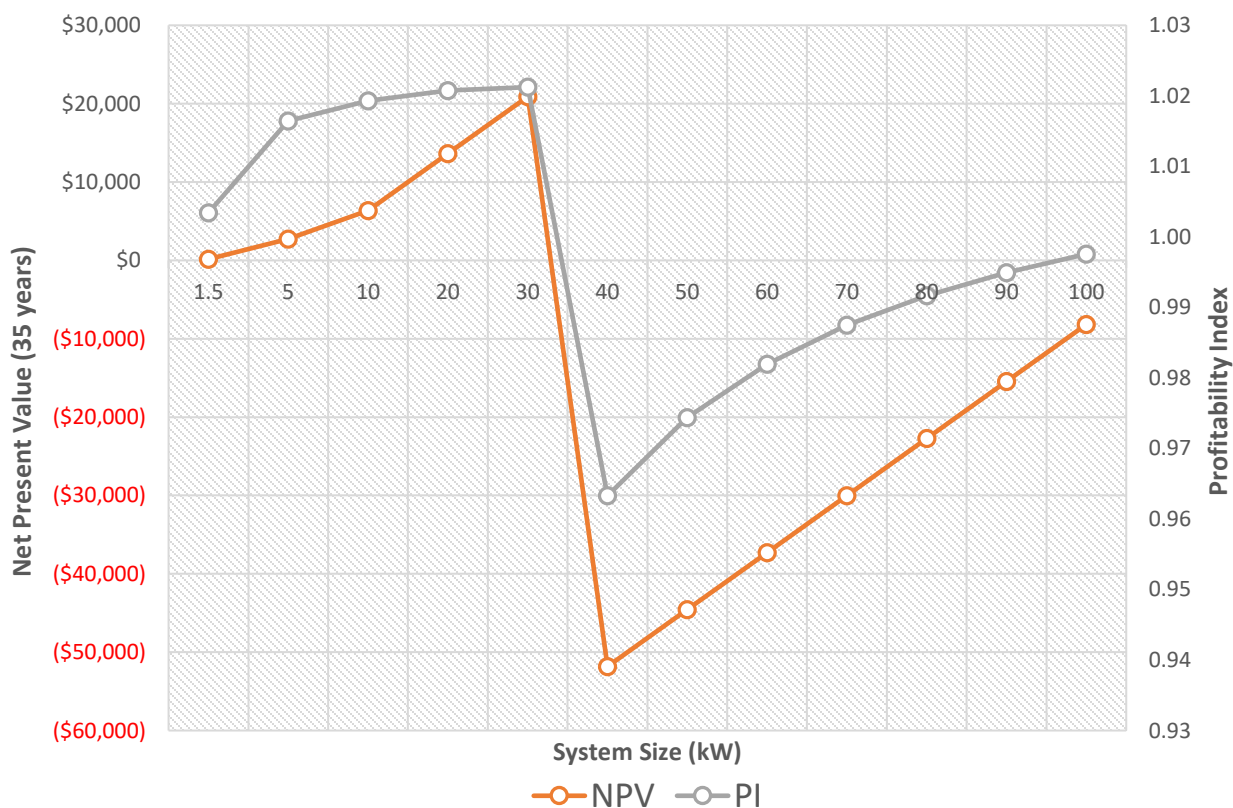
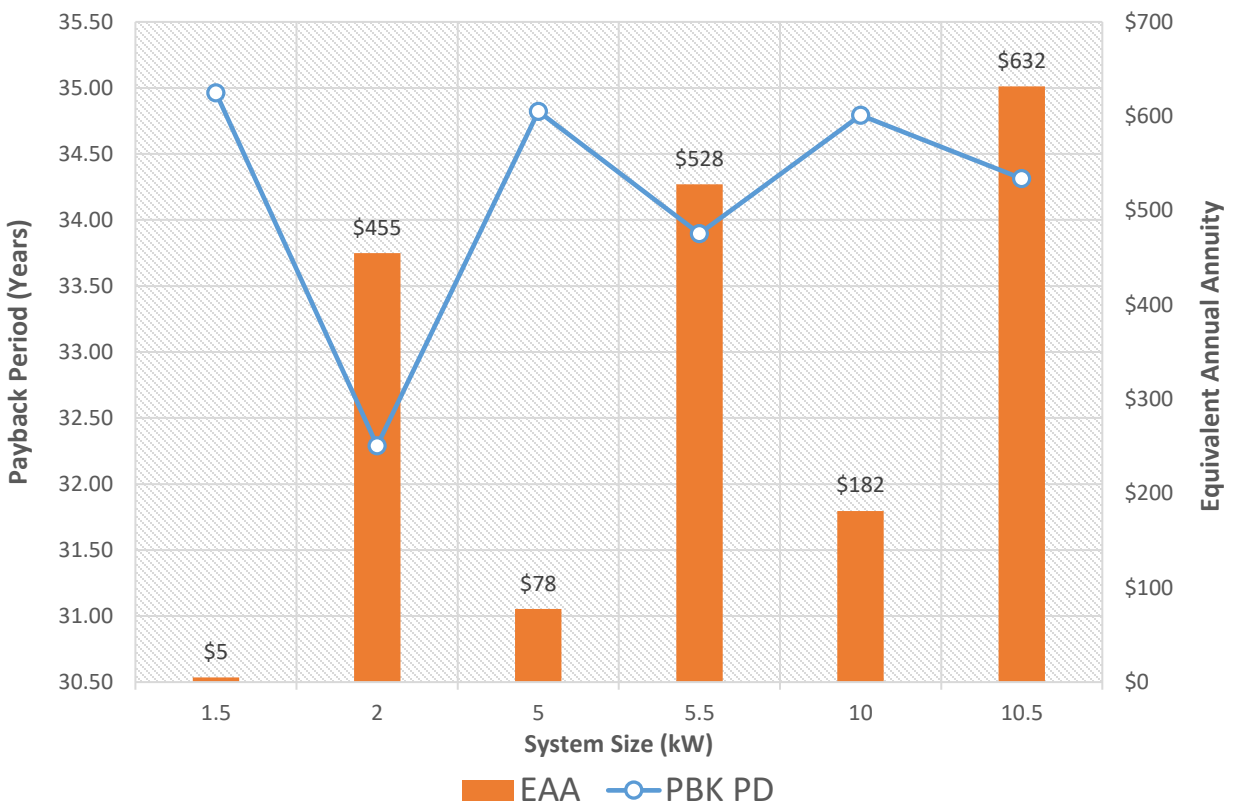


Figure 12 indicates that PI levels off at just over 1.02 for systems between 10 and 30 kW due to the fixed capital cost per FC module. In reality, the capital expense will likely decrease with system size due to economics of scale involved with manufacturing and commissioning, so PI can be expected to level off at some higher value. NPVs increase exponentially as energy offsets accumulate proportional to the rated power’s accumulation (energy production) over the system

lifetime. Both metrics are shown to decrease dramatically for system sizes over 30 kW, the threshold imposed by BGE for when to investigate retrofitting the surrounding grid with utility substations or new T&D equipment to make it “smart” enough to handle two-way flow and accommodate the additional power transmitted. DG systems exceeding 30 kW are required to undergo an intensive interconnection review process, which greatly reduces investment attractiveness.

The incentive to redeploy the 0.5 kW FC currently onsite was evaluated further; its financial model was combined with the smallest three systems (1.5, from the primary deployment options, and 5 and 10 kW in the extrapolated set presented above) to evaluate system sizes of 2, 5.5 and 10.5 kW. The simulated output metrics, two of which are displayed in Figure 13, show benefits for combining the 0.5 kW FC with another FC systems.

Figure 13: System Performance Augmentations with Existing 0.5 kW FC System



Payback period (PBK PD) is defined as the length of time required for the system’s NPV to reach zero and become non-negative. This is the point when the initial investment is fully recovered; the shorter the PBK PD, the better. Equivalent annual annuities (EAA) are the average operational incomes generated by each system per year, which is calculated by dividing the NPV by the system lifespan; the higher the EAA, the better.

The addition of the 0.5 kW FC impacts these metrics more than does the system size itself, as is apparent in the difference between the amount of change created by moving up 0.5 kW and that created by moving up by 3.5 kW and 5 kW per the extrapolation described earlier. For example,

the addition of the 0.5 kW FC to the 1.5 kW FC increases the EAA from \$5 to \$455 and lowers the PBK PD from 35 to 32.25 years, whereas the addition of FCs not already owned by MDOT MPA to bring the electrical output up from 1.5 kW to 5 kW increases the EAA from \$5 to \$78 and decreases the PBK PD from 35 to 34.75 years. This can be explained by the fact that the 0.5 kW of the ARP500 is free of capital cost, whereas additional upfront payment is required for each conjoined 1.5 kW FC system.

Table 6: Financial Analysis Output Table

System Size (kW)	AES (kWh)	GHG RED (MT CO _{2eq})	CAPX	OPX	NPV	PI	IRR	PBK PD (years)	EAA	LCCA	LCOE	COE
0.5	4,380	75.43	\$ 3,000.00	\$ 15,408.91	\$15,753	6.2510	11.88%	7.17	\$450	\$0.16	\$0.12	\$0.10
1.5	13,140	226.28	\$ 50,310.00	\$ 63,777.11	\$171	1.0034	0.01%	34.96	\$5	\$0.08	\$0.25	\$0.14
2	17,520	301.71	\$ 51,660.00	\$ 79,186.01	\$15,924	1.3083	1.10%	32.29	\$455	\$0.09	\$0.21	\$0.13
"5"	43,800	754.28	\$ 68,850.00	\$ 213,278.02	\$79,100	2.1489	3.05%	27.30	\$2,260	\$0.11	\$0.18	\$0.14
5	43,800	754.28	\$ 165,016.67	\$ 212,590.36	\$2,717	1.0165	0.06%	34.82	\$78	\$0.08	\$0.25	\$0.14
"5.5"	48,180	829.71	\$ 70,200.00	\$ 228,686.92	\$94,853	2.3512	3.50%	26.64	\$2,710	\$0.11	\$0.18	\$0.14
5.5	48,180	829.71	\$ 165,466.67	\$ 227,999.26	\$18,470	1.1116	0.42%	33.90	\$528	\$0.08	\$0.23	\$0.14
10	87,600	1,508.56	\$ 328,883.33	\$ 425,180.72	\$6,354	1.0193	0.07%	34.79	\$182	\$0.08	\$0.25	\$0.14
10.5	91,980	1,583.99	\$ 330,683.33	\$ 440,589.62	\$22,107	1.0669	0.26%	34.31	\$632	\$0.08	\$0.24	\$0.14
20	175,200	3,017.12	\$ 656,616.67	\$ 850,361.43	\$13,628	1.0208	0.08%	34.78	\$389	\$0.08	\$0.25	\$0.14
30	262,800	4,525.69	\$ 984,350.00	\$ 1,275,542.15	\$20,902	1.0212	0.08%	34.77	\$597	\$0.08	\$0.25	\$0.14
40	350,400	6,034.25	\$ 1,412,083.33	\$ 1,700,722.87	(\$51,824)	0.9633	-0.15%	35.68	(\$1,481)	\$0.08	\$0.25	\$0.14
50	438,000	7,542.81	\$ 1,739,816.67	\$ 2,125,903.59	(\$44,551)	0.9744	-0.10%	35.55	(\$1,273)	\$0.08	\$0.25	\$0.14
60	525,600	9,051.37	\$ 2,067,550.00	\$ 2,647,941.53	(\$37,277)	0.9820	-0.07%	35.47	(\$1,065)	\$0.08	\$0.26	\$0.14
70	613,200	10,559.93	\$ 2,395,283.33	\$ 2,976,265.02	(\$30,003)	0.9875	-0.05%	35.40	(\$857)	\$0.08	\$0.25	\$0.14
80	700,800	12,068.50	\$ 2,723,016.67	\$ 3,401,445.74	(\$22,729)	0.9917	-0.03%	35.36	(\$649)	\$0.08	\$0.25	\$0.14
90	788,400	13,577.06	\$ 3,050,750.00	\$ 3,826,626.45	(\$15,455)	0.9949	-0.02%	35.32	(\$442)	\$0.08	\$0.25	\$0.14
100	876,000	15,085.62	\$ 3,378,483.33	\$ 4,251,807.17	(\$8,181)	0.9976	-0.01%	35.29	(\$234)	\$0.08	\$0.25	\$0.14
~200	1,752,000	30,171.24	\$ 1,750,000.00	\$ 1,650,015.00	\$3,845,253	3.1973	7.45%	13.96	\$109,864	\$0.35	\$0.06	\$0.03
200	1,752,000	30,171.24	\$ 3,500,000.00	\$ 1,875,015.00	\$3,616,853	2.0334	4.48%	18.18	\$103,339	\$0.22	\$0.09	\$0.03

Table 6 shows the data outputs tabulated in the CCFAT. Quotation marks and the “~” tilde notation were used to differentiate system projections of the same nominal power rating but different model inputs. This was necessary for the 5-kW size because specifications for Atrex’s soon-to-be released can only be considered tentative (Cheekatamarla, 2018). So, for accuracy, a 5-kW figure was included in the regression to provide a window of potential costs for an Atrex system of that size. The tilde-denoted 200 kW system by Bloom Energy has a different implementation scenario consisting of a microgrid. Just the microgrid, without a battery bank added, is assumed to have a lower capital cost than the interconnection fee, so it appears to be the more financially beneficial option of the two 200 kW systems.

For the numerical-order ranking of all projected systems according to several metrics in Table 6, refer to Figures B-1 to B-5 in Appendix B.

6. REGULATORY CONSIDERATIONS

Given the system's ultra-low emissions and no solid waste production aside from periodic stack replacements, SOFCs have significant permitting advantages compared with conventional NGDG technologies. Certain requirements for grid interconnection, for instance, can be streamlined for a project such as this according to BGE. To meet power infrastructure requirements of reliability and integrity, however, a strict engineering design/review process would have to ensue. Although concerns have been raised regarding the safety of FC vehicles, stationary FCs are of little concern if they comply with universal electrical code. Of course, the specific location of the system matters as much as it is a safe distance away from traffic and is at no risk of incurring a collision or any accidental damage. Spaces such as this exist behind Buildings 91A, B, and C. This goes for security purposes as well, including the protection from weather hazards. Lastly, the FC system must comply with any federal, state, and local regulatory authorities for building construction regulations and zoning ordinances.

7. CONCLUSION AND NEXT STEPS

The purpose of this project was to find a place for FCs in POB's energy portfolio where they would not only benefit onsite operations and local environmental conditions but also contribute to the reduce dependency on electric grid and serve as an example to all industrial sectors of best-practice grid modernization strategies. SOFCs fit particularly well in RE system implementation strategy as they facilitate end-use electrification and distributed generation while maintaining reliability and autonomy from environmental and sometimes geopolitical conditions. Evidence indicates that the SOFC technology needs to take a larger role in present-day fuel cell solutions, as the technology's fuel flexibility eliminates the issue of completely overhauling existing energy source and transportation infrastructure.

The process for FC deployment was detailed for future use of this document as a template or guide for future project development in this field. Rationale for different FC types, options for designing their surrounding system components, characterizations of load compatibilities with different operation modes, and an in-depth economic and emissions analysis were included to provide a complete picture of an accurate functional outline of an FC power system for various scenarios involving stationary power generation.

This project indicates that a deployment of the MDOT MPA-owned 0.5 kW SOFC is most favorable based on economic assessments of commercially available or almost commercially available 0.5 kW, 1.5 kW, 5 kW, and 200 kW FCs as well as extrapolated systems ranging from 10 kW to 100 kW. Other system sizes recommended for POB are 200 kW, 5.5 kW, 5 kW, 2 kW, 10.5 kW, 30 kW, 20 kW, 10 kW, and 1.5 kW because they all returned positive cash flow during their assumed 35-year lifespans. In general, while the larger units have a costlier capital outlay, the time to positive cash flow is shorter and the savings accumulated in later years can be substantial. Moreover, the financial advantage for the larger units may even be higher since the economic assessments did not include potential incentives for greenhouse gas reductions. The

LCOEs of these systems, displayed in Figure B-4 Appendix B, are competitive with other RE technologies and even the regional utility grid itself, which is very competitive at 8 cents/kWh. The top scenarios performed at a range from 6-18 cents/kWh. Prior studies of maritime port FC applications, reliant on PEMFC technologies, had actual LCOEs of \$1.38/kWh (Pratt & Chan, 2017) and projected ones of 10-16 cents/kWh with the added feature of CHP technology to boost efficiency (MacKinnon & Samuelsen, 2016).

FCs are an attractive financial and economic investment for stationary deployment at POB when applied with a systems-based approach. With this in mind, MDOT MPA has many options to consider moving forward in the implementation of corresponding onsite NGDG. To fulfill all aspects of deployment (capital costs, operational expenses, interconnection logistics, etc.), a small-scale FC deployment of 0.5 kW or 5.5 kW is the most advisable energy solution. With the utilization of financing options, larger systems and maybe even a microgrid or large-scale cogeneration may become economically possible.

REFERENCES


- Abbaspour, A., Parsa, N., & Sadeghi, M. (2014, July). A new feedback Linearization-NSGA-II based control design for PEM fuel cell. *International Journal of Computer Applications*, 97(10), 25-32. doi:10.5120/17044-7354
- Ahead of the curve: Proactive plan positions Baltimore to gain Panama Canal traffic. (2016). *Special Advertising Section of The Journal of Commerce*, 48-50.
- American Association of Port Authorities. (2016). *Infrastructure investment plans for U.S. ports and their private-sector partners, 2016 through 2020*. Seaports Deliver Prosperity.
- American Association of Port Authorities. (n.d.). *Exports, Jobs & Economic Growth*. Retrieved from <http://www.aapa-ports.org/advocating/content.aspx?ItemNumber=21150>
- Battelle. (2017). *Manufacturing cost analysis of 100 and 250 kW fuel cell systems for primary power and combined heat and power applications*. U.S. Department of Energy. Columbus: Battelle Memorial Institute.
- Bloom, A. (2018). *Interconnections seam study*. Ames: National Renewable Energy Lab.
- Braun, R. J. (2001). Optimal design and operation of solid oxide fuel cell systems for distributed generation. (B. J. Thompson, Ed.) *Research Papers of the Link Foundation Fellows*.
- Cheekatamarla, P. (2018, June 29). Atrex Energy/MPA business call. (J. Krupa, Interviewer)
- Chen, I.-C. (2018, April 20). Toyota, Shell move forward with hydrogen facility at Port of Long Beach. *L.A. Biz*. Retrieved from <https://www.bizjournals.com/losangeles/news/2018/04/20/toyota-shell-move-forward-with-hydrogen-facility.html>
- Chick, L., Weimar, M., Whyatt, G., & Powell, M. (2014). The case for natural gas fuelled solid oxide fuel cell power systems for distributed generation. *Fuel Cells*, 15(1), 49-60. doi:10.1002/face.201400103
- Cohn, L. (2018, July 2). Port of San Diego to demonstrate how microgrids benefit ports worldwide. *Microgrid Knowledge*. Retrieved from <https://microgridknowledge.com/microgrids-benefit-ports-san-diego/>
- Curtin, S., & Gangi, J. (2015). *The business case for fuel cells 2015: powering corporate sustainability*. U.S. Department of Energy. Washington DC: Fuel Cell & Hydrogen Energy Association.
- Dinsmore, C. (2017, November 17). Record growth continues at port of Baltimore. *The Baltimore Sun*.
- E4tech. (2017). *The fuel Cell Industry Review 2017*. Retrieved from <http://www.fuelcellindustryreview.com/>
- Fuel Cell Technologies Office. (2018). *Hydrogen Resources*. (O. o. Energy, Producer, & Department of Energy) Retrieved from [energy.gov: https://www.energy.gov/eere/fuelcells/hydrogen-resources](https://www.energy.gov/eere/fuelcells/hydrogen-resources)
- Gur, T. M. (2016). Comprehensive review of methane conversion in solid oxide fuel cells: Prospects for efficient electricity generation from natural gas. *Progress in Energy and Combustion Science*, 54, 1-64. doi:<http://dx.doi.org/10.1016/j.pecs.2015.10.004>
- ICF. (2018). *Implications of policy-driven residential electrification*. American Gas Association.

- ICF International. (2016). *National port strategy assessment: Reducing air pollution and greenhouse gases at U.S. ports*. Office of Transportation and Air Quality. Washington DC: U.S. Environmental Protection Agency.
- ICF International. (2017). *Catalog of CHP technologies: Section 6. Technology characterization - Fuel cells*. U.S. Department of Energy. Washington DC: U.S. Environmental Protection Agency.
- Incantalupo, T. (2011, March 29). First hydrogen fuel cell station on LI. *Newsday*. Retrieved from <https://www.newsday.com/business/first-hydrogen-fuel-cell-station-on-li-1.2787459>
- International Maritime Organization. (2015). *Third IMO greenhouse gas study 2014*. London.
- J. Thijssen, LLC. (2009). *Natural gas-fueled distributed generation solid oxide fuel cell systems*. National Energy Technology Laboratory. Pittsburgh: U.S. Department of Energy.
- Klippenstein, M. (2017, December 27). *Fuel cells in 2017 are where solar was in 2002*. Retrieved from gtm: a Wood Mackenzie Business: <https://www.greentechmedia.com/amp/article/fuel-cells-in-2017-are-where-solar-was-in-2002>
- MacKinnon, M. A., & Samuelsen, S. (2016). *Assessment of fuel cell technologies to address power requirements at the Port of Long Beach*. University of California Irvine, Advanced Power & Energy Program. Long Beach: Port of Long Beach.
- Mirabile, J. A. (2018, June 14). Review of Interconnection Restrictions. (J. Krupa, Interviewer)
- Najafi, B., Mamaghani, A. H., Rinaldi, F., & Casalegno, A. (2015). Fuel partialization and power/heat shifting strategies applied to a 30 kWel high temperature PEM fuel cell based residential micro cogeneration plant. *International Journal of Hydrogen Energy*, 40, 14224-14234. doi:<http://dx.doi.org/10.1016/j.ijhydene.2015.08.088>
- Newby, R., & Keairns, D. (2013). *Analysis of natural gas fuel cell plant configurations - Revision 1*. National Energy Technology Laboratory, Office of Fossil Energy. Washington DC: U.S. Department of Energy.
- O'Connor, T. (2018, July 26). *Environmental Defense Fund*. Retrieved from www.edf.org/blog/2018/07/26/what-summers-heatwaves-tell-us-about-americas-electric-grid
- Orrell, A., Homer, J., & Tang, Y. (2018). *Distributed Generation Valuation and Compensation*. Richland, WA: Pacific Northwest National Laboratory.
- Port of Baltimore. (2015). *Port of Baltimore port report 2015: Growing our market*. Baltimore: Today Media Custom Communications.
- Pratt, J. W., & Chan, S. H. (2017). *Maritime Fuel Cell Generator Project*. Sandia National Laboratories. Albuquerque: U.S. Department of Energy.
- Productivity at its finest: Baltimore again named most efficient US container port. (2017). *Special Advertising Section of The Journal of Commerce*, 50-51.
- Reinish, J. (2014, February 10). *State & Alternative Fuel Provider Fleets*. Retrieved from U.S. Department of Energy: <https://epact.energy.gov/case-studies/port-authority>
- Schmitt, G. (2001). *Fuel cells for today's energy needs*. Retrieved from archives.evergreen.edu: <http://archives.evergreen.edu/webpages/curricular/2000-2001/ENVANA/Fuel%20Cells/report.htm>

- State of Maryland. (2016). *Ten-year plan (2016-2025) of electric companies in Maryland*. Public Service Commission, Energy Analysis and Planning Division. Baltimore: Maryland Department of Natural Resources.
- van Beurden, P. (2004). *On the catalytic aspects of steam-methane reforming: A literature survey*. ECN.
- Wachsman, E. D., & Lee, K. T. (2011, November 18). Lowering the temperature of solid oxide fuel cells. *Science*, 334(6058), pp. 935-939. doi:10.1126/science.1204090
- Wolfe, C. (2015, July 7). Houston as a hydrogen haven? *Texas Clean Air Matters Blog*. Retrieved from <http://blogs.edf.org/texascleanairmatters/2015/07/07/houston-as-a-hydrogen-haven/>

APPENDIX

Figure A-1: Atrex Energy FC Specification Sheet

	Atrex Energy, Inc. Remote Power Generator Technical Data			
	RP250	ARP500	ARP1000	ARP1500
Series	RP Series	ARP Series	ARP Series	ARP Series
Electricity Efficiency	~25%	~25%	~30%	~35%
DC Output Power Max	250W	500W	1000W	1500W
DC Output Voltage	12 or 24 VDC	2-60VDC	2-60VDC	2-60VDC
DC Output Current Max ¹	25A	100A	100A	100A
Operating Modes	Current Control (CC) Voltage Control (VC) Battery Charge (Bx, x=12, 24 or 48VDC)			
Start-up Time to Max Outpower Power	<60 minutes			
Propane Fuel Series P/N ²	RP250P	ARP500Px	ARP1000Px	ARP1500Px
Natural Gas Fuel Series P/N ²	RP250N	ARP500Nx	RP1000Nx	ARP1500Nx
CSA Certification Available	No	Yes	Yes	Yes
Fuel Cell Inlet Supply Pressure	2 psig - 5 psig (13.8kPa - 34.5kPa)			
Fuel Supply Pressure with High Pressure Regulator Kit (RP-HWN/RP-HWP)	10 psig - 125 psig (68.9kPa - 861.8kPa)			
Max Sulfur Content	<60ppmw (42mg/m ³)			
Max Water Content	<5000ppmv for standard system, non-condensing at operating temperature & pressure			
Fuel Consumption-Propane (HD5)	1.2G/day	2.4G/day	3.6G/day	5.2G/day
	4.5L/day	9.0L/day	13.5L/day	19.6L/day
Fuel Consumption-Natural Gas	116ft ³ /day	185ft ³ /day	298ft ³ /day	398ft ³ /day
	3.3m ³ /day	5.3m ³ /day	8.4m ³ /day	11.3m ³ /day
Operating Temperature	-40°C to +50°C (-40°F to +122°F)			
Storage Temperature	-40°C to +55°C (-40°F to +131°F)			
Humidity	5% to 95% (non-condensing)			
Operating & Storage Altitude	0 to 8,000 feet (2,438 meters)			
Unit Dimensions (H x W x D)	22"x22"x39"	26"x22"x39"	26"x28"x39"	
	(56cm x 56cm x 99cm)	(66cm x 56cm x 99cm)	(66cm x 71cm x 99cm)	
Unit Weight	280lbs (127kg)	293lbs (133kg)	351lbs (160kg)	358lbs (163kg)
Shipping Dimensions (H x W x D)	45" x 46" x 38"		48" x 46" x 38"	
	(114cm x 117cm x 97cm)		(122cm x 117cm x 97cm)	
Shipping Weight	346lbs (157kg)	359lbs (163kg)	419lbs (190kg)	426lbs (194kg)
Noise Levels (at 1m)	52dBA			
Fuel Connection-Propane into ARP-HWP	1/2" FNPT			
Fuel Connection-Propane into Fuel Cell	1/4" MNPT			
Fuel Connection-Natural Gas into ARP-HWN	1/2" FNPT			
Fuel Connection-Natural Gas into Fuel Cell	3/8" Swagelok type compression tube fitting			
Data Interface	MODBUS RTU via DB9 Connector (Requires RP-RS option)	MODBUS RTU via Terminal Strip (Requires ARP-RSC8 option)		
Local Computer Interface	RJ45			
Electrical Interface	Terminal Block 2/0 - 8 AWG			
Enclosure IP Category	IP23			
Enclosure Construction	Powder Coated Galvanized Steel			
Warranty	12 Months after Installation or 13 months after Date of Shipment			

¹ - Current will also be limited by maximum output power of unit

² - x = CSA Certification (C = CSA Certified, U = non CSA Certified)

Figure A-2: Bloom Energy FC Specification Sheet

Technical Highlights (ES5-BABAAA)	
Outputs	
Nameplate power output (net AC)	210 kW
Base load output (net AC)	200 kW
Electrical connection	480 V, 3-phase, 60 Hz
Inputs	
Fuels	Natural gas, directed biogas
Input fuel pressure	10-18 psig (15 psig nominal)
Water	None during normal operation
Efficiency	
Cumulative electrical efficiency (LHV net AC)*	65-53%
Heat rate (HHV)	5,811-7,127 Btu/kWh
Emissions	
NOx	< 0.01 lbs/MWh
SOx	Negligible
CO	< 0.05 lbs/MWh
VOCs	< 0.02 lbs/MWh
CO ₂ @ stated efficiency	679-833 lbs/MWh on natural gas; carbon neutral on directed biogas
Physical Attributes and Environment	
Weight	12.6 tons
Dimensions (variable layouts)	14' 9" x 8' 8" x 7' 0" or 25' 9" x 4' 5" x 7' 5"
Temperature range	-20° to 45° C
Humidity	0% - 100%
Seismic vibration	IBC site class D
Location	Outdoor
Noise	< 70 dBA @ 6 feet
Codes and Standards	
Complies with Rule 21 interconnection and IEEE1547 standards	
Exempt from CA Air District permitting; meets stringent CARB 2007 emissions standards	
An Energy Server is a Stationary Fuel Cell Power System. It is Listed by Underwriters Laboratories, Inc. (UL) as a 'Stationary Fuel Cell Power System' to ANSI/CSA FC1-2014 under UL Category IRGZ and UL File Number MH45102.	
Additional Notes	
Access to a secure website to monitor system performance & environmental benefits	
Remotely managed and monitored by Bloom Energy	
Capable of emergency stop based on input from the site	

Figure B-1: Deployment Option PIs Ranked

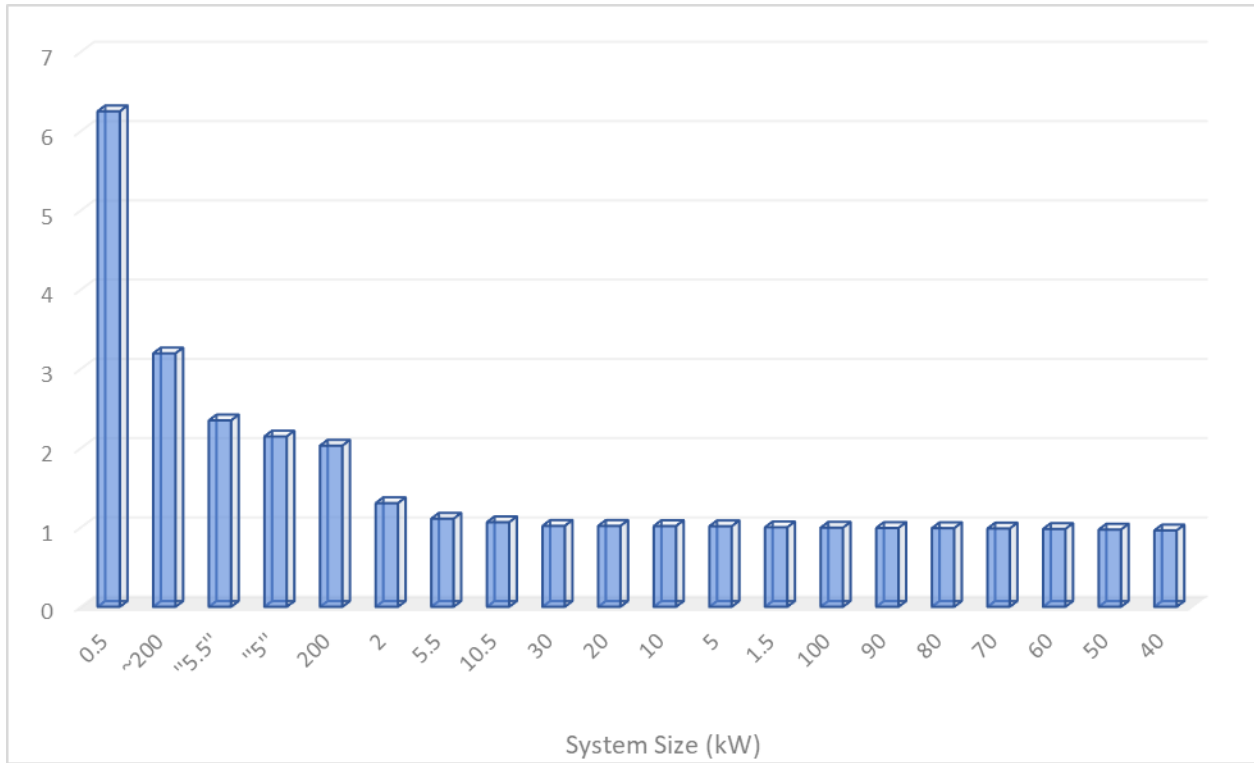


Figure B-2: Deployment Option IRRs Ranked

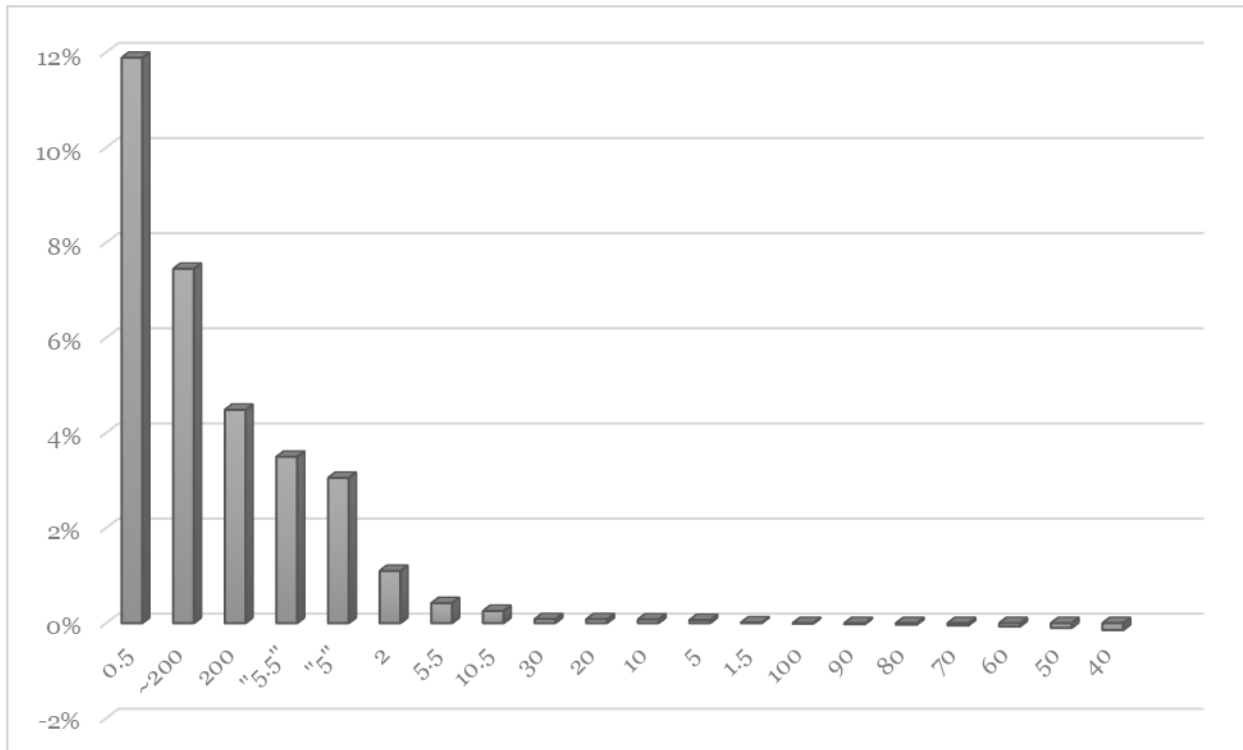


Figure B-3: Deployment Option Payback Periods Ranked

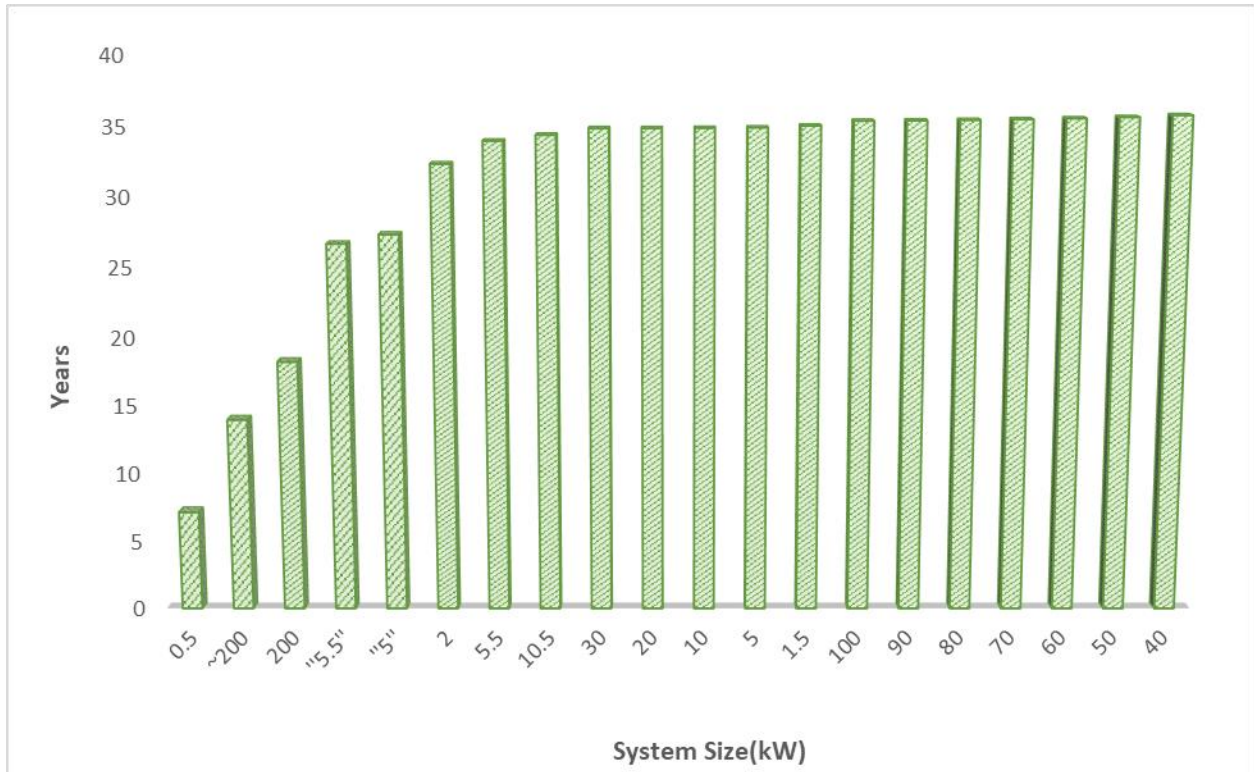


Figure B-4: Deployment Option LCOEs Ranked

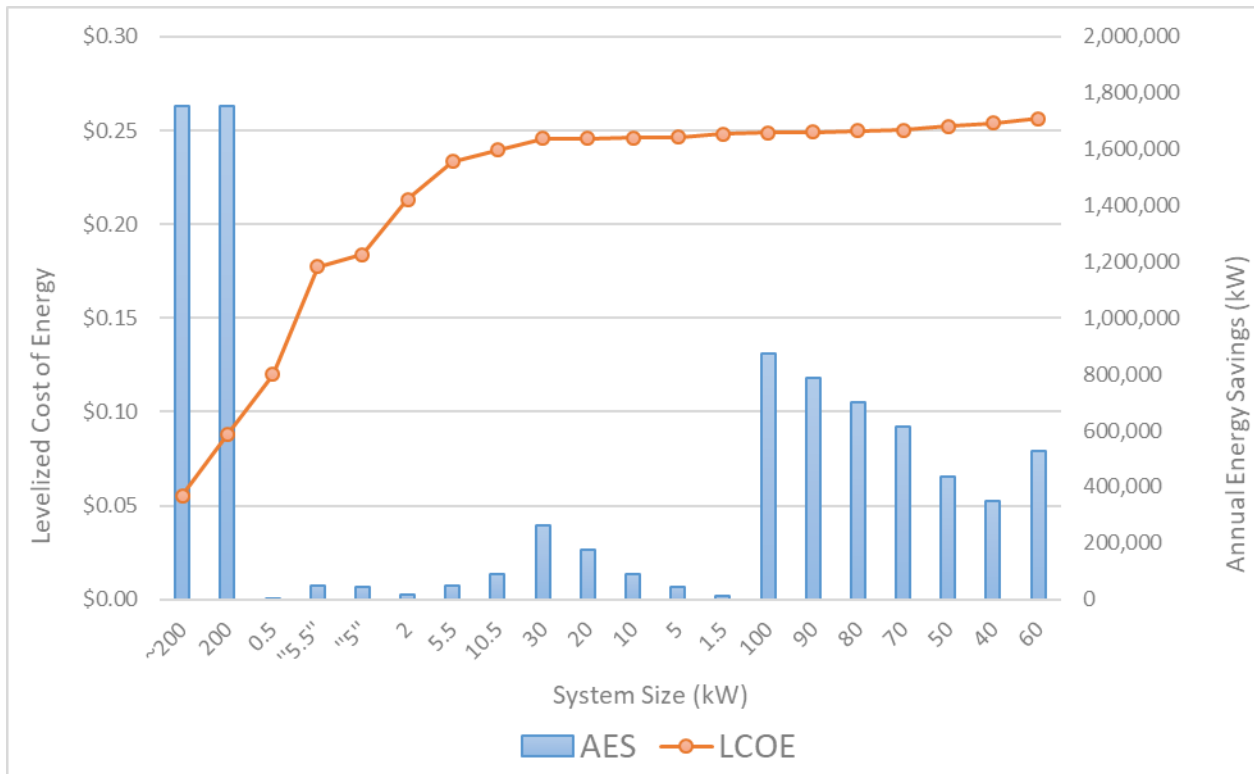


Figure B-5: Deployment Option LCCAs Ranked

